

The research of population structure in evolutionary algorithms

Yirui Wang

Affiliated to the major of
Advanced Mathematics and Human Mechanism
in Graduate School of Science and Engineering for Education



University of Toyama
Gofuku 3190, Toyama-shi, Toyama 930-8555 Japan

2020

Acknowledgements

Time goes by so fast, my doctoral career is coming to an end. During these three years, I have learned a lot of professional knowledge and improved own practical ability. I will never forget the University of Toyama which educates and cares for me. Before my graduation, I would like to express sincere gratitude to my teachers, schoolmates and family.

First of all, I would like to thank my supervisor Prof. Zheng Tang who is very responsible for my study and life. He guides and helps to solve various difficulties I meet. As a superior teacher and example, he encourages and supports schoolmates to make progress toward dreams. I will follow his belief to become a better man.

Then, I would like to appreciate my another supervisor Prof. Shangce Gao. His strict requirements in academic domain and conscientious attitude in work profoundly affect me. Especially for my research, he provides a number of constructive feedback and valuable discussion. Without his considerate care and helpful suggestions, I cannot achieve my current academic status.

Next, I would like to thank schoolmates and friends in our laboratory. During my doctoral period, we help each other in both study and life. Mutual promotion and improvement make us better and happier. I really enjoy those unforgettable time which becomes eternity. Hereby, I hope that everyone will live happily and everything will go well.

Finally, I am very grateful to my family. Without their encouragement and support, I cannot be who I am. As my spiritual pillar and motivation, they pay too many emotions and time. In the future, I will live up to their expectations and endeavour to become an outstanding person.

Abstract

Complex networks have been attracting much attention and developed rapidly over the past two decades. In nature and society, numerous networks have been described widely, such as Internet, E-mail, interpersonal relationship, collaboration, citation and so on. Investigations in various networks demonstrate these networks have some identical characteristics of topologies including small world, scale free, community structure and hierarchical framework. The discovery of these characteristics can make people better understand inherent regulation of abstract networks. Therefore, the complex network is regarded as an effective tool to depict and interpret the elusive phenomenon generated by real world. The aim involves two aspects where one is to cognize and analyze the essence of complicated system in terms of multiple viewpoints and the other is to enhance the application of research objective.

Evolutionary algorithms (EAs) such as genetic algorithm (GA), particle swarm optimization (PSO) and ant colony optimization (ACO) are effective methods to resolve various problems. As population-based algorithms, EAs continually evolve their populations to derive better results on optimization problems. Their population structures can influence interaction among individuals such that their performances are also determined. Adjusting population structures can become a kind of methods to improve performance of EAs. Studies have proved that population structures can remarkably help the evolution of individuals so as to reinforce the properties of EAs.

In this thesis, three kinds of EAs including differential evolution (DE), brain storm optimization (BSO) and gravitational search algorithm (GSA) are researched from the viewpoint of population structure. For them, my work mainly focuses on the following aspects: (1) Construction and implementation of complex networks; (2) Relationship between population structures and transmitting information; (3) Interaction among individuals in different population structures; (4) New proposals to modify population topologies for improving performance of EAs. The specific contents are given as follows.

(1) For DE, a population interaction network (PIN) is proposed to investigate the rela-

tionship constituted by populations. The cumulative distribution function (CDF) of degree in PIN is analyzed by five fitting models on twelve benchmark functions. The goodness of fit is used to measure fitting results. Experimental results demonstrate that CDF meets cumulative Poisson distribution. Besides, the number of nodes in PIN and the rate parameter λ in the fitted Poisson distribution are further studied using different control parameters of DE, which exhibits the effect and characteristic of the population interaction.

(2) For BSO, to theoretically analyze its performance from the viewpoint of population evolution, the PIN is used to construct the relationship among individuals. Four experiments in different dimensions, parameters, combinatorial parameter settings and related algorithms are implemented, respectively. Experimental results indicate the frequency of average degree of BSO meets a power law distribution on functions with low dimension, which shows the best performance of algorithm among three kinds of dimensions. The parameters of BSO are investigated to find the influence of population interaction with the power law distribution on the performance of algorithm, and respective parameter can change the relationship among individuals. In addition, mutual effect among parameters is analyzed to find the best combinatorial result to significantly enhance the performance of BSO. Contrast among BSO, DE and PSO demonstrates a power law distribution is more effective for boosting the population interaction to enhance the performance of BSO.

(3) For GSA, a hierarchical GSA with an effective gravitational constant (HGSA) is proposed to address premature convergence and low search ability. Three contrastive experiments are carried out to analyze the performances between HGSA and other GSAs, heuristic algorithms and PSOs on function optimization. Experimental results demonstrate the effective property of HGSA due to its hierarchical structure and gravitational constant. A component-wise experiment is also established to further verify the superiority of HGSA. Additionally, HGSA is applied to several real-world optimization problems so as to verify its good practicability and performance. Finally, time complexity analysis is discussed to conclude that HGSA has the same computational efficiency in comparison with other GSAs.

The thesis is organized as follows. Chapter 1 introduces background and related work of EAs as well as contributions of this thesis. Chapter 2 presents the research of population structure on DE. Chapter 3 describes several characteristics of population structure on BSO. Chapter 4 gives an improved GSA based on a modified population structure. Chapter 5 summarizes some general conclusions and points out several future work.

Contents

Acknowledgements	ii
Abstract	iii
1 Introduction	1
1.1 Background of EAs	1
1.2 Related work of EAs	2
1.2.1 Population structure	2
1.2.2 An overview of BSO	5
1.2.3 An overview of GSA	5
1.3 Contributions of this thesis	6
2 The research of differential evolution	8
2.1 Introduction	8
2.2 Conventional DE	8
2.3 Population interaction network	9
2.4 Experiment and analysis	12
2.4.1 Fitting results for PIN	17
2.4.2 Analysis for parameters	20
2.5 Conclusions	23
3 The research of brain storm optimization	25
3.1 Introduction	25
3.2 Conventional BSO	26
3.2.1 Basic principle of BSO	26
3.2.2 Characteristics of BSO	29
3.3 Construction of PIN	30
3.4 Experiment and analysis	32

3.4.1	Experimental setup	32
3.4.2	Results in different dimensions	34
3.4.3	Results in different parameters	39
3.4.4	Analysis for combinatorial parameter settings	48
3.4.5	Analysis for different related algorithms	52
3.5	Conclusions	54
4	The research of gravitational search algorithm	56
4.1	Introduction	56
4.2	Conventional GSA	57
4.3	Hierarchical GSA	59
4.3.1	Motivation	59
4.3.2	Proposed HGSA	60
4.4	Experiment and analysis	67
4.4.1	Experimental setup	67
4.4.2	Comparison between HGSA and other GSAs	68
4.4.3	Comparison between HGSA and other heuristic algorithms	76
4.4.4	Comparison between HGSA and other PSOs	77
4.5	Discussion	83
4.5.1	Parameter sensitivity analysis	83
4.5.2	Component-wise analysis	87
4.5.3	Real-world optimization problems	89
4.5.4	Time complexity analysis	91
4.6	Conclusions	92
5	Conclusions	93
5.1	Some general remarks	93
5.2	Future work	94
	Bibliography	95

List of Figures

2.1	(a) The structured diagram, and (b) framework of population interaction network in DE.	10
2.2	An illustrative graph of population interaction network in DE.	11
2.3	The box-and-whisker diagram of best fitness of DE on six standard benchmark functions and six CEC'05 benchmark functions.	14
2.4	The 2-dimensional sketch of PIN of DE on six standard benchmark functions.	15
2.5	The general changing process of PIN of DE on Sphere function.	16
2.6	The cumulative distribution graphs between the original data and fitting models of DE.	19
2.7	The number of nodes and the value of λ under DE with different parameters.	22
3.1	A descriptive diagram of PIN in BSO.	31
3.2	The box-and-whisker diagrams of optimal solutions obtained by BSO on Sphere, F6 and F18 with 2, 10, 30 dimensions.	36
3.3	Two-log curves of the average degree distribution of BSO on Sphere, F6 and F18 with 2, 10, 30 dimensions.	37
3.4	The power law distribution of average degree of BSO on other nine functions with 2 dimension.	38
3.5	The value of power exponent γ obtained by various parameters of BSO on six benchmark functions.	47
4.1	The graphs of conventional and new gravitational constant $G(t)$	62
4.2	A three-layered structure of HGSA.	64
4.3	The curves of two weighted coefficients $w_1(t)$ and $w_2(t)$	65
4.4	The illustrative graphs of the operating principle of HGSA.	67
4.5	The box-and-whisker diagrams of optimal solutions obtained by seven kinds of GSAs on F7 and F38 with 10, 30 and 50 dimensions.	75

4.6	The convergence graphs of average best-so-far solutions obtained by seven kinds of GSAs on F2 and F39 with 10, 30 and 50 dimensions.	75
4.7	The box-and-whisker diagrams of optimal solutions obtained by HGSA and five heuristic algorithms on F17, F27 and F53 with 30 dimensions.	79
4.8	The convergence graphs of average best-so-far solutions obtained by HGSA and five heuristic algorithms on F14, F29 and F39 with 30 dimensions. . . .	79
4.9	The curves of (a) log-sigmoid function with five different L values and (b) five different K value intervals.	86

List of Tables

1.1	A list of various metaheuristic algorithms.	2
2.1	The concrete description of twelve benchmark functions.	13
2.2	The best fitness value obtained by DE on twelve benchmark functions.	14
2.3	Fitting results of twelve functions with five models.	21
3.1	The experimental results obtained by BSO on benchmark functions and CEC'05 test functions with different dimensions.	35
3.2	The experimental results obtained by BSO with different number of clusters c on benchmark functions.	40
3.3	The statistical results of parameter c obtained by the Friedman test, where * indicates the best average rank of parameter.	40
3.4	The experimental results obtained by BSO with different number of populations p on benchmark functions.	40
3.5	The statistical results of parameter p obtained by the Friedman test, where * indicates the best average rank of parameter.	41
3.6	The experimental results obtained by BSO with different replacement rate p_c on benchmark functions.	41
3.7	The statistical results of parameter p_c obtained by the Friedman test, where * indicates the best average rank of parameter.	42
3.8	The experimental results obtained by BSO with different selected probability p_g on benchmark functions.	42
3.9	The statistical results of parameter p_g obtained by the Friedman test, where * indicates the best average rank of parameter.	43
3.10	The experimental results obtained by BSO with different p_{c1} on benchmark functions.	43
3.11	The statistical results of parameter p_{c1} obtained by the Friedman test, where * indicates the best average rank of parameter.	44

3.12	The experimental results obtained by BSO with different p_{c2} on benchmark functions.	44
3.13	The statistical results of parameter p_{c2} obtained by the Friedman test, where * indicates the best average rank of parameter.	45
3.14	Parameter results based on the $L_{25}(5^6)$ orthogonal array for six benchmark functions.	49
3.15	Statistical results of parameter settings obtained by the Friedman test, where * indicates the best average rank of parameter setting.	50
3.16	The experimental results obtained by BSO_{bp} on benchmark functions and CEC'05 test functions with three dimensions.	51
3.17	Statistical results obtained by the Wilcoxon signed ranks test between BSO_{bp} and BSO_{op} in three dimensions.	52
3.18	The experimental results obtained by BSO_{bp} , DE and PSO on CEC'05 test functions with three dimensions.	53
3.19	Statistical results obtained by the Wilcoxon signed ranks test among BSO_{bp} , DE and PSO on CEC'05 test functions with three dimensions.	54
4.1	Parameter settings of HGSA and other GSAs.	70
4.2	Experimental results of benchmark functions (F1-F57) with $D = 10$ dimensions using HGSA, GSA, GGSA, CGSA-M, PSOGSA, MGSA and DNLGSA.	71
4.3	Experimental results of benchmark functions (F1-F57) with $D = 30$ dimensions using HGSA, GSA, GGSA, CGSA-M, PSOGSA, MGSA and DNLGSA.	72
4.4	Experimental results of benchmark functions (F1-F57) with $D = 50$ dimensions using HGSA, GSA, GGSA, CGSA-M, PSOGSA, MGSA and DNLGSA.	73
4.5	Statistical results obtained by the Wilcoxon signed ranks test between HGSA and GSA, GGSA, CGSA-M, PSOGSA, MGSA and DNLGSA in $D = 10, 30$ and 50 dimensions.	74
4.6	Experimental results of benchmark functions (F1-F57) with $D = 30$ dimensions using HGSA, DE, CMA-ES, GABC, GWO and SCA.	78
4.7	Statistical results obtained by the Wilcoxon signed ranks test between HGSA and DE, CMA-ES, GABC, GWO and SCA in $D = 30$ dimensions.	79
4.8	Parameter settings of seven variants of PSO.	81
4.9	Experimental results of error values of CEC2013 test functions (F1-F28) with $D = 30$ dimensions using HGSA, FIPS, GPSO, CLPSO, OLPSO, GAPSO, DEPSO and GL-PSO.	82

4.10	Statistical results obtained by the Wilcoxon signed ranks test between HGSA and FIPS, GPSO, CLPSO, OLPSO, GAPSO, DEPSO and GL-PSO in $D = 30$ dimensions.	82
4.11	Experimental results of benchmark functions (F1-F57) with $D = 30$ dimensions using HGSA with five different L values.	84
4.12	Statistical results of parameter L obtained by the Friedman test, where * indicates the best average rank of parameter.	84
4.13	Experimental results of benchmark functions (F1-F57) with $D = 30$ dimensions using HGSA with five different K value intervals, where $n = 100$	85
4.14	Statistical results of parameter K obtained by the Friedman test, where * indicates the best average rank of parameter.	85
4.15	Experimental results of benchmark functions (F1-F57) with $D = 30$ dimensions using HGSA, HGSA-OG and GSA-IG.	88
4.16	Statistical results obtained by the Wilcoxon signed ranks test between HGSA and HGSA-OG and GSA-IG in $D = 30$ dimensions.	88
4.17	Experimental results of four real-world optimization problems using HGSA, GSA, GGSA, CGSA-M, MGSA, PSO-GSA and DNLGSA.	90

Chapter 1

Introduction

1.1 Background of EAs

Nowadays, a number of optimization problems are complex and difficult owing to their high dimensional spaces [1, 2]. Traditional mathematical methods cannot use effective formulas to resolve these problems. Thus, more and more attention have been attracted toward metaheuristic algorithms because they generally find a global optimal solution via continuous iterations [3–6].

Metaheuristic algorithms can be divided into two classes, i.e., single-point search algorithms and population-based search algorithms. Single-point search algorithms use an old individual to produce new one over iterations, such as simulated annealing (SA) [7] and Tabu search (TS) [8]. Population-based search algorithms utilize the population to gradually converge into a global optimal solution via some cooperative operators, such as GA [9], evolutionary programming (EP) [10], DE [11–13], ACO [14], PSO [15], BSO [16] and GSA [17].

Besides, metaheuristic algorithms can also be classified into three categories: biology-based algorithms, physics-based algorithms and geography-based algorithms. Biology-based algorithms are inspired from natural evolution and biological behaviors, which consist of swarm-based algorithms and evolution-based algorithms. Swarm-based algorithms mimic cooperative behaviors of social nature, such as ACO and PSO. A swarm consists of many distinctive individuals and shows global social behaviors without central control. Individuals in a swarm are relatively simple whereas their collaboration can exert remarkable effect to handle different missions. Evolution-based algorithms are inspired from biological evolution. Biological operators including natural selection, crossover and mutation are introduced into algorithms to improve their search ability. Thus, these al-

Table 1.1: A list of various metaheuristic algorithms.

Biology-based algorithms	
Genetic algorithm (GA) [9]	Evolutionary programming (EP) [10]
Evolutionary strategy (ES) [19]	Differential evolution (DE) [11]
Harmony search algorithm (HSA) [20]	Artificial immune system (AIS) [21]
Particle swarm optimization (PSO) [15]	Bacterial foraging optimization (BFO) [22]
Cuckoo search algorithm (CS) [23]	Artificial bee colony algorithm (ABC) [24]
Ant colony optimization (ACO) [14]	Coral reef optimization (CRO) [25]
Firefly algorithm (FA) [26]	Teaching-learning based optimization (TLBO) [27]
Shuffled frog leaping algorithm (SFLA) [28]	Pigeon inspired optimization (PIO) [29]
Brain storm optimization (BSO) [16]	
Physics-based algorithms	
Simulated annealing (SA) [7]	Gravitational search algorithm (GSA) [17]
Chaotic optimization algorithm (COA) [30]	Intelligent water drops algorithm (IWD) [31]
Magnetic optimization algorithm (MOA) [32]	
Geography-based algorithms	
Tabu search algorithm (TS) [8]	Imperialistic competition algorithm (ICA) [18]

gorithms have learning, adaptive and evolutionary capabilities, such as GA, EP and DE. Physics-based algorithms are designed from physical phenomenon and rules, such as SA and GSA. Geography-based algorithms are to search space according to geography, such as TS and imperialistic competition algorithm (ICA) [18]. More algorithms can be referred in Table 1.1.

These algorithms have two crucial properties, i.e., exploration and exploitation. Exploration means that algorithms sufficiently search an entire space without trapping into local optima. Exploitation indicates that algorithms further optimize the search space in order to find a better solution. To obtain better results, the balance between exploration and exploitation should be considered. Consequently, numerous researchers focus on them to improve performances of algorithms.

1.2 Related work of EAs

1.2.1 Population structure

There are enormous complicated relationships among things or people in the real world, which constructs different kinds of characteristic networks called complex networks via the mutual collaboration and communication. In the last decades, the complex network as a hot topic has been studied extensively and developed quickly to apply for a great number of research fields, such as transportation network, Internet, mobile phone network, neural network and collaboration network [33–38]. The characteristics of complex networks

are dynamic, random and complicated, which can be reflected by the numerous nodes and edges in the networks. At present, the wide and main emergence among heterogeneous networks is the scale-free network [39], small-world network [40, 41], random network [42] and weighted network [43] which show the distinctive property for the structure of network, respectively. Therefore, massive researches concerned about complex network have demonstrated the structure of network can significantly influence the attribute of network measured by the degree of nodes, shortest paths, clustering coefficient or motifs [44–46].

In fact, the structure of network shows the general process of evolution of nodes and controls the entire property of network. Understanding and analyzing the essence of network is beneficial for better profoundly acquainting the evolutionary mechanism of nodes so as to enhance the attribute of other networks according to this mechanism or change this mechanism to improve itself. Based on this point of view, a majority of researchers have paid attention to the performance of complex network mostly modeled by the relationship among individuals in EAs [47–50].

EAs as population-based swarm intelligent approaches have been used and developed for addressing various optimization problems such as single objective optimization [51], multi-objective optimization [52] and combinatorial optimization [53, 54]. These wide applications indicate that EAs possess tremendous potential and play important roles in the field of optimization. Thus, their performances are persistently paid attention and investigated in order to further enhance their effectiveness and efficiency. Since EAs consist of individuals in the population, their population structures influence the organization and evolution of individuals so as to determine the performances of algorithms. Researches have demonstrated that a novel population structure can be beneficial for significantly improving the performances of EAs for resolving a number of optimization problems [55–57].

At present, several population structures have been found and integrated into EAs to strengthen their properties. A simple population topology is panmictic, where the interaction among individuals is randomly achieved during the execution of algorithm [48]. Although this kind of structure can facilitate the quick information interaction of all individuals in the population, its population diversity is low such that premature convergence is prone to occur. Hence, a population structure with neighborhood or other topologies are devised to handle this issue [58]. Due to the characteristics of new population structure, the information interaction among individuals is slowed so as to alleviate the stagnation of algorithm. The population structure with neighborhood is generally called cellular structure [59]. Its population is trimly arranged and each individual only interacts with

its neighborhood. Based on this kind of mechanism, the slow spread of information from neighborhood to neighborhood decreases the possibility of premature convergence. The distributed structure as a kind of topology is also proposed to improve the performances of EAs [56]. It divides a complete population into several smaller subpopulations. In each subpopulation, individuals are independently evolved. Migration strategies implement the information interaction from subpopulation to subpopulation. This structure not only explores diverse search ranges but also accomplishes the communication among individuals in different spaces such that population diversity can be maintained [60]. The cellular structure and distributed structure have been applied to GA, PSO and DE to enhance their performances [61–66].

Besides, a hierarchical structure which divides all individuals in the population into several levels/layers is also an effective topology [57]. In the same level/layer, each individual has an identical property. Different levels/layers play distinctive roles in the evolution of individuals. This structure can hierarchically hybridize the cellular structure and distributed structure so that the population can be evolved better according to both properties. In [67], a two-layered hierarchical structure was introduced into a backtracking search optimization algorithm to generate new individuals. Two layers adopted a multi-swarm learning strategy based on DE and teaching-learning-based optimization, respectively. In [68], a complete hierarchical multi-objective GA was proposed to address a transit network design problem from three levels, namely routes construction, networks design and multi-objective analysis. In [69], a hierarchical GA was used to optimize modular neural networks. It adopted four elitism methods to optimize multiple architectures of modular neural networks. A hierarchical PSO was designed to learn the fuzzy logic system's parameters of a Takagi-Sugeno fuzzy model [70]. It used a six-level hierarchy to decrease the complexity of learning method as well as enhance its computational efficiency and performance. In [71], a hierarchical operator was introduced into the grey wolf optimizer algorithm to change the hunting mechanism of grey wolf, where a fuzzy variant of hierarchical operator based on fuzzy logic was used to effectively improve the performance of algorithm. Thus, a hierarchical structure can also been demonstrated to change the distribution of individuals in EAs to strengthen their search performances [48, 49, 72]. Conclusively, these population topologies can implement the effective information interaction among individuals according to their distinctive architectures. Moreover, theoretical analyses with respect to population structures have been discussed to profoundly understand their inherent attribute and essence for refining the performances of EAs [44, 47, 50].

1.2.2 An overview of BSO

BSO proposed by Shi [16] is a novel swarm intelligent algorithm involving two features consisting of the cluster and evolution of population. The cluster of population reflects the performances of individuals in the search space of problem, while the evolution of population associates individuals in various clusters to produce new better individuals. These two procedures lead to the persistent convergence and divergence of solutions during the execution of BSO, which can ultimately acquire an optimal solution in the search space. For the original BSO, the k-means clustering algorithm is used to classify individuals into several classes. Subsequently, several different clustering strategies are devised to enhance the clustering performance, such as random grouping method [73], k-medians clustering algorithm [74] and so on. These clustering methods effectively decrease the computational complexity of BSO. Moreover, several variants of BSO are proposed on the basis of different ways to generate new individuals [51, 75, 76]. An adaptive step-size, new selection and generation strategy was proposed to enhance the performance of BSO [77]. The chaotic operation was added into BSO to avoid trapping into the premature convergence [78]. An advanced discussion mechanism including inter- and intra- cluster discussions, and a differential step method were introduced to improve the optimization of BSO [79]. The combination between BSO and other EAs such as SA [80] and DE [81] have demonstrated the effectiveness and efficiency of hybrid algorithms. Based on the characteristics of BSO, substantial problems have been addressed, such as multiobjective optimization, multimodal optimization, electric power systems and so on [82]. Thus, BSO possesses potential capacity to show superior performances for various optimization problems, while it is still in its infancy.

1.2.3 An overview of GSA

GSA is one of novel and effective EAs [17]. It attempts to use the gravitational force among individuals to implement the information interaction of population so as to find an optimal solution. This mechanism brings about exploration and exploitation abilities of GSA and guarantees both balance. Although GSA has the potential for obtaining an optimum, it usually may be trapped into the local optima due to its limited search ability [83]. To resolve this issue, various strategies and approaches have been proposed to further enhance the performance of GSA. The self-adaptive strategies are conducive to balancing exploration and exploitation abilities of GSA in the search process. In [84], each individual self-adaptively

chose two updating methods to find a better solution, where one achieved the communication among individuals and the other assisted individuals in getting out of the local optima. The chaotic strategies are effective for enhancing the search ability of GSA according to its ergodicity and stochasticity. In [85], GSA was improved by two chaotic strategies where one was to use chaotic sequences to replace random sequences and the other was to embed a chaotic local search to optimize solutions. Due to the effectiveness of chaos, multiple chaotic maps were incorporated into GSA to investigate their properties [86]. Hybrid strategies which combine several methods also show the distinct performance to address the disadvantage of GSA. The GSA combined with PSO to sufficiently utilize both characteristics to reinforce its exploration and exploitation process [87]. An improved GSA hybridized an orthogonal crossover to boost its exploration ability and convergence [88]. An opposition-based learning was incorporated into GSA to initialize its population and guide the evolution of individuals [89]. The quantum mechanics was added into the GSA to enhance its population diversity and help it escape from the premature convergence [90]. A novel alpha adjusting method based on agents' positions and fitness was proposed to address the premature convergence issue of GSA. Meanwhile, a boundary constraint based on stability conditions further improved the effect of alpha value for GSA [91]. A global best solution was used to guide the movement of agents according to the gravitational force in GSA, and the improved GSA showed a good performance on the benchmark functions and the training of feedforward neural networks [92]. Fuzzy GSAs based on fuzzy logic were proposed to resolve the optimal architecture of modular neural networks for the pattern recognition of medical images [93, 94]. A niching method was incorporated into GSA to control the interaction among individuals for multimodal optimization problems [95]. GSA with an offspring repair technique was introduced to solve dynamic constrained optimization problems [96]. A discrete GSA was proposed to solve 0-1 knapsack problem [97] and graph planarization problem [98]. The combination between GSA and PSO was used to optimize the optimal multi-robot path [99] and designs of complementary metal oxide semiconductor analog circuits [100]. These strategies and approaches effectively develop GSA and enhance its search property.

1.3 Contributions of this thesis

In this thesis, three kinds of EAs including DE, BSO and GSA are investigated in chapters 2, 3 and 4, respectively. Each chapter shows characteristics of population structure of

one algorithm. Thus, contributions of this thesis mainly consist of these three chapters, summarized as follows:

(1) Contributions of chapter 2 are: 1) PIN is proposed to depict the information interaction of populations in DE. 2) Comparative experiments are implemented to observe five candidate fitting models. 3) Goodness of fit demonstrates the cumulative frequency of degree in PIN satisfies a cumulative Poisson distribution. 4) Sensitivity analyses for nodes and λ are accomplished using different population sizes, dimensions, F and CR , respectively.

(2) Contributions of chapter 3 are: 1) Based on the perspective of population structure, PIN of BSO is established as a theoretically analytical approach to research its performance on functions with low, medium and high dimensions. 2) BSO whose frequency of average degree meets a power law distribution possesses the best performance on the functions with low dimension, whereas it can not completely obey a power law distribution in high dimension so as to obtain inferior performance. 3) Different parameters of BSO are investigated to illustrate that they can influence the population interaction in an inefficient way, thus the performance of algorithm can not be significantly improved. 4) Mutual effect among parameters is further analyzed by an orthogonal array to find the best combinatorial result for boosting the performance of BSO. 5) BSO is compared with DE and PSO to discuss their relationship between performances and characteristics of distributions.

(3) Contributions of chapter 4 are: 1) A three-layered hierarchical structure is proposed to guide the population interaction in HGSA from the perspective of population topology. 2) An improved gravitational constant is developed to extend the exploration period of HGSA such that HGSA has sufficient time and capacity to find an approximately optimal solution. 3) Two weighted coefficients with time are introduced to not only reinforce the relationship among three layers but also balance the transition between exploration and exploitation abilities in HGSA. 4) Extensive experiments are conducted and results suggest that HGSA can help individuals escape from the premature convergence or accelerate normal convergence.

Chapter 2

The research of differential evolution

2.1 Introduction

To analyze the characteristics of population in DE, this chapter proposes a population interaction network (PIN) to establish the connection among individuals of the population. Five models including exponential, gamma, logistic, poisson and normal distributions are used to fit for the cumulative frequency of degree in PIN. The goodness of fit is adopted to determine the fitting results. Subsequently, the number of nodes in PIN and the value of fitting rate parameter λ derived from poisson distribution are discussed based on different population sizes, dimensions, F and CR of DE.

2.2 Conventional DE

DE proposed by Storn and Price is a population-based global optimization algorithm. It has many advantages such as simple structure, good convergence, few control parameters and strong robustness for solving optimization problems [101]. The diagram of DE is shown in Fig. 2.1(a), including initialization, mutation, crossover and "one-to-one" selection. The initialization of each individual $X_i, i \in \{1, 2, \dots, NP\}$ in DE is described as follow:

$$X_i^d = X_i^{dl} + rand(0, 1) \cdot (X_i^{du} - X_i^{dl}), \quad (2.1)$$

where NP is the scale of population and $d \in \{1, 2, \dots, D\}$ indicates the dimension. du and dl represent the upper and lower bounds of X_i in d -th dimension, respectively.

The second process in DE is a differential mutation which can distinctively generate a

mutant vector to be an intermediate variable V_i of evolution according to:

$$V_i = X_{r1} + F \cdot (X_{r2} - X_{r3}), \quad (2.2)$$

where $r1, r2, r3 \in \{1, 2, \dots, NP\}$ are random indexes and $i \neq r1 \neq r2 \neq r3$. F is a constant factor indicating the degree of amplification. It should be noticed that the individual V_i uses the initialization in Eq. (1) to renew some genes which can not satisfy the condition of bounds in order to guarantee the effectiveness of solutions during the execution of evolution, i.e., $V_i^{dl} \leq V_i^d \leq V_i^{du}$.

The third process is crossover which can increase the diversity of new individuals U_i via combining the original individual X_i with the intermediate variable V_i , which is shown as follow:

$$U_i^d = \begin{cases} V_i^d & \text{if } rand(0, 1) \leq CR \text{ or } d = d_{rand} \\ X_i^d & \text{otherwise} \end{cases}, \quad (2.3)$$

where CR is a crossover control parameter and $d_{rand} \in [1, 2, \dots, D]$ indicates a random integer.

In the end of an iteration, the selection is implemented by comparing U_i with X_i using a greedy criterion to make the better individual reserve in the population for the next iteration. Through these processes, DE can gradually converge and ultimately derive the global optimum.

2.3 Population interaction network

Although DE has achieved tremendous successes on a great number of applications [102], most of their performances are evaluated empirically, implying a great lack of theoretical analysis. The rigorous analysis of DE is difficult, but such a theory can help to understand, design, and teach DE. Pioneering research works have been proposed to theoretically analyze EAs, including schema theory [103], Markov chains theory together with first hitting time [104], takeover time analysis [105], and statistical physics analysis [106]. Although these analytical methods are capable of addressing the fundamental issues in EAs involving convergence proofs, performance measures, and balance of exploration and exploitation, their applicability is limited because these methods are proposed for some specific EAs rather than all of them. Moreover, such theoretical analysis for DE is not yet explored to the best knowledge of the authors. Thus, an urgent and challenging task is to propose a gen-

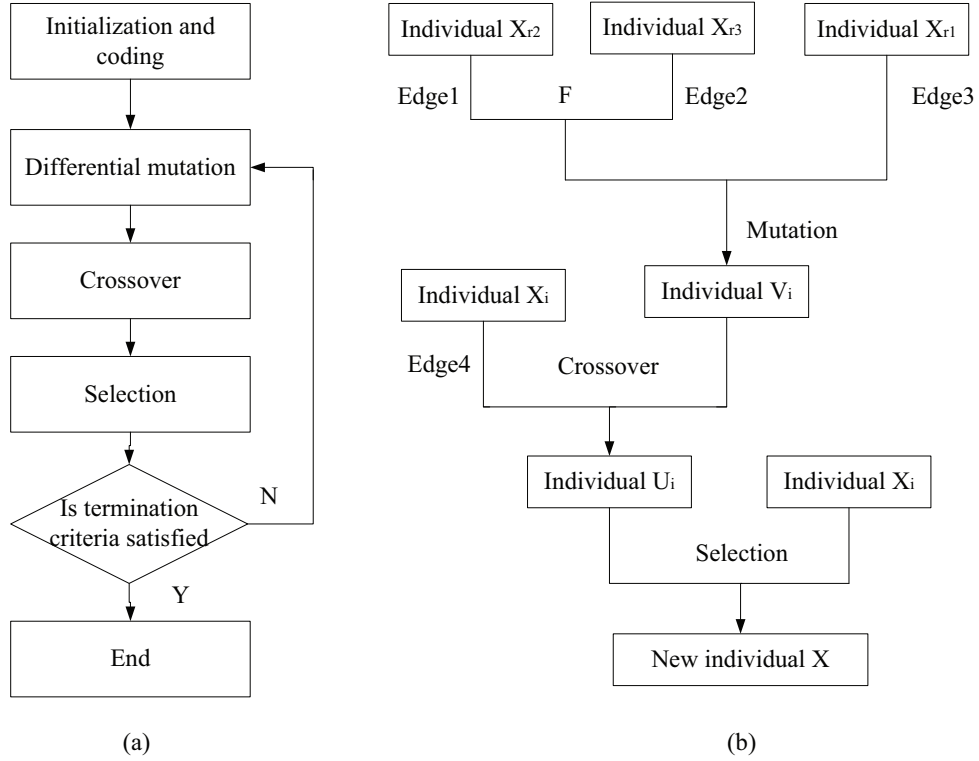


Figure 2.1: (a) The structured diagram, and (b) framework of population interaction network in DE.

eral analytical methodology which can deal with all DEs. It thus motivates us to propose the following population interaction network (PIN) to theoretically analyze DE.

In the complex network, generally, each individual represents a node and the relation between two individuals indicates an edge. The inherent regulation of some networks usually can be reflected by their nodes or edges [107–109]. In fact, these nodes and edges can explicitly exhibit the information interaction of evolutionary populations. The proposed PIN is used to investigate the property of population in DE. Since DE adopts the differential mutation, crossover and selection operations to generate new offsprings to replace those worse parents, the offsprings can obtain vital information from their parents during the evolutionary process. PIN not only captures such information but also illustrates the connection among them.

In DE, the new generated individual is associated with four current individuals which come from the mutation and crossover respectively. Fig. 2.1(b) shows the framework of PIN in DE. In the beginning, three randomly selected individuals X_{r1} , X_{r2} , X_{r3} are recombined to form an intermediate variable V_i through the mutation, hence there are four nodes and three edges. Then the intermediate variable V_i and the original individual X_i jointly

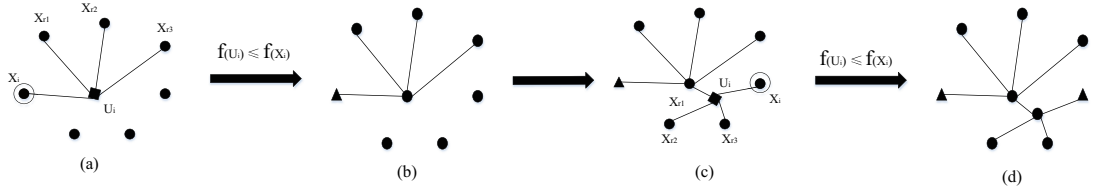


Figure 2.2: An illustrative graph of population interaction network in DE.

generate an individual U_i via the crossover. The resultant nodes and edges increase two, respectively. Finally, the selection determines the next offspring between individuals U_i and X_i without generating any new nodes and edges. In this way, we just consider the successful evolutionary process in order to observe the effective population interaction and information dissemination. To be specific, the individual U_i , which is superior to the original individual X_i , should be primarily taken into account. Meanwhile, to simplify the structure of network, we neglect the nodes and edges formed by the intermediate variables, and reserve the actual individuals and their relationship. Considering the fact that intermediate variables which only play a connecting role in constructing new individuals is meaningless, the parents and offsprings possess the entire information. In other words, when DE successfully evolves, the overall process involves five individuals composed of $X_{r1}, X_{r2}, X_{r3}, X_i$ and U_i . Consequently, each evolution can generate one new node and four new edges. Until the end of algorithm, the whole recorded populations are able to establish a complex network, which shows the information interaction and population topology.

Fig. 2.2 illustratively depicts the construction of PIN involving the connection of edges and evolution of vertices. Circle, square and triangle indicate current, new formed and old substituted vertices, respectively. The concrete procedure of construction is listed as follows:

(1) DE randomly selects three vertices X_{r1}, X_{r2}, X_{r3} to connect with new formed vertex U_i according to the mutation operation;

(2) The original vertex X_i connects with U_i in terms of the crossover operation, shown as Fig. 2.2(a);

(3) If $f(U_i) \leq f(X_i)$, new vertex U_i substitutes original vertex X_i in current population due to the selection operation, exhibited as Fig. 2.2(b);

(4) Repeat procedure (1)-(3) (i.e., Figs. 2.2(c) and (d)) to eventually reach the termination of algorithm and obtain the topology of PIN.

2.4 Experiment and analysis

To evaluate the characteristics of population interaction in conventional DE, twelve benchmark functions are adopted in Table 2.1, including six standard benchmark functions commonly tested on numerous optimization approaches such as GA, PSO and DE [110–112] to analyze and assess their optimization performances and six CEC'05 benchmark functions [113] which further enhance the complexity of functions via shift or rotation to measure the properties of algorithms.

In Table 2.1, Sphere, Rosenbrock, F_1 , F_2 and F_4 are unimodal functions. Griewank, Rastrigin, Schwefel, Ackley, F_6 , F_8 and F_9 are multimodal functions with many local minima, and the number of these local minima increases exponentially according to the dimension of functions. Sphere function has a global optimum due to its continuous and convex property. Rosenbrock function is difficult to converge into the global optimum since the global optimum is located in a long, narrow and parabolic valley. Ackley function has an almost flat outer range and a deep hole in the center, thus it has not only a global optimum but also a risk to enable algorithms to trap into many local optima. Griewank function has a global optimum and massive widespread local optima which overall show a convex shape. Rastrigin function possesses several regularly distributed local optima and a global optimum. It is complicated and difficult for many algorithms to resolve Schwefel function because the complex structure of function may enable algorithms to converge into a local optimum by mistake rather than its global optimum. F_1 is a separable function, whereas F_2 and F_4 are non-separable functions without and with noise, respectively. F_6 is a non-separable function which has a similar valley with Rosenbrock function. F_8 is a rotated and non-separable function whose global optimum lies on the bound. F_9 has separable characteristic and a great deal of local optima. More information regarding these functions can be referred in [113, 114]. Using these functions which have different structures can eliminate the misgiving where the population interaction of DE only takes place in particular occasions. Then, the parameters of DE are set as follows. The essential factors $F = 0.5$ and $CR = 0.9$ are referred in the literatures [101, 111]. Both the dimension of functions and the population sizes are 30. The maximum number of iterations is 5000. All the experiments are implemented by Matlab on a personal PC.

The performance of DE for twelve functions is shown in Table 2.2. By 50 runs for each function, the minimum, median, maximum, mean and standard deviation of best fitness values are attained, respectively. The corresponding box-and-whisker diagram is plotted in Fig. 2.3. It is found from Table 2.2 and Fig. 2.3 that DE has different performance on

Table 2.1: The concrete description of twelve benchmark functions.

Function	Definition	Domain	Global minimum
Sphere	$f(x) = \sum_{i=1}^D x_i^2$	$[-100, 100]$	0
Rosenbrock	$f(x) = \sum_{i=1}^{D-1} [100(x_{i+1} - x_i^2)^2 + (x_i - 1)^2]$	$[-30, 30]$	0
Griewank	$f(x) = \frac{1}{4000} \sum_{i=1}^D x_i^2 - \prod_{i=1}^D \cos(\frac{x_i}{\sqrt{i}}) + 1$	$[-600, 600]$	0
Rastrigin	$f(x) = 10D + \sum_{i=1}^D [x_i^2 - 10 \cos(2\pi x_i)]$	$[-5.12, 5.12]$	0
Schwefel	$f(x) = 418.9829D - \sum_{i=1}^D x_i \sin(\sqrt{ x_i })$	$[-500, 500]$	0
Ackley	$f(x) = -20 \exp(-0.2 \sqrt{\frac{1}{D} \sum_{i=1}^D x_i^2})$	$[-32, 32]$	0
F_1	$-\exp(\frac{1}{D} \sum_{i=1}^D \cos(2\pi x_i)) + 20 + \exp(1)$	$[-100, 100]$	-450
F_2	$f(x) = \sum_{i=1}^D z_i^2 + f_{bias_1}$	$[-100, 100]$	-450
F_4	$f(x) = \sum_{i=1}^D (\sum_{j=1}^i z_j)^2 + f_{bias_2}$	$[-100, 100]$	-450
F_6	$f(x) = (\sum_{i=1}^D (\sum_{j=1}^i z_j)^2)(1 + 0.4 N(0, 1)) + f_{bias_4}$	$[-100, 100]$	390
F_8	$f(x) = \sum_{i=1}^{D-1} (100(z_i^2 - z_{i+1})^2 + (z_i - 1)^2) + f_{bias_6}$	$[-100, 100]$	-140
F_9	$f(x) = -20 \exp(-0.2 \sqrt{\frac{1}{D} \sum_{i=1}^D z_i^2})$ $-\exp(\frac{1}{D} \sum_{i=1}^D \cos(2\pi z_i)) + 20 + e + f_{bias_8}$ $f(x) = \sum_{i=1}^D (z_i^2 - 10 \cos(2\pi z_i) + 10) + f_{bias_9}$	$[-32, 32]$ $[-5, 5]$	-330

Table 2.2: The best fitness value obtained by DE on twelve benchmark functions.

Function	Minimum	Median	Maximum	Mean(\pm Std)
Griewank	0	0.04	0.66	0.08(\pm 0.12)
Rastrigin	6.97	19.06	50.94	20.14(\pm 7.91)
Rosenbrock	1.00	96.72	13939.84	1062.66(\pm 2504.11)
Schwefel	592.19	1423.04	2718.73	1458.09(\pm 474.12)
Sphere	1.80E-21	0.01	29.68	2.09(\pm 5.66)
Ackley	4.19E-07	1.16	3.34	1.07(\pm 0.87)
F_1	-450	-449.99	18.17	-434.31(\pm 68.97)
F_2	-450	-449.16	356.31	-395.52(\pm 149.84)
F_4	-449.25	-363.67	626.42	-254.01(\pm 257.16)
F_6	485.27	3.99E+05	2.05E+08	9.35E+06(\pm 3.27E+07)
F_8	-119.15	-119.02	-118.95	-119.02(\pm 0.04)
F_9	-320.05	-304.11	-279.10	-302.08(\pm 8.49)

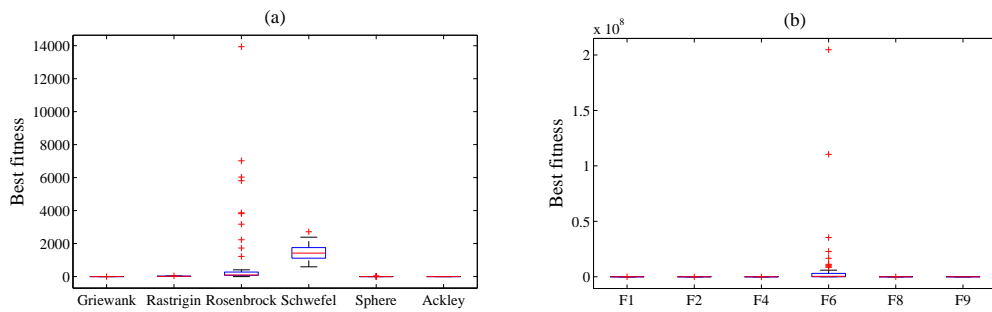


Figure 2.3: The box-and-whisker diagram of best fitness of DE on six standard benchmark functions and six CEC'05 benchmark functions.

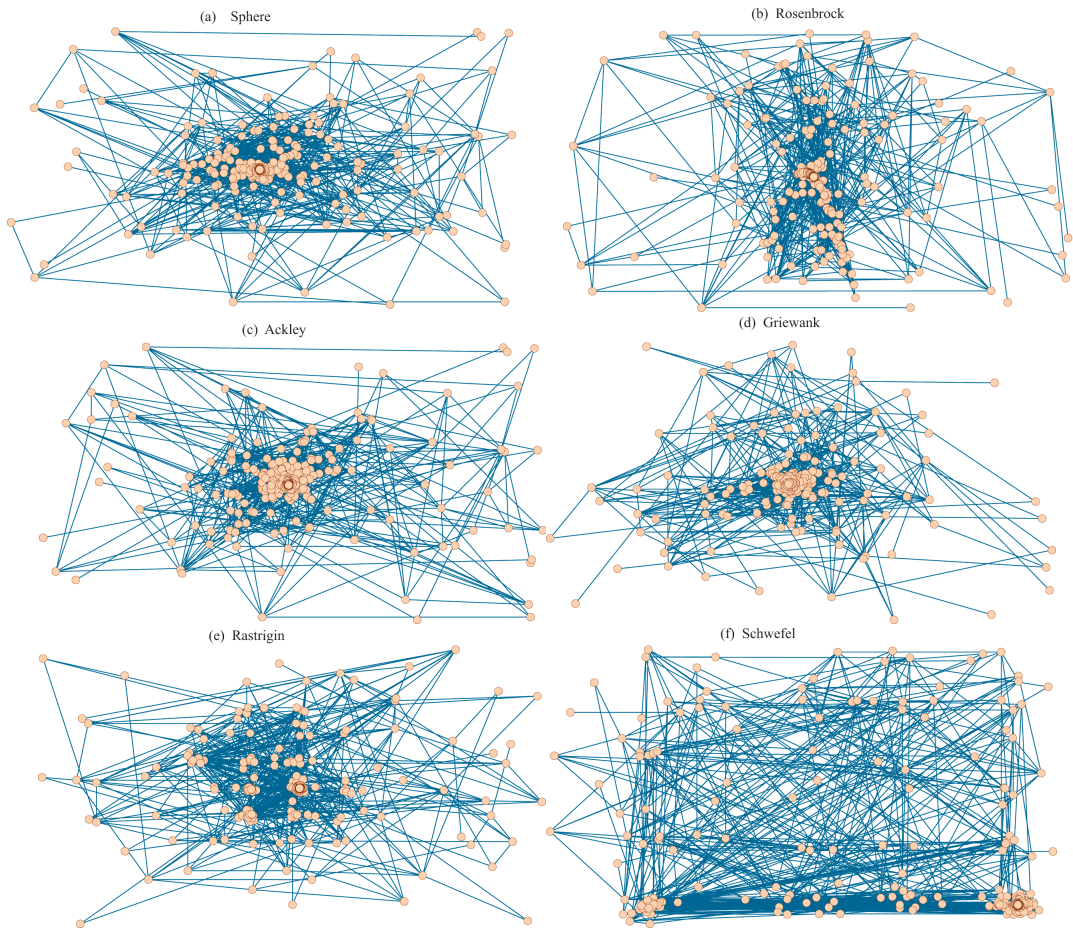


Figure 2.4: The 2-dimensional sketch of PIN of DE on six standard benchmark functions.

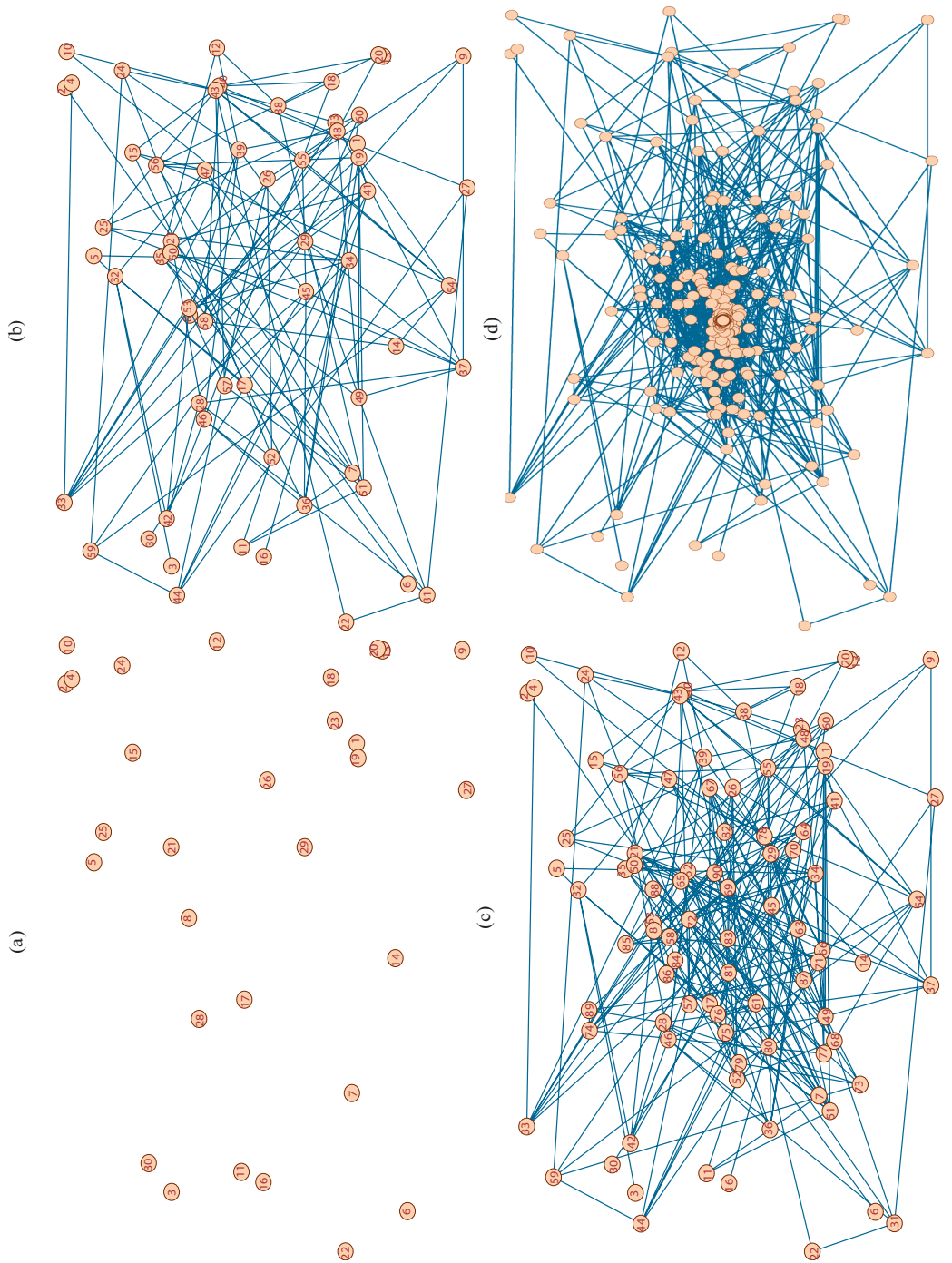


Figure 2.5: The general changing process of PIN of DE on Sphere function.

different functions, thus indicating that the performance of DE is problem-dependent. Since the dimension is 30 which has enhanced the computational complexity, the best fitness value is difficult to be acquired. On standard benchmark functions, the performance of DE is superior for Griewank, Sphere and Ackley. However, the weak circumstance occurs on the other functions, especially Rosenbrock and Schwefel. On CEC'05 benchmark functions, even though the results regarding F_1 , F_8 and F_9 are relatively preferable comparing with those obtained in F_2 , F_4 and F_6 , the overall performance of DE is inferior to that on standard functions. The results suggest that: (1) high dimension changes the structure of standard functions and significantly influences Rastrigin, Rosenbrock and Schwefel; (2) the search mechanism of DE is proper for resolving Sphere, Ackley and Griewank with high dimension; (3) CEC'05 benchmark functions with high dimension intensify complexity of functions to notably interfere with the search performance of DE.

In order to intuitively observe information interaction among individuals of the population, Fig. 2.4 is plotted to show the planar PIN using a 2-dimensional sketch. The coordinate of node depends on the components of solution, and the values of the first two dimensions (i.e., X_i^1 and X_i^2) are used to plot the figure. From Figs. 2.4(a)-(e), we can find that nodes finally converge at the center, illustrating individuals constantly evolve and solutions are progressively improved. Nevertheless, Fig. 2.4(f) displays more nodes locate at the right corner rather than the center where the global minimal solution exists. This is because the components of optimal solution (both X_i^1 and X_i^2) in Figs. 2.4(a)-(e) are equal or approximate to 0, whereas in Schwefel, the solutions are trapped around the search boundaries. Fig. 2.5 is plotted to be an example for showing a general changing process of PIN on Sphere function. Fig. 2.5(a) indicates thirty initial individuals. Fig. 2.5(b) shows thirty new generated individuals and the connection between new and old ones. Fig. 2.5(c) continues to exhibit new formed individuals over iterations and Fig. 2.5(d) is the ultimate full-connection graph of PIN. Thus, Figs. 2.4 and 2.5 distinctly demonstrate the emergence of PIN and relation among individuals in the evolutionary process.

2.4.1 Fitting results for PIN

The complex network of DE is constructed by PIN, which indicates the relationship between the degree of nodes and its cumulative distribution. The degree of a node represents the number of nodes connecting with this node, namely the number of edges. To observe the property of PIN, five models involving exponential, gamma, logistic, poisson and normal are utilized to fit via the maximum likelihood estimation. Since the fitting results are

similar on both six standard benchmark functions and six CEC'05 benchmark functions, Fig. 2.6 only shows the fitting results regarding six standard benchmark functions. The horizontal axis is the degree of nodes in a non-direct graph constituted by PIN and the vertical axis is CDF which depicts the cumulative distribution function of degree. From this figure, we can notice that, although the total degree of PIN is different on six functions, the general distribution of respective CDF is similar. It demonstrates that the population interaction of DE is common and appears to be uninfluenced by the structure of functions. Its frequency is nearly 0 when the degree is less than 5 or greater than 20, whereas the CDF obviously increases when the degree is in the interval [5, 20]. Furthermore, the significant increase of CDF mainly occurs in the interval [5, 7]. Since each evolutionary node generates 4 edges, it has a high potential to be the parent for next evolution. Thus, the frequency of degree mostly concentrating on the interval [5, 7] suggests a new node can become a parent with 1, 2 and 3 times, respectively. Afterwards, the frequency of degree gradually declines, suggesting that it is difficult for a new node to sustain a parent within numerous times. In other words, most of nodes need to be evolved continuously in order to enhance the quality of solution. As for those nodes whose degree are less than 5, they absolutely belong to initial individuals which are firstly evolved.

Fig. 2.6 can distinctly show the exponential distribution is not eligible for the CDF of PIN and other models have similar fitting results. To further discern the characteristics regarding the CDF of PIN, the goodness of fit is used to assess which model the CDF of PIN accords with. For analyzing the goodness-of-fit statistics, we adopt the sum of square due to error (*SSE*) and R-square (R^2) to compare their differences. The *SSE*, which measures the total square deviation from the fit to the original data, is described as follow:

$$SSE = \sum_{i=1}^n (\hat{y}_i - y_i)^2, \quad (2.4)$$

where \hat{y}_i and y_i indicate the fit and original data respectively. The *SSE* closer to 0 means the smaller fitting error. The R^2 indicates the square of the correlation between the fit and original data, explaining the level of the fitting results. It is defined as the ratio of the sum of squares of the regression (*SSR*) and the total sum of squares (*SST*), where $SSR = \sum_{i=1}^n (\hat{y}_i - \bar{y})^2$ and $SST = \sum_{i=1}^n (y_i - \bar{y})^2$. \bar{y} is the mean of the original data. Hence, R^2 is expressed as follow:

$$R^2 = \frac{SSR}{SST} = \frac{\sum_{i=1}^n (\hat{y}_i - \bar{y})^2}{\sum_{i=1}^n (y_i - \bar{y})^2}. \quad (2.5)$$

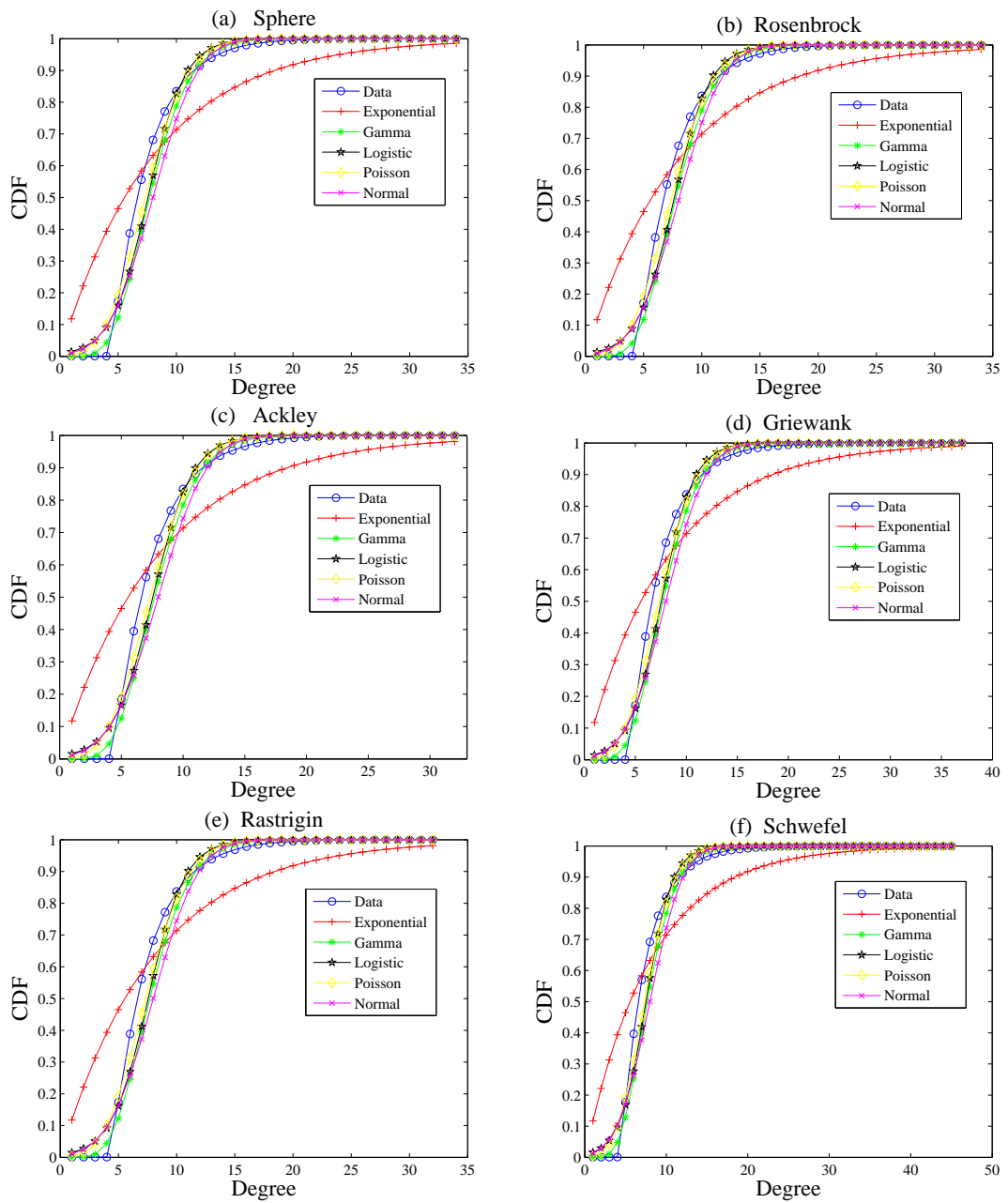


Figure 2.6: The cumulative distribution graphs between the original data and fitting models of DE.

The R^2 closer to 1 indicates the fitting result is better. The goodness of fit with five models on twelve functions calculated by these two methods is listed in Table 2.3. From Table 2.3, we can observe that the SSE of exponential is the maximum and its R^2 is the minimum. It corresponds with the phenomenon that Fig. 2.6 reveals, which shows significant error between the exponential and original data. Additionally, despite Fig. 2.6 unsuccessfully distinguishes the relationship between other four models and the CDF of PIN, the poisson exhibits the best fitting performance according to its smallest SSE and greatest R^2 on the whole functions in Table 2.3. Consequently, the CDF of PIN in DE can be appropriately regarded as a cumulative poisson distribution.

To better implement a cumulative poisson distribution, the maximum likelihood estimation of poisson distribution is specifically described as follows:

(1) The probability density function of poisson distribution is $f(x, \lambda) = \frac{\lambda^x}{x!} e^{-\lambda}$, $x = 0, 1, 2, \dots$;

(2) The likelihood function is formulated by $L(\lambda) = \prod_{i=1}^n f(x_i, \lambda) = \prod_{i=1}^n \frac{\lambda^{x_i}}{x_i!} e^{-\lambda}$;

(3) Then the log-likelihood equation is obtained, expressed as $\ln L(\lambda) = \ln \lambda^{\sum_{i=1}^n x_i} - \ln \prod_{i=1}^n x_i! - n\lambda$;

(4) Setting $\frac{\partial \ln L(\lambda)}{\partial \lambda} = 0$, the estimated value of λ is derived finally, which is shown as $\lambda = \frac{1}{n} \sum_{i=1}^n x_i = \bar{x}$.

2.4.2 Analysis for parameters

After determining that the cumulative poisson distribution is proper for the CDF of PIN in DE, we discuss about the nodes of PIN and the rate parameter λ of the fitted poisson model under different parameters. Fig. 2.7 shows the experimental results regarding diverse sizes of populations, dimensions of functions, control parameters F and CR in DE on six standard benchmark functions. In each sub-figure, the values of other parameters are the same as above mention except for the respective analytical parameters.

Firstly, four populations whose sizes are 10, 30, 50 and 100 are investigated. Fig. 2.7(a) indicates the nodes gradually increase in terms of the population size, whereas two exceptions, where the nodes decrease, occur on Rastrigin and Schwefel since a number of populations unsuitable for their complex functional structures may influence evolutionary process to generate less new individuals. The corresponding value of λ decreases and two exceptions show the notable decline in Fig. 2.7(b). This means the frequency of each degree diminishes, illustrating the weak interaction of nodes.

Secondly, Figs. 2.7(c) and (d) describe the affect of 2, 10, 30 and 50 dimensions for

Table 2.3: Fitting results of twelve functions with five models.

Function	Exponential		Gamma		Logistic		Poisson		Normal	
	SSE	R^2	SSE	R^2	SSE	R^2	SSE	R^2	SSE	R^2
Sphere	0.604	0.850	0.082	0.980	0.067	0.983	0.042	0.990	0.127	0.969
Rosenbrock	0.609	0.849	0.079	0.981	0.065	0.984	0.039	0.990	0.121	0.970
Ackley	0.588	0.849	0.084	0.979	0.069	0.982	0.044	0.989	0.131	0.966
Griewank	0.603	0.854	0.085	0.980	0.068	0.984	0.045	0.989	0.133	0.968
Rastrigin	0.601	0.847	0.084	0.979	0.068	0.983	0.044	0.989	0.131	0.967
Schwefel	0.592	0.864	0.090	0.979	0.073	0.983	0.050	0.989	0.144	0.967
F_1	0.603	0.863	0.086	0.981	0.069	0.984	0.045	0.990	0.134	0.970
F_2	0.588	0.853	0.077	0.981	0.065	0.984	0.037	0.991	0.118	0.971
F_4	0.541	0.858	0.077	0.980	0.070	0.982	0.043	0.989	0.126	0.967
F_6	0.606	0.840	0.079	0.979	0.065	0.983	0.039	0.990	0.122	0.968
F_8	0.404	0.864	0.044	0.985	0.048	0.984	0.022	0.993	0.091	0.969
F_9	0.601	0.864	0.089	0.980	0.071	0.984	0.049	0.989	0.143	0.968

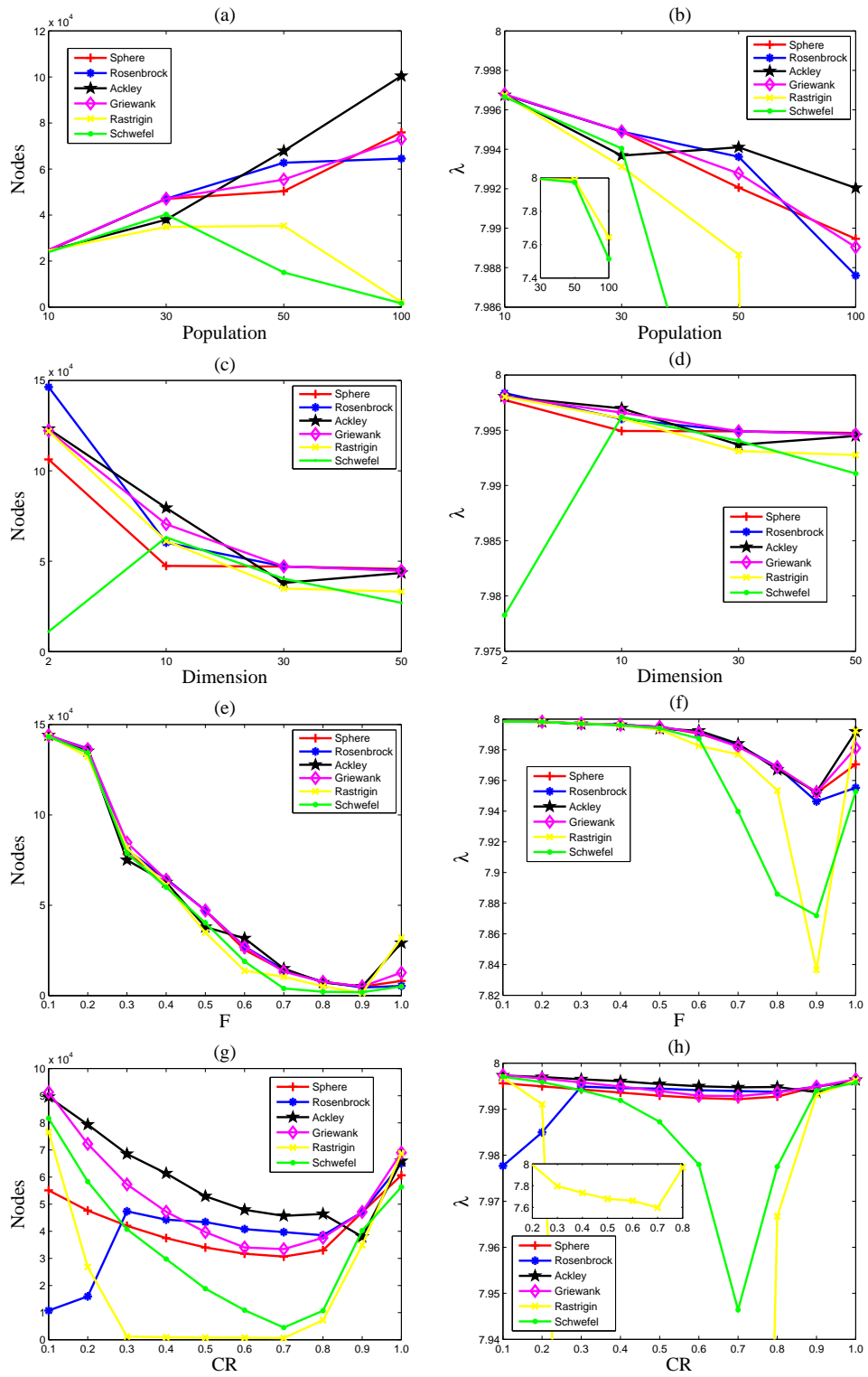


Figure 2.7: The number of nodes and the value of λ under DE with different parameters.

nodes and λ . Due to the special functional structure, the least nodes are formed on Schwefel with 2 dimensions. Except for this, the number of nodes and the value of λ decrease when the dimension of the function increases. The dimension enhances the computational complexity of algorithm, thereby reducing generation and connection of new individuals.

Thirdly, F in the interval $[0.1, 1.0]$ is studied. Fig. 2.7(e) denotes the number of nodes gradually declines from intervals 0.1 to 0.9 and slightly ascends on 1.0. Meanwhile, the λ shows the similar circumstances in Fig. 2.7(f), where the value of λ on Rastrigin and Schwefel sharply descends when $F = 0.9$. It seems to be that the smaller F prompts connections between two individuals and constantly implements the evolutionary process, and $F = 0.9$ indicates that it is ineligible to conduct the population interaction for DE.

Finally, CR located in the interval $[0.1, 1.0]$ is analyzed. Figs. 2.7(g) and (h) display a majority of nodes and λ firstly reduce and later increase, suggesting CR plays an important role in controlling the number of nodes. Especially on Rastrigin and Schwefel, the number of nodes and the corresponding value of λ significantly decline on the interval $[0.2, 0.7]$. Afterwards, they quickly rise to maintain identical characteristics with other functions. This is because the greater CR can efficiently recombine the information among individuals and thus to generate better solutions. The smaller CR also leads to the generation of new individuals but the quality of solution is inferior. As for the median interval, CR might not provide effective information for population interaction. Thus, the evolutionary nodes relatively decrease. Furthermore, the structure of Rastrigin and Schwefel is sensitive for solutions obtained by different CR . Accordingly, their nodes and λ have distinctive changes.

In addition, it is interesting to point out that the observations derived from PIN are roughly consistently with those empirically obtained from other researches [115].

2.5 Conclusions

In this chapter, a population interaction network (PIN) is proposed to analyze the complex network in DE. Via calculating the original CDF of PIN on twelve benchmark functions, we find that the whole original CDFs are similar, suggesting that the characteristics of population interaction in DE are common. Moreover, these CDFs show that the frequency of degree mostly focuses on the interval $[5, 7]$, indicating a majority of individuals are evolved within three generations of being parents. The goodness of fit including the sum of square due to error and R-square is utilized to measure the fitting models. The fitting results

demonstrate that the CDF of PIN generally accords with a cumulative poisson distribution.

Furthermore, parameters are investigated to illustrate the number of nodes and the corresponding rate parameter λ . We find that (1) most of nodes increase along with the population size except for two special functions, and the corresponding value of λ decreases. The decline of the value of λ indicates that the frequency of degree reduces, i.e., the interaction of population attenuates. (2) The high dimension reduces the generation of nodes and the value of λ . (3) Since the small F effectively motivates communication among individuals, the number of nodes and the value of λ are great. (4) The greater CR is beneficial for taking advantage of useful information among individuals to produce new solutions, showing a prospective method for enhancing the number of nodes and the value of λ .

Chapter 3

The research of brain storm optimization

3.1 Introduction

In this chapter, to investigate the inherent property of BSO from the point of view of population structure, a PIN is constructed to analyze the relationship between the evolutionary process of individuals and the performance of algorithm. Four experiments are implemented to show the experimental results in different dimensions, parameters, combinatorial parameter settings and related algorithms, respectively. The first experiment demonstrates the emergence of power law distribution in the PIN for thirty one functions with 2 dimension rather than 10 and 30 dimensions and the performance of BSO is the best in 2 dimension, suggesting the power law distribution represents the good performance of BSO and effectively guides the evolution of individuals in the functions with low dimension. The second experiment illustrates the influence of different parameters on the PIN with the power law distribution. The value of each parameter in BSO can change the power exponent γ of power law distribution so as to affect the population interaction of algorithm. The third experiment analyzes the interactive influence among parameters to obtain the best combinatorial parameter setting for improving the performance of BSO. The last experiment discusses the characteristics of distributions and performances among BSO, DE and PSO to demonstrate that the power law distribution is a better method of population interaction for enhancing the property of BSO.

3.2 Conventional BSO

The BSO is inspired by the interactive action of human beings called the brainstorming process in a group. The mutual collaboration results in various fantastic ideas which can effectively resolve a hard problem. Based on this mechanism, BSO is used to handle a great deal of combinatorial optimization problems [82] due to its clustering and evolutionary characteristics. In BSO, there are two essential process including divergence and convergence of solutions. Solutions are obtained by several classes, and better solutions are generated by the evolution of current solutions. Through the continuous transformation of solutions between divergence and convergence, the best solution will be derived finally in the whole search range.

3.2.1 Basic principle of BSO

It is an original innovation that the BSO combines the swarm intelligence with clustering algorithm to optimize problems. All the solutions are divided into several classes, and new solutions are formed to replace previous solutions from one or two classes. Subsequently, the whole solutions are classified afresh. This operation not only implements the evolution of solutions in different space to transmit information from one class to other classes but also enhances both the exploration of algorithm and the diversity of solutions so that BSO can exploit the eventual search range when those classes maintain invariant. The original BSO primarily contains four procedures: the classification of individuals, the replacement of cluster center, the generation of new individuals and the selection between previous and new individuals.

(A) The classification of individuals: The original BSO utilizes the k-means clustering algorithm to classify individuals in current population into several classes. Individuals in the same class have similar characteristics, and each class indicates a search range. Individuals are continually evolved, in the meantime, the distribution of individuals also changes towards smaller and smaller range according to the clustering algorithm over iterations during the execution of algorithm. Therefore, for a problem, the clustering results can show the distribution of individuals in search space, meaning the landscape of this problem.

(B) The replacement of cluster center: To enhance the diversity of population, the random replacement is adopted to substitute a cluster center via a randomly generated individual in terms of a probability value p_c . This operation is beneficial for the algorithm to avoid trapping into the premature convergence, which is similar to the mutation of cluster

center.

(C) The generation of new individuals: After the clustering and replacing process, new individuals are generated by selecting one or two individuals to be the parents. A probability value p_g controls the number of selected individuals. In fact, when one individual is used to generate new individual, the exploitation capacity of BSO plays an important role since new individual needs to make use of information of the parent to evolve. Nevertheless, if two individuals are applied for generating new individual, the exploration capacity of BSO influences the quality of offspring owing to the uncertainty of information of the diverse parents. In addition to the p_g , there are another two parameters p_{c1} and p_{c2} which confirm the selected individuals from one and two cluster centers, respectively. To be specific, new generated individual from one cluster center or one general individual is decided by p_{c1} . Similarly, p_{c2} determines new generated individual from two cluster centers or two general individuals. The utilization of cluster centers can accelerate the convergence of algorithm, whereas the employment of general individuals can expand the search space to enhance the diversity of population. After determining the selected individuals, new individual begins to form according to the following formulas:

$$U_n^d = X_s^d + N(\mu, \sigma^2) \cdot \xi(t), \quad (3.1)$$

$$\xi(t) = \text{logsig}\left(\frac{0.5 \times T - t}{k}\right) \cdot \text{rand}(0, 1), \quad (3.2)$$

where U_n^d and X_s^d indicate the d -th dimension of new and selected individuals, respectively. It should be noted that X_s means the combination of both if two selected individuals are used. $N(\mu, \sigma^2)$ is a Gaussian distribution with mean μ and variance σ^2 . $\xi(t)$ is a step size function which determines the direction of evolution. $\text{logsig}()$ denotes a logarithmic sigmoid transfer function. T and t represent the maximum and current number of iteration, respectively. k is a constant. $\text{rand}(0, 1)$ is a random variable uniformly distributed in the interval $(0,1)$. These two formulas can effectively guide selected individuals to generate new individuals with nice quality.

(D) The selection between previous and new individuals: The comparison between previous and new individuals is manipulated to select which possesses better performance. If new individual is superior to previous one, the replacement is operated to reserve new individual. Otherwise, there is no operation. The selection operation guarantees the successful evolution of individuals over iterations and outputs the whole individuals as the next population.

Algorithm 1: BSO

Input: Parameters $p, c, p_c, p_g, p_{c1}, p_{c2}, k, T$

Output: The optimal solution

```
1 Initialization:  $p$  individuals are randomly generated to be the initial population and
   assessed;
2 while the termination criterion is not satisfied do
3   Classify  $p$  individuals into  $c$  classes via a k-means clustering algorithm;
4   Find the best individual in each class to be a cluster center;
5   if  $\text{rand}(0, 1) < p_c$  then
6     An individual is randomly generated to randomly replace a cluster center;
7   for  $i = 1$  to  $p$  do
8     if  $\text{rand}(0, 1) < p_g$  then
9       Select a class by the roulette;
10      if  $\text{rand}(0, 1) < p_{c1}$  then
11        Select the cluster center in this class to generate new individual
12        according to Eqs. (3.1) and (3.2);
13      else
14        Randomly select a general individual in this class to generate new
15        individual according to Eqs. (3.1) and (3.2);
16      else
17        Randomly select two classes;
18        if  $\text{rand}(0, 1) < p_{c2}$  then
19          Select two cluster centers to incorporate to generate new individual
20          according to Eqs. (3.1) and (3.2);
21        else
22          Randomly select one general individual in each class and two
23          individuals are incorporated to generate new individual according to
24          Eqs. (3.1) and (3.2);
25      The selection is executed to retain the better individual;
26   Iteration +1;
27   Output the best solution;
28 return
```

Based on the above procedures, BSO can finally acquire the optimal solution with the continuous iterations. The entire process of BSO is shown in Algorithm 1.

3.2.2 Characteristics of BSO

Swarm intelligent algorithms possess two capacities, i.e., exploration and exploitation, so as to optimize the search space of problem. In BSO, these capacities are embodied by the convergence and divergence of individuals. To be specific, convergence means that massive individuals gather on the same position whereas divergence signifies numerous individuals are distributed on different positions. Thus, the convergence characteristic is beneficial for exploiting current search range of solutions and the divergence characteristic is conducive to exploring new different search space to find a possibly better solution. BSO uses a k-means clustering algorithm to classify individuals into different classes according to their distances in order to implement the convergence operation. The divergence operation is that new individuals are generated by the previous individuals in one or two classes. New individuals correspond to new underlying search space, thereby implying that better solutions exist in a more promising region.

BSO has several merits according to its basic principle as follows: (1) A novel clustering method can categorize the whole population into several sub-populations so as to effectively manage each individual's distribution in search space. (2) The generation of individuals depends on one or two general or best individuals. This operation not only enhances the diversity of population but also guarantees the speed of convergence, suggesting an effective balance between the exploration and exploitation of algorithm. (3) A number of applications have demonstrated that BSO has the potential practicability and expansibility for various optimization and real-world problems [82].

However, apart from its advantages, BSO also has some drawbacks which need to be refined as follows: (1) The number of parameters in BSO is too many to enhance its robustness and performance. (2) The k-means clustering algorithm based on distance is restrained on a high dimension of problem to cause the inferior performance. (3) The k-means is a user-defined clustering algorithm and its computational efficiency is low. Consequently, there is a big space for BSO to enhance its performance according to the above characteristics. New theoretical analyses or new strategies should be proposed to develop the BSO better in the future works.

3.3 Construction of PIN

BSO have successfully resolved various optimization problems [82]. The fact verifies BSO is a promising and potential algorithm applied for diverse kinds of problems. Therefore, enhancing the property of BSO is crucial for obtaining nice optimized results. A good result usually indicates the validity and capacity of algorithm for handling problems. A theoretical analysis is beneficial for interpreting the essence of algorithm and discovering certain methods to overcome its drawback so as to better develop the performance of algorithm. Nowadays, there are a few literatures for investigating the performance of BSO in terms of its parameters [116, 117]. It is obvious that the value of parameters determine the property of algorithm. However, the actual research regarding systematically analyzing the inherent attribute of BSO is deficient. As a matter of fact, the theoretical analyses are helpful and vital for understanding and modifying the characteristics of BSO, which can provide a guideline to implement the improvement of algorithm. For this purpose, we utilize the PIN [47] to establish the relationship among individuals in BSO to explore and analyze the concrete phenomenon occurring in the population structure.

Population structures are built by the existing vertices and edges which represent individuals and connection among individuals, respectively. To characterize the population structures is an essential measure for comparing and analyzing their properties. Generally, the population topology shows the ultimate outcome of continuous evolution of populations and evidently influences the performance of algorithm [48, 118]. The reason why the population topology leads to the certain result is that the knowledge carried by individuals is transmitted by a specific evolutionary mechanism, at the same time, the interaction of individuals (i.e., the update of knowledge) is achieved. The eventual graph of population structure exhibits the result of transmission of knowledge in the whole populations and certain regulation. The PIN describes the interaction of individuals. In BSO, each individual can be regarded as a vertex and the update among individuals indicates the generation of edges. Although BSO uses the clustering method to classify individuals, the knowledge of individuals is still effectively applied for delivering. Taking advantage of PIN can acquire both the intrinsic communication of knowledge and the characteristic of population structure.

The PIN used to construct the interaction of population in BSO is described as follows: The initial individuals indicate the original vertices, and there is no edge among them. Then the clustering algorithm classifies individuals and the best individual in each class is reserved, which is unrelated to the interaction of individuals. Thus, the operation of PIN

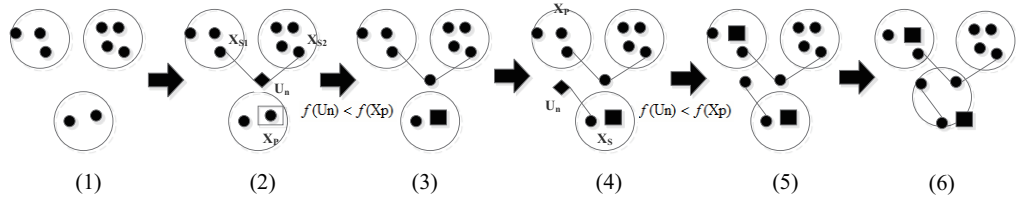


Figure 3.1: A descriptive diagram of PIN in BSO.

is not considered in these two process. Next, the behavior of changing the cluster center can be regarded as the mutation operation to increase the diversity of population if the replacement is carried out. It should be noticed that even if a new cluster center is generated, this cluster center will be regarded as the previous one to take part in the next generation of individuals. Hence, a new vertex is not generated but to sequentially maintain the vertex corresponding to the previous cluster center. Thereafter, the generation of new individuals is executed by selecting one or two individuals. If one class is selected, new individual as an offspring will be produced by either the cluster center or a general individual as a parent according to the parameter p_{c1} . Then the new individual denotes the generation of new vertex, and one edge between the offspring and parent is formed. Otherwise, one new individual will be generated by either two cluster centers or two general individuals on the basis of the parameter p_{c2} . Meanwhile, two edges between the offspring and two parents are established to manifest their relationship. In the end, the selection operation determines whether the connection is valid or not. If new individual is superior to previous individual, the previous one is replaced by new one, and new generated vertex and edges are actually retained. On the contrary, the generated vertex and edges are abandoned if new individual is inferior to previous one. Since the successful population interaction means the result of evolution is better and better, it is worth considering a better individual which signifies a transition in the whole evolutionary process. By this means, when the BSO reaches the termination, the ultimate population interaction network of BSO is constructed to show the interaction of knowledge among individuals and the attribute of complete network.

Fig. 3.1 is plot to specifically illustrate the construction process of PIN in BSO. Black circles indicate the individuals (vertices) in the current population. Transparent circles denote the classes. Transparent rectangles mean the individuals X_p which will be replaced. Black rectangles represent the individuals which have been replaced. Black rhombuses manifest the new generated individual U_n . Therefore, in Fig. 3.1, a primary construction process of PIN can be elucidated as follows:

- (1) There are nine initial individuals and three classes in the population;

(2) Two selected individuals X_{s1} and X_{s2} from two classes produce the new individual U_n to compare with the previous individual X_p . A vertex and two edges are simultaneously formed;

(3) If the new individual U_n outperforms the previous individual X_p ($f(U_n) < f(X_p)$), the individual U_n replaces the individual X_p ;

(4) Another selected individual X_s from one class generates the individual U_n to replace the individual X_p , meaning a vertex and an edge are formed;

(5) When $f(U_n) < f(X_p)$, the replacement is achieved again;

(6) Enter into next iteration, the clustering algorithm resumes classifying individuals into three classes.

From Figs. 3.1(1) and (6), it can be observed that the distribution of individuals have changed in the whole population and the number of individuals in each class correspondingly alter, suggesting the interaction of individuals promote the evolution of population towards better results.

3.4 Experiment and analysis

In order to explore the attribute and relationship of population interaction in BSO, the first experiment is carried out to investigate the performance of the algorithm under different dimensions. Dimensions can significantly not only enhance the complicated structure of problem but also change the effect of population interaction. After determining the emergence of the power law distribution obtained by the connections among individuals in specific dimension, the second experiment which analyzes the influence of power law distribution on population interaction under diverse parameters of BSO is implemented. The exponent γ of power law distribution shows evident results that different parameters of BSO have respective characteristics, indicating the population interaction depends on the value of parameters in BSO. The third experiment using an orthogonal array analyzes the best combinatorial parameter setting of BSO for improving its performance. The last experiment compares BSO with two related algorithms, i.e., DE and PSO, to discuss their performances according to their characteristics of distributions.

3.4.1 Experimental setup

To assess the property of BSO for optimization functions with different dimensions, thirty one functions composed of six benchmark functions and twenty five CEC'05 test functions

are used to guarantee the generalization and validity of experimental results. Using numerous functions can reduce the potential risk of algorithm trapped into local or specific situations which can not exhibit the actual property of algorithm, and provide a fair comparison so as to come to a general conclusion. In these functions, Sphere, Rosenbrock, Quartic and F1-F5 belong to unimodal functions, whereas Griewank, Rastrigin, Schwefel and F6-F25 are multimodal functions. Compared with unimodal functions which have no local optima, multimodal functions have plenty of local optima or some local optima. In addition, the number of local optima in multimodal functions will increase exponentially along with the increment of dimensions of problem, which will become more difficult to resolve. A more detailed information of these functions can be referred in [10, 113]. Therefore, it is useful and critical for analyzing the performance of BSO and avoiding some uncertain circumstances via adopting these functions which possess heterogeneous structures.

The construction of PIN in BSO is comprised of the edges and vertices. Vertices and edges represent individuals and their connections, respectively. When the algorithm reaches the termination condition, the whole individuals and connections among them generate the complex network (PIN) which has a great deal of vertices and edges. To extract and analyze the characteristic of PIN, the degree of vertex, which denotes the number of edges linked to this vertex, is utilized. Moreover, it should be noticed that the constructed PIN is a non-directed graph, which indicates the connections among individuals have no direction. The purpose of this paper is to investigate the influence of distribution of frequency of average degree on the performance of BSO. Thus, a power law distribution reveals the relationship between degree and its frequency in BSO for several functions with specific dimension. The power law distribution is expressed as $P(k) \propto k^{-\gamma}$ [119], where $P(k)$ indicates the probability distribution of variable k and γ denotes the power exponent. According to this definition, the power exponent γ in the PIN can be calculated as follow:

$$\gamma = \frac{\ln P(k_1) - \ln P(k_2)}{\ln k_2 - \ln k_1}, \quad (3.3)$$

where $P(k_1)$ and $P(k_2)$ indicate the frequencies of degrees k_1 and k_2 , respectively. Furthermore, the power law distribution can be shown as a straight line in the two-log figure and the slope of line represents the value of power exponent γ [119]. Therefore, it can be obviously judged whether a curve meets the power law distribution in terms of the characteristic of straight line in two-log axes.

To conduct the comparative experiment in different dimensions, the parameters of BSO are set in terms of the literature [16]. The population size p is 100. The number of clusters

c is 5. The replacement rate p_c is 0.2. The selected probability p_g is 0.8. The parameters p_{c1} and p_{c2} are 0.4 and 0.5, respectively. The constant k is set to be 20, and the number of maximum iteration T is 2000. The dimensions of each function are set to be 2, 10 and 30, implying low, medium and high dimensions, respectively. The BSO is independently run 30 times for each function to derive the average optimal solution and the distribution of average degree. All the experiments are achieved by a Matlab software on a computer with 3.30GHz Intel(R) Core(TM) i5 CPU and 8GB RAM.

3.4.2 Results in different dimensions

The experimental results obtained by BSO on benchmark functions and CEC'05 test functions with three kinds of dimensions are shown in Table 3.1, where values in and out of the parenthesis indicate the standard deviation and mean of thirty optimal solutions, respectively. It can be found from Table 3.1 that the experimental results in $D = 2$ are the least among three kinds of dimensions and most of them belong to the known best-so-far solutions, suggesting the performance of BSO is the best on all the functions with 2 dimension and the optimization of BSO for functions is valid. Since the increase of dimension can result in the more complicated structures of functions, high dimension can significantly intensify the complexity of functions which can influence the capacity of algorithm for searching optimal solution. Based on this reason, the performance of BSO in the functions with 10 and 30 dimensions notably declines, which is reflected by the worse experimental results in $D = 10$ and $D = 30$. The higher dimension the function has, the worse optimal solution the BSO ultimately acquires. This circumstance primarily occurs in CEC'05 test functions because the CEC'05 test functions possess the characteristics of shift or rotation which can be remarkably altered via the increasing dimension so that the searching capacity of BSO is insufficient for CEC'05 test functions with high dimension comparing with those benchmark functions. Consequently, Table 3.1 verifies the effective and efficient property of BSO for the functions with low dimension.

To detect the inherent essence of significant differences of experimental results among the functions with three dimensions, the average degree is adopted to analyze the relationship between the population interaction and the performance of algorithm. In consideration of the generally similar status exhibited by numerous experimental results from Table 3.1, Fig. 3.2 is given to show the box-and-whisker diagrams of optimal solutions on three functions including Sphere, F6 and F18 with three dimensions, and the corresponding two-log curves of the average degree distribution are plotted in Fig. 3.3. In Fig. 3.2, the horizontal

Table 3.1: The experimental results obtained by BSO on benchmark functions and CEC'05 test functions with different dimensions.

Function	$D = 2$	$D = 10$	$D = 30$
Sphere	$7.35E - 48(\pm 5.03E - 48)$	$3.80E - 44(\pm 8.04E - 45)$	$6.56E - 43(\pm 1.1E - 43)$
Rosenbrock	$0(\pm 0)$	$6.32(\pm 1.77)$	$39.61(\pm 26.16)$
Quartic	$4.92E - 05(\pm 3.72E - 05)$	$2.92E - 04(\pm 1.52E - 04)$	$9.70E - 03(\pm 5.68E - 03)$
Griewank	$1.60E - 02(\pm 2.52E - 02)$	$1.37(\pm 0.43)$	$1.12E - 02(\pm 1.25E - 02)$
Rastrigin	$0(\pm 0)$	$3.98(\pm 1.36)$	$31.11(\pm 5.92)$
Schwefel	$8.70(\pm 30.00)$	$1453.08(\pm 364.62)$	$5466.16(\pm 789.72)$
F1	$-450(\pm 0)$	$-450(\pm 0)$	$-450(\pm 2.11E - 14)$
F2	$-450(\pm 0)$	$-450(\pm 0)$	$-448.61(\pm 0.60)$
F3	$-445.92(\pm 16.96)$	$69997.08(\pm 42493.28)$	$2045349(\pm 603296.7)$
F4	$-450(\pm 0)$	$-410.79(\pm 136.32)$	$23353.16(\pm 5163.39)$
F5	$-310(\pm 0)$	$-309.80(\pm 0.37)$	$4255.53(\pm 946.41)$
F6	$390(\pm 0)$	$595.24(\pm 752.78)$	$1440.30(\pm 1897.79)$
F7	$-138.60(\pm 3.80)$	$1239.78(\pm 84.82)$	$6342.76(\pm 280.88)$
F8	$-133.93(\pm 8.89)$	$-119.94(\pm 3.17E - 02)$	$-119.65(\pm 7.92E - 02)$
F9	$-330(\pm 0)$	$-325.95(\pm 1.17)$	$-290.93(\pm 10.14)$
F10	$-330(\pm 0)$	$-325.19(\pm 1.63)$	$-291.66(\pm 7.85)$
F11	$90(\pm 0)$	$90.58(\pm 0.74)$	$107.07(\pm 1.89)$
F12	$-460(\pm 0)$	$-450.21(\pm 11.48)$	$15496.47(\pm 10756.5)$
F13	$-130(\pm 0)$	$-129.26(\pm 0.22)$	$-125.75(\pm 1.13)$
F14	$-300(\pm 7.37E - 03)$	$-296.33(\pm 0.29)$	$-286.92(\pm 0.39)$
F15	$120(\pm 0)$	$395.44(\pm 167.04)$	$525.22(\pm 78.41)$
F16	$120(\pm 0)$	$214.91(\pm 8.23)$	$267.82(\pm 133.56)$
F17	$120(\pm 0)$	$217.66(\pm 19.20)$	$284.55(\pm 151.11)$
F18	$13.33(\pm 18.26)$	$710.96(\pm 227.61)$	$901.95(\pm 46.81)$
F19	$160(\pm 77.68)$	$675.84(\pm 246.05)$	$913.54(\pm 35.17)$
F20	$176.67(\pm 84.42)$	$699.51(\pm 219.82)$	$901.65(\pm 46.64)$
F21	$433.33(\pm 98.03)$	$868.41(\pm 227.64)$	$880(\pm 76.11)$
F22	$487.09(\pm 97.48)$	$1020.04(\pm 184.83)$	$1239.01(\pm 9.86)$
F23	$453.09(\pm 124.44)$	$1182.27(\pm 168.29)$	$940.80(\pm 145.47)$
F24	$453.33(\pm 25.37)$	$550(\pm 180.71)$	$460(\pm 5.71E - 13)$
F25	$360(\pm 0)$	$1998.84(\pm 7.61)$	$1924.83(\pm 7.54)$

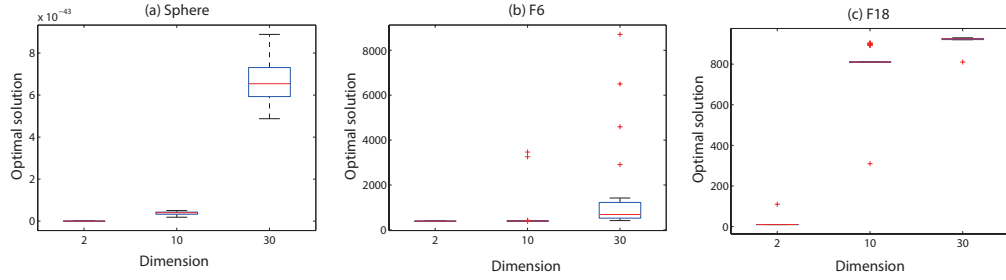


Figure 3.2: The box-and-whisker diagrams of optimal solutions obtained by BSO on Sphere, F6 and F18 with 2, 10, 30 dimensions.

axis indicates dimension and the vertical axis manifests optimal solution. It is obvious from Fig. 3.2 that the total optimal solutions of each function in 2 dimension are much less than those in 10 and 30 dimensions, and optimal solutions of each function are worse and worse along with the increase of dimension, illustrating the performance of BSO in the functions with 2 dimension is superior to that on the functions with 10 and 30 dimensions once again. In Fig. 3.3, the horizontal axis denotes the value of average degree and the vertical axis represents the frequency of average degree. According to Fig. 3.3, it can be seen that the power law distribution shown by the black dash line occurs in Figs. 3.3(a) (d) and (g), indicating the population interaction of BSO meets a power law distribution on the functions with 2 dimension. Nevertheless, in the other subfigures which display the average degree distribution on the functions with 10 and 30 dimensions, it can be evidently observed that the overall frequency of average degree shows a convex shape rather than a straight line, implying the population interaction of BSO is significantly influenced and changed by the dimensions of functions so that the average degree distribution can not completely meet a power law distribution anymore and the performance of BSO declines.

From Figs. 3.2 and 3.3, it can be concluded that the reason why BSO performs best on the functions with 2 dimension instead of 10 and 30 dimensions is that the population interaction of BSO which indicates a power law distribution is effective and efficient for seeking an optimal solution in low dimension of functions, whereas the high dimension enhances the complexity of functions to lead to the descend of property regarding the population interaction whose structure is transformed and incompletely obeys a power law distribution, and eventually cause the inferior quality of optimal solution. Therefore, the power law distribution can stand for the good population interaction of BSO as well as the robust capacity for exploring and exploiting an optimal solution in heterogeneous functions.

Fig. 3.4 is depicted to further demonstrate that the performance of BSO generally de-

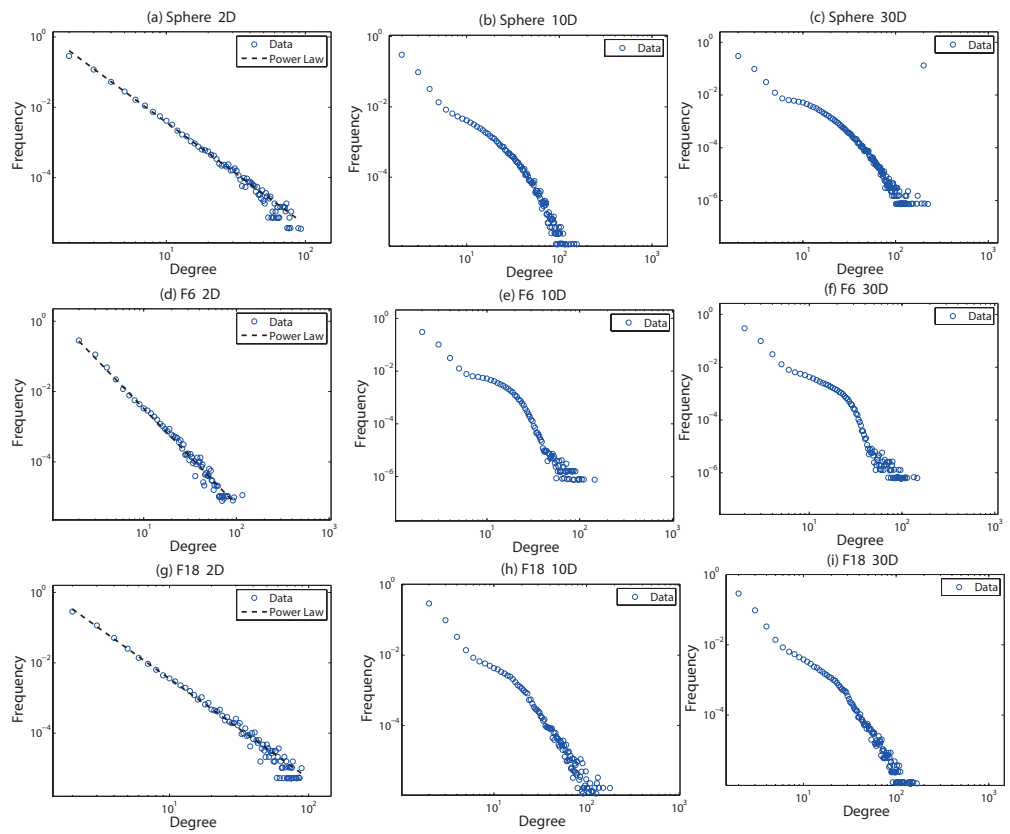


Figure 3.3: Two-log curves of the average degree distribution of BSO on Sphere, F6 and F18 with 2, 10, 30 dimensions.

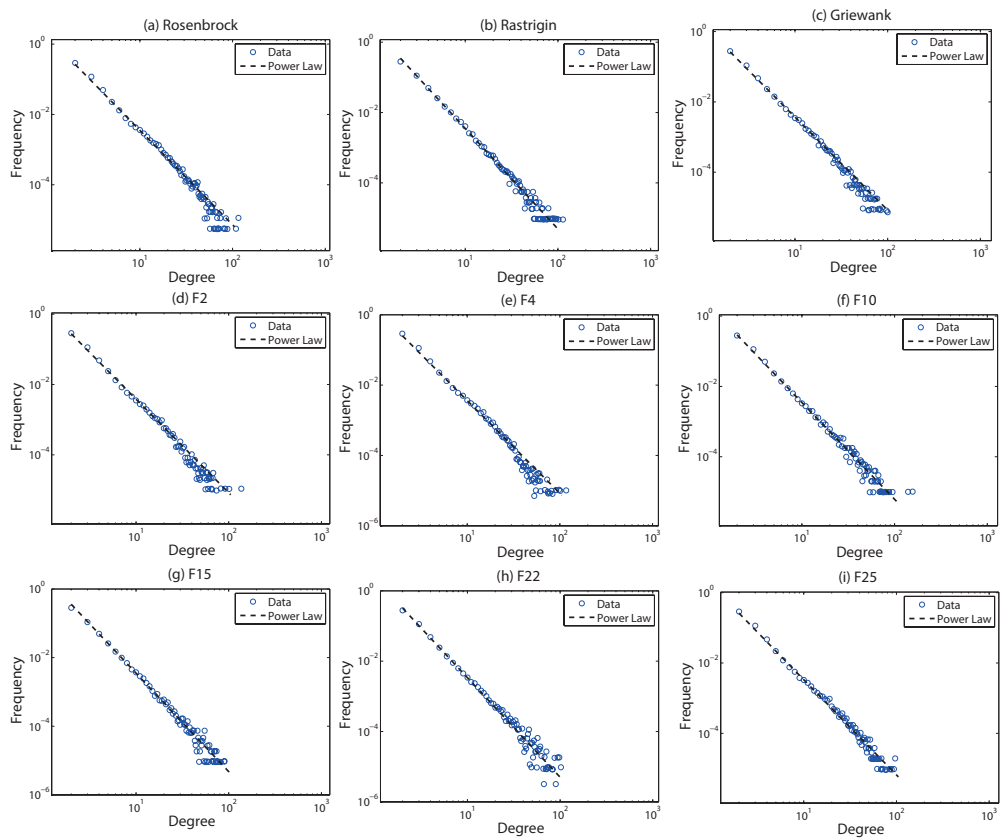


Figure 3.4: The power law distribution of average degree of BSO on other nine functions with 2 dimension.

depends on the power law distribution of population interaction on nine functions with 2 dimension, including Rosenbrock, Rastrigin, Griewank, F2, F4, F10, F15, F22 and F25. In Fig. 3.4, it can be observed that the frequency of average degree of BSO in each function also reveals a power law distribution. Meanwhile, the optimal solution of corresponding each function is superior in Table 3.1. Hence, it can be declared that the population interaction of BSO obeying a power law distribution can effectively guide the evolution of individuals and efficiently acquire an optimal solution on the functions with low dimension. The power law distribution not only determines the population structure but also influences the direction of evolution among populations, suggesting it plays a crucial role in the evolutionary process of BSO. As a result, the power law distribution shows a promising pattern of population interaction which is beneficial for boosting the performance of BSO. A novel perspective which is to change the population structure of BSO to completely satisfy a power law distribution in high dimension is worth considering in order to reinforce the quality of individuals and the capacity of exploration and exploitation of the algorithm in search space.

3.4.3 Results in different parameters

BSO shows an outstanding attribute owing to its distinctive framework and the effective application of its parameters. Thus, it is necessary to investigate and analyze the impact of each parameter on the performance of BSO via a theoretical method. Six parameters including the number of clusters c , the number of population p , the replacement rate p_c , the selected probability p_g and two parameters p_{c1} and p_{c2} are studied, respectively. Since the power law distribution of population interaction emerges on the whole functions with low dimension, six benchmark functions with 2 dimension are adopted to measure the effect of parameters. When one parameter is analyzed, the other parameters maintain the values mentioned in the experiment regarding dimensions. For each parameter, the experiment is run 30 times for obtaining the mean and standard deviation of optimal solutions. Tables 3.2, 3.4, 3.6, 3.8, 3.10 and 3.12 indicate the experimental results obtained by BSO with analytical parameters on six benchmark functions, respectively. The corresponding statistical results obtained by the Friedman test and post-hoc test [120] at a significant level of $\alpha = 0.05$ are shown in Tables 3.3, 4.1, 3.7, 3.9, 3.11 and 3.13, respectively. Fig. 3.5 is plotted to denote the obtained value of power exponent γ for each analytical parameter on six benchmark functions. The specific analyses of experiment are described as follow.

- (1) The analysis of the number of clusters: The parameter c is set to be six values from

Table 3.2: The experimental results obtained by BSO with different number of clusters c on benchmark functions.

Function	$c = 3$	$c = 5$	$c = 7$	$c = 9$	$c = 11$	$c = 13$
Sphere	$6.05E - 48$ ($\pm 5.43E - 48$)	$7.35E - 48$ ($\pm 5.03E - 48$)	$1.02E - 47$ ($\pm 9.91E - 48$)	$9.72E - 48$ ($\pm 8.93E - 48$)	$8.33E - 48$ ($\pm 6.39E - 48$)	$1.13E - 47$ ($\pm 1.11E - 47$)
Rosenbrock	0 (± 0)					
Quartic	$3.85E - 05$ ($\pm 3.12E - 05$)	$4.92E - 05$ ($\pm 3.72E - 05$)	$3.62E - 05$ ($\pm 3.02E - 05$)	$4.20E - 05$ ($\pm 2.65E - 05$)	$4.17E - 05$ ($\pm 3.54E - 05$)	$4.94E - 05$ ($\pm 2.96E - 05$)
Griewank	$2.49E - 02$ ($\pm 2.58E - 02$)	$1.60E - 02$ ($\pm 2.52E - 02$)	$2.16E - 02$ ($\pm 3.18E - 02$)	$3.07E - 02$ ($\pm 4.25E - 02$)	$3.18E - 02$ ($\pm 3.32E - 02$)	$1.72E - 02$ ($\pm 2.07E - 02$)
Rastrigin	0 (± 0)					
Schwefel	10.02 (± 30.77)	8.70 (± 30.00)	11.84 (± 36.14)	11.13 (± 33.08)	24.69 (± 47.80)	24.04 (± 48.03)

Table 3.3: The statistical results of parameter c obtained by the Friedman test, where * indicates the best average rank of parameter.

Parameter	Average rank	Unadjusted p	p_{Bonf}	p_{Holm}	$p_{Hochberg}$	$\alpha = 0.05$
$c = 3$	3.0833	0.877371	1	1	0.877371	No
* $c = 5$	2.9167					
$c = 7$	3.0833	0.877371	1	1	0.877371	No
$c = 9$	3.75	0.440401	1	1	0.877371	No
$c = 11$	4.25	0.217044	1	1	0.877371	No
$c = 13$	3.9167	0.354539	1	1	0.877371	No

Table 3.4: The experimental results obtained by BSO with different number of populations p on benchmark functions.

Function	$p = 10$	$p = 50$	$p = 100$	$p = 200$
Sphere	$1.06E - 46$ ($\pm 1.17E - 46$)	$1.38E - 47$ ($\pm 1.37E - 47$)	$7.35E - 48$ ($\pm 5.03E - 48$)	$3.47E - 48$ ($\pm 3.58E - 48$)
Rosenbrock	$3.13E - 06$ ($\pm 1.53E - 05$)	0 (± 0)	0 (± 0)	0 (± 0)
Quartic	$2.99E - 04$ ($\pm 2.49E - 04$)	$8.15E - 05$ ($\pm 5.67E - 05$)	$4.92E - 05$ ($\pm 3.72E - 05$)	$2.21E - 05$ ($\pm 1.69E - 05$)
Griewank	$1.89E - 01$ ($\pm 1.85E - 01$)	$3.91E - 02$ ($\pm 6.28E - 02$)	$1.60E - 02$ ($\pm 2.52E - 02$)	$7.76E - 03$ ($\pm 1.00E - 02$)
Rastrigin	0 (± 0)			
Schwefel	49.29 (± 61.15)	29.61 (± 48.27)	8.07 (± 30.00)	7.90 (± 30.05)

Table 3.5: The statistical results of parameter p obtained by the Friedman test, where * indicates the best average rank of parameter.

Parameter	Average rank	Unadjusted p	p_{Bonf}	p_{Holm}	$p_{Hochberg}$	$\alpha = 0.05$
$p = 10$	3.5	0.013906	0.041719	0.041719	0.041719	Yes
$p = 50$	2.6667	0.179712	0.539137	0.359425	0.359425	No
$p = 100$	2.1667	0.502335	1	0.502335	0.502335	No
* $p = 200$	1.6667					

Table 3.6: The experimental results obtained by BSO with different replacement rate p_c on benchmark functions.

Function	$p_c = 0.1$	$p_c = 0.2$	$p_c = 0.3$	$p_c = 0.4$	$p_c = 0.5$
Sphere	$6.72E - 48$ ($\pm 6.84E - 48$)	$7.35E - 48$ ($\pm 5.03E - 48$)	$7.78E - 48$ ($\pm 8.22E - 48$)	$9.42E - 48$ ($\pm 8.66E - 48$)	$5.74E - 48$ ($\pm 5.00E - 48$)
Rosenbrock	0 (± 0)				
Quartic	$4.02E - 05$ ($\pm 3.40E - 05$)	$4.92E - 05$ ($\pm 3.72E - 05$)	$4.20E - 05$ ($\pm 2.80E - 05$)	$4.33E - 05$ ($\pm 2.55E - 05$)	$3.68E - 05$ ($\pm 2.55E - 05$)
Griewank	$1.95E - 02$ ($\pm 2.87E - 02$)	$1.60E - 02$ ($\pm 2.52E - 02$)	$1.90E - 02$ ($\pm 2.20E - 02$)	$1.72E - 02$ ($\pm 1.85E - 02$)	$1.65E - 02$ ($\pm 2.34E - 02$)
Rastrigin	0 (± 0)				
Schwefel	27.92 (± 50.81)	8.07 (± 30.00)	4.00 (± 21.62)	4.29 (± 21.64)	$2.55E - 05$ (± 0)
Function	$p_c = 0.6$	$p_c = 0.7$	$p_c = 0.8$	$p_c = 0.9$	
Sphere	$7.11E - 48$ ($\pm 8.28E - 48$)	$9.85E - 48$ ($\pm 8.19E - 48$)	$7.46E - 48$ ($\pm 7.33E - 48$)	$7.02E - 48$ ($\pm 9.22E - 48$)	
Rosenbrock	0 (± 0)				
Quartic	$3.77E - 05$ ($\pm 3.50E - 05$)	$3.74E - 05$ ($\pm 2.80E - 05$)	$4.99E - 05$ ($\pm 4.65E - 05$)	$3.47E - 05$ ($\pm 4.13E - 05$)	
Griewank	$1.90E - 02$ ($\pm 1.85E - 02$)	$1.25E - 02$ ($\pm 1.49E - 02$)	$1.51E - 02$ ($\pm 1.52E - 02$)	$1.28E - 02$ ($\pm 1.26E - 02$)	
Rastrigin	0 (± 0)				
Schwefel	$5.33E - 02$ ($\pm 2.05E - 01$)	$5.20E - 02$ ($\pm 2.85E - 01$)	$2.55E - 05$ (± 0)	$2.55E - 05$ (± 0)	

Table 3.7: The statistical results of parameter p_c obtained by the Friedman test, where * indicates the best average rank of parameter.

Parameter	Average rank	Unadjusted p	p_{Bonf}	p_{Holm}	$p_{Hochberg}$	$\alpha = 0.05$
$p_c = 0.1$	6.3333	0.05778	0.462237	0.462237	0.462237	No
$p_c = 0.2$	5.8333	0.113846	0.91077	0.796924	0.683078	No
$p_c = 0.3$	5.6667	0.140017	1	0.796924	0.700083	No
$p_c = 0.4$	5.8333	0.113846	0.91077	0.796924	0.683078	No
$p_c = 0.5$	4	0.67329	1	1	0.75183	No
$p_c = 0.6$	5.3333	0.205903	1	0.823613	0.75183	No
$p_c = 0.7$	3.8333	0.75183	1	1	0.75183	No
$p_c = 0.8$	4.8333	0.342782	1	1	0.75183	No
* $p_c = 0.9$	3.3333					

Table 3.8: The experimental results obtained by BSO with different selected probability p_g on benchmark functions.

Function	$p_g = 0.1$	$p_g = 0.2$	$p_g = 0.3$	$p_g = 0.4$	$p_g = 0.5$
Sphere	$7.90E - 48$ ($\pm 7.83E - 48$)	$7.70E - 48$ ($\pm 5.71E - 48$)	$7.51E - 48$ ($\pm 8.21E - 48$)	$8.16E - 48$ ($\pm 8.33E - 48$)	$8.08E - 48$ ($\pm 8.92E - 48$)
Rosenbrock	0 (± 0)				
Quartic	$2.42E - 05$ ($\pm 1.88E - 05$)	$2.80E - 05$ ($\pm 2.08E - 05$)	$3.06E - 05$ ($\pm 1.89E - 05$)	$3.16E - 05$ ($\pm 1.60E - 05$)	$2.60E - 05$ ($\pm 1.84E - 05$)
Griewank	$1.40E - 03$ ($\pm 4.13E - 03$)	$1.13E - 03$ ($\pm 2.62E - 03$)	$7.40E - 04$ ($\pm 2.26E - 03$)	$2.47E - 03$ ($\pm 4.53E - 03$)	$5.19E - 03$ ($\pm 9.14E - 03$)
Rastrigin	0 (± 0)				
Schwefel	3.47 (± 15.90)	3.98 (± 19.16)	7.94 (± 30.04)	16.72 (± 40.89)	3.22 (± 15.21)
Function	$p_g = 0.6$	$p_g = 0.7$	$p_g = 0.8$	$p_g = 0.9$	
Sphere	$7.22E - 48$ ($\pm 6.82E - 48$)	$9.88E - 48$ ($\pm 8.80E - 48$)	$7.35E - 48$ ($\pm 5.03E - 48$)	$8.79E - 48$ ($\pm 8.40E - 48$)	
Rosenbrock	0 (± 0)				
Quartic	$2.76E - 05$ ($\pm 1.60E - 05$)	$3.25E - 05$ ($\pm 2.35E - 05$)	$4.92E - 05$ ($\pm 3.72E - 05$)	$4.75E - 05$ ($\pm 3.68E - 05$)	
Griewank	$5.75E - 03$ ($\pm 8.07E - 03$)	$8.38E - 03$ ($\pm 1.20E - 02$)	$1.60E - 02$ ($\pm 2.52E - 02$)	$4.83E - 02$ ($\pm 3.53E - 02$)	
Rastrigin	0 (± 0)				
Schwefel	3.96 (± 21.62)	5.23 (± 22.17)	8.07 (± 30.00)	3.95 (± 21.62)	

Table 3.9: The statistical results of parameter p_g obtained by the Friedman test, where * indicates the best average rank of parameter.

Parameter	Average rank	Unadjusted p	p_{Bonf}	p_{Holm}	$p_{Hochberg}$	$\alpha = 0.05$
* $p_g = 0.1$	3.5					
$p_g = 0.2$	4.3333	0.598161	1	1	0.833029	No
$p_g = 0.3$	4.6667	0.460597	1	1	0.833029	No
$p_g = 0.4$	5.6667	0.170587	1	0.980116	0.833029	No
$p_g = 0.5$	3.8333	0.833029	1	1	0.833029	No
$p_g = 0.6$	4.6667	0.460597	1	1	0.833029	No
$p_g = 0.7$	5.8333	0.140017	1	0.980116	0.833029	No
$p_g = 0.8$	6.6667	0.045201	0.361611	0.361611	0.361611	Yes
$p_g = 0.9$	5.8333	0.140017	1	0.980116	0.833029	No

Table 3.10: The experimental results obtained by BSO with different p_{c1} on benchmark functions.

Function	$p_{c1} = 0.1$	$p_{c1} = 0.2$	$p_{c1} = 0.3$	$p_{c1} = 0.4$	$p_{c1} = 0.5$
Sphere	$8.70E - 48$ ($\pm 7.56E - 48$)	$7.99E - 48$ ($\pm 6.16E - 48$)	$5.81E - 48$ ($\pm 6.67E - 48$)	$7.35E - 48$ ($\pm 5.03E - 48$)	$8.24E - 48$ ($\pm 6.46E - 48$)
Rosenbrock	0 (± 0)				
Quartic	$4.26E - 05$ ($\pm 3.61E - 05$)	$3.73E - 05$ ($\pm 3.40E - 05$)	$2.71E - 05$ ($\pm 1.99E - 05$)	$4.92E - 05$ ($\pm 3.72E - 05$)	$3.06E - 05$ ($\pm 2.51E - 05$)
Griewank	$9.70E - 03$ ($\pm 9.54E - 03$)	$1.42E - 02$ ($\pm 2.30E - 02$)	$2.38E - 02$ ($\pm 3.86E - 02$)	$1.60E - 02$ ($\pm 2.52E - 02$)	$2.08E - 02$ ($\pm 2.17E - 02$)
Rastrigin	0 (± 0)				
Schwefel	12.81 (± 36.02)	12.26 (± 37.56)	14.69 (± 38.40)	8.07 (± 30.00)	3.95 (± 21.62)
Function	$p_{c1} = 0.6$	$p_{c1} = 0.7$	$p_{c1} = 0.8$	$p_{c1} = 0.9$	
Sphere	$6.64E - 48$ ($\pm 7.60E - 48$)	$5.93E - 48$ ($\pm 4.80E - 48$)	$5.29E - 48$ ($\pm 4.03E - 48$)	$5.17E - 48$ ($\pm 6.48E - 48$)	
Rosenbrock	0 (± 0)				
Quartic	$3.98E - 05$ ($\pm 3.44E - 05$)	$2.98E - 05$ ($\pm 2.25E - 05$)	$4.60E - 05$ ($\pm 2.87E - 05$)	$3.28E - 05$ ($\pm 2.23E - 05$)	
Griewank	$2.70E - 02$ ($\pm 2.44E - 02$)	$3.14E - 02$ ($\pm 3.18E - 02$)	$3.01E - 02$ ($\pm 2.53E - 02$)	$2.17E - 02$ ($\pm 2.64E - 02$)	
Rastrigin	0 (± 0)				
Schwefel	9.69 (± 30.17)	7.51 (± 25.82)	14.39 (± 36.43)	5.54 (± 22.77)	

Table 3.11: The statistical results of parameter p_{c1} obtained by the Friedman test, where * indicates the best average rank of parameter.

Parameter	Average rank	Unadjusted p	p_{Bonf}	p_{Holm}	$p_{Hochberg}$	$\alpha = 0.05$
$p_{c1} = 0.1$	5	0.460597	1	1	0.75183	No
$p_{c1} = 0.2$	4.6667	0.598161	1	1	0.75183	No
$p_{c1} = 0.3$	5.1667	0.399075	1	1	0.75183	No
$p_{c1} = 0.4$	5.1667	0.399075	1	1	0.75183	No
* $p_{c1} = 0.5$	3.8333					
$p_{c1} = 0.6$	5.5	0.291841	1	1	0.75183	No
$p_{c1} = 0.7$	4.8333	0.527089	1	1	0.75183	No
$p_{c1} = 0.8$	6.5	0.09169	0.733522	0.733522	0.733522	No
$p_{c1} = 0.9$	4.3333	0.75183	1	1	0.75183	No

Table 3.12: The experimental results obtained by BSO with different p_{c2} on benchmark functions.

Function	$p_{c2} = 0.1$	$p_{c2} = 0.2$	$p_{c2} = 0.3$	$p_{c2} = 0.4$	$p_{c2} = 0.5$
Sphere	$6.98E - 48$ ($\pm 6.94E - 48$)	$6.08E - 48$ ($\pm 7.01E - 48$)	$5.53E - 48$ ($\pm 5.29E - 48$)	$8.91E - 48$ ($\pm 6.59E - 48$)	$7.35E - 48$ ($\pm 5.03E - 48$)
Rosenbrock	0 (± 0)				
Quartic	$3.16E - 05$ ($\pm 2.20E - 05$)	$4.44E - 05$ ($\pm 3.48E - 05$)	$3.36E - 05$ ($\pm 2.65E - 05$)	$3.96E - 05$ ($\pm 2.71E - 05$)	$4.92E - 05$ ($\pm 3.72E - 05$)
Griewank	$3.56E - 02$ ($\pm 8.21E - 02$)	$1.80E - 02$ ($\pm 2.48E - 02$)	$2.65E - 02$ ($\pm 2.44E - 02$)	$1.04E - 02$ ($\pm 1.37E - 02$)	$1.60E - 02$ ($\pm 2.52E - 02$)
Rastrigin	0 (± 0)				
Schwefel	4.22 (± 21.60)	4.90 (± 21.72)	11.97 (± 33.17)	4.68 (± 21.72)	8.07 (± 30.00)
Function	$p_{c2} = 0.6$	$p_{c2} = 0.7$	$p_{c2} = 0.8$	$p_{c2} = 0.9$	
Sphere	$7.96E - 48$ ($\pm 6.07E - 48$)	$6.55E - 48$ ($\pm 5.91E - 48$)	$6.04E - 48$ ($\pm 6.78E - 48$)	$5.77E - 48$ ($\pm 6.53E - 48$)	
Rosenbrock	0 (± 0)				
Quartic	$4.33E - 05$ ($\pm 2.86E - 05$)	$3.83E - 05$ ($\pm 4.45E - 05$)	$3.62E - 05$ ($\pm 2.69E - 05$)	$4.06E - 05$ ($\pm 3.38E - 05$)	
Griewank	$2.34E - 02$ ($\pm 2.29E - 02$)	$2.98E - 02$ ($\pm 2.94E - 02$)	$1.38E - 02$ ($\pm 1.53E - 02$)	$1.94E - 02$ ($\pm 1.95E - 02$)	
Rastrigin	0 (± 0)				
Schwefel	9.37 (± 30.33)	21.63 (± 44.58)	3.95 (± 21.62)	4.63 (± 21.80)	

Table 3.13: The statistical results of parameter p_{c2} obtained by the Friedman test, where * indicates the best average rank of parameter.

Parameter	Average rank	Unadjusted p	p_{Bonf}	p_{Holm}	$p_{Hochberg}$	$\alpha = 0.05$
$p_{c2} = 0.1$	4.5	0.527089	1	1	0.67329	No
$p_{c2} = 0.2$	5.3333	0.246252	1	1	0.67329	No
$p_{c2} = 0.3$	5.3333	0.246252	1	1	0.67329	No
$p_{c2} = 0.4$	4.1667	0.67329	1	1	0.67329	No
$p_{c2} = 0.5$	5.5	0.205903	1	1	0.67329	No
$p_{c2} = 0.6$	5.8333	0.140017	1	0.980116	0.67329	No
$p_{c2} = 0.7$	6	0.113846	0.91077	0.91077	0.67329	No
* $p_{c2} = 0.8$	3.5					
$p_{c2} = 0.9$	4.8333	0.399075	1	1	0.67329	No

3 to 13 with 2 difference, respectively. From Table 3.3, it can be found that the performance of BSO is the best in $c = 5$ according to the average rank whereas it is not significantly different from other values of c . In Fig. 3.5(a), the values of γ of the power law distribution on six functions significantly increase with the increment of the number of clusters, meaning the frequencies of average degree in the population interaction significantly decrease. That is to say, the connections among individuals are reduced so that the transmission of knowledge carried by individuals is not completely implemented, suggesting the effect of population interaction is gradually weakened with the increment of the number of clusters. This is because individuals are excessively separated by too many clusters, resulting in the deficient relationship among individuals. Accordingly, the experiment demonstrates a small number of clusters which shows a small value of γ can facilitate the population interaction better and be an appropriate value for optimization though it slightly influences the performance of BSO.

(2) The analysis of the number of population: The parameter p is set to be 10, 50, 100 and 200, which indicate a tiny, small, medium and large scale of population, respectively. Tables 3.4 and 4.1 show BSO performs best in $p = 200$ on the basis of the experimental results and average rank, respectively. However, the statistical results validate the fact that the performance of BSO in $p = 200$ is superior to that in $p = 10$ and has no significant difference with that in $p = 50$ and $p = 100$. Fig. 3.5(b) indicates the values of γ in six functions sharply decline from $p = 10$ to $p = 50$ and subsequently slowly decrease from $p = 50$ to $p = 200$, implying the frequencies of average degree in the population interaction increasingly enlarge, which enhances the relationship among individuals. It should be noted that the values of γ in $p = 10$ are abnormally large since the number of individuals

is so small that the population interaction is difficult to achieve a global search. Thus, in fact, the frequency of average degree can not meet a power law distribution in $p = 10$. The impact of population interaction is improved by the increasing number of population since more individuals can generate more connections among them so as to tighten up the structure of entire network and the relationship among individuals. Consequently, a large number of population which shows a small value of γ is more suitable for enhancing the population interaction of BSO.

(3) The analysis of the replacement rate: The parameter p_c is set in the interval [0.1, 0.9]. Table 3.7 reveals that $p_c = 0.9$ is the best but without significant difference comparing with other values of p_c . Fig. 3.5(c) shows the values of γ frequently change and exhibit fluctuant shapes on six functions according to diverse values of p_c , signifying the frequencies of average degree are arbitrarily influenced by the p_c . This is because the p_c brings the diversity of population to BSO whereas this kind of diversity has no effective guidance for the population interaction. Thus, the p_c is incompletely beneficial for improving the performance of BSO. This conclusion is the same as that in the reference [116].

(4) The analysis of the selected probability: The parameter p_g is also set in the interval [0.1, 0.9]. It can be seen that there is no significant difference among experimental results in different values of p_g except for $p_g = 0.8$ though $p_g = 0.1$ indicates the best performance in terms of the average rank. In Fig. 3.5(d), irregularly fluctuant shapes on six functions occur due to the changing values of γ , which illustrates the selected number of individuals determined by the p_g notably affects the population interaction but without adequate effectiveness. The quality of new individual generated by one or two selected individuals is not enormously different since the BSO only considers to enhance the diversity of population but not provides a mechanism for reinforcing the quality of new solution between one and two selected individuals. Hence, the BSO should be further improved to enable the p_g to be more effective for intensifying the population interaction so that the algorithm can get a better optimal solution.

(5) The analysis of two parameters p_{c1} and p_{c2} : The p_{c1} and p_{c2} are tested in the interval [0.1, 0.9], respectively. From Tables 3.11 and 3.13, it can be observed that the overall experimental results in $p_{c1} = 0.5$ and $p_{c2} = 0.8$ show the best property whereas they are similar with experimental results under other values, respectively. Figs. 3.5(e) and (f) display the values of γ on six functions decrease with the increase of the p_{c1} and p_{c2} , respectively, indicating the frequencies of average degree progressively ascend and the population interaction is increasingly enhanced. In Fig. 3.5(e), it is obvious that the values

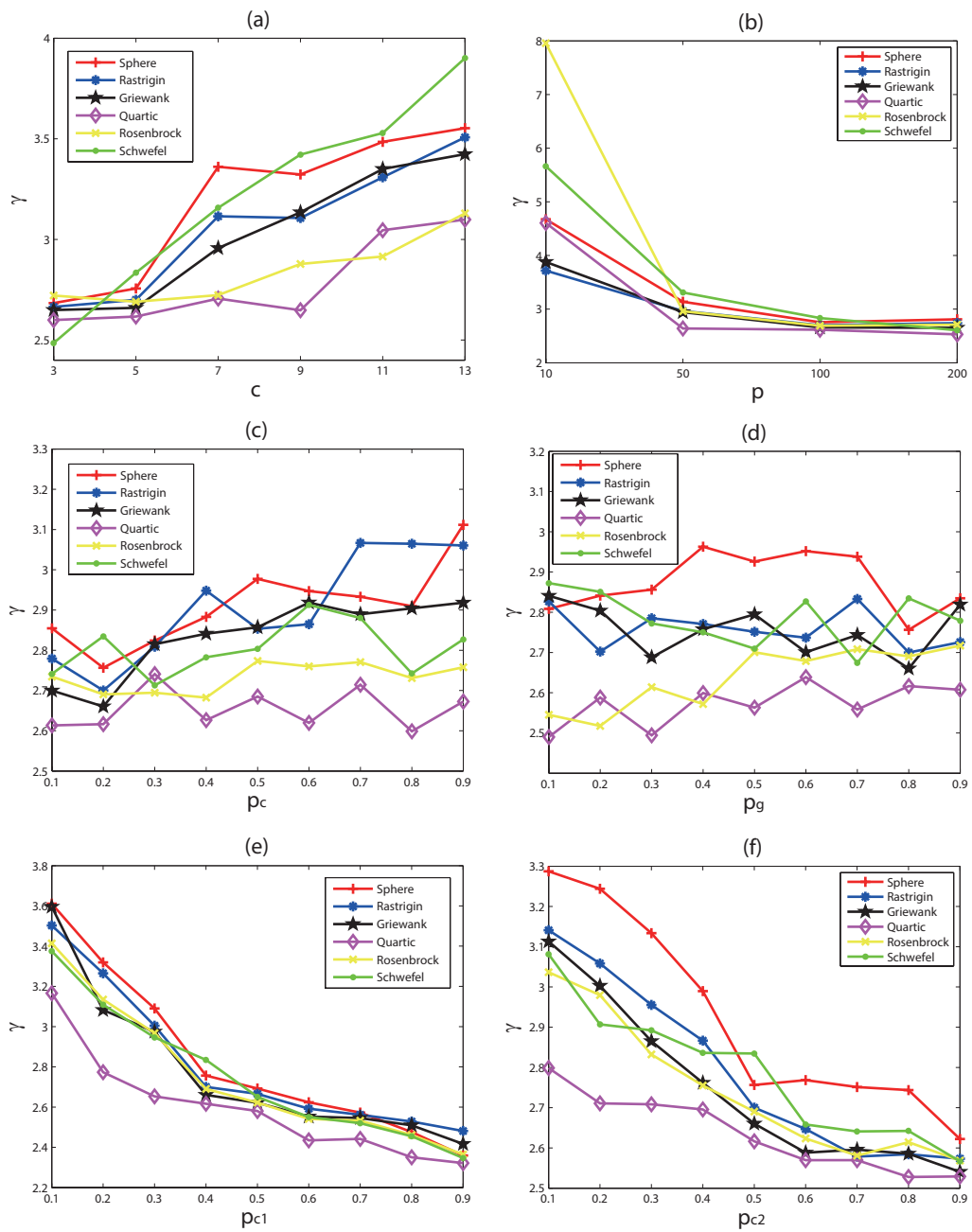


Figure 3.5: The value of power exponent γ obtained by various parameters of BSO on six benchmark functions.

of γ significantly decline in the interval [0.1, 0.4] and gradually decrease in the interval [0.4, 0.9]. However, in Fig. 3.5(f), the similar situation occurs in the interval [0.1, 0.5] and [0.5, 0.9], respectively. A small value of p_{c1} or p_{c2} means to generate new individual by one or two general individuals with a high probability, which leads to the more exploration and exploitation of solutions so as to make the population interaction weak. When a large value of p_{c1} or p_{c2} is adopted, it is more likely to use one or two cluster centers to generate new individual to accelerate the convergence of BSO. One or two good optimal solutions used to offer more effective knowledge can strengthen the connection among individuals so that the population interaction becomes strong. Thus, the parameters p_{c1} and p_{c2} exhibit the similarly changing process of population interaction, suggesting the relationship among individuals generated by the general individuals or cluster centers makes difference. On the basis of this circumstance, a balance between p_{c1} and p_{c2} should be taken into account to further improve the population interaction to acquire a better property of BSO.

3.4.4 Analysis for combinatorial parameter settings

The above analyses of parameters focus on each independent parameter. That is to say, for discussing a parameter, only it remains variant while other parameters are fixed. To further investigate the interactive influence among these parameters, six parameters are combined according to their different values to optimize six benchmark functions in 2 dimension. Each parameter is set as follows: $c \in \{3, 5, 7, 9, 10\}$, $p \in \{10, 30, 50, 100, 200\}$, $p_g \in \{0.1, 0.3, 0.5, 0.7, 0.9\}$, $p_c \in \{0.1, 0.3, 0.5, 0.7, 0.9\}$, $p_{c1} \in \{0.1, 0.3, 0.5, 0.7, 0.9\}$, $p_{c2} \in \{0.1, 0.3, 0.5, 0.7, 0.9\}$. Since a thorough analysis of parameter settings needs $5^6 = 15625$ experiments, we use the Taguchi's method [121] to reasonably decrease the number of experiments so as to derive the best combinatorial parameter setting. The Taguchi's method uses an orthogonal array to measure a portion of possible combinations instead of all the combinations, meaning the best evaluation of combinations can be acquired by the least experimental runs. As a result, in our experiment, an orthogonal array $L_{25}(5^6)$ is utilized to assess the best combinatorial result among twenty five kinds of parameter settings. Each combinatorial parameter setting is run 30 times and mean is obtained in Table 3.14. Table 3.15 shows the statistical results of the Friedman test.

From Table 3.15, we can see that the No.15 combinatorial parameter setting has the best average rank and significantly outperforms eight groups among the whole parameter settings. Therefore, $c = 7, p = 200, p_g = 0.1, p_c = 0.9, p_{c1} = 0.7, p_{c2} = 0.3$ can be regarded as the best combinatorial parameter setting. In order to evaluate its effect, we

Table 3.14: Parameter results based on the $L_{25}(5^6)$ orthogonal array for six benchmark functions.

No.	c	p	P_g	P_c	P_{c1}	P_{c2}	Function					
							Sphere	Rosenbrock	Quartic	Griewank	Rastrigin	Schwefel
1	3	10	0.1	0.1	0.1	0.1	9.06E-47	7.74E-06	1.26E-04	7.58E-02	0	166.31
2	3	30	0.3	0.5	0.7	0.9	4.00E-47	1.07E-12	1.06E-04	7.83E-03	0	3.95
3	3	50	0.5	0.7	0.9	0.3	1.88E-47	0	5.54E-05	9.46E-03	0	2.55E-05
4	3	100	0.7	0.9	0.3	0.5	8.79E-48	0	3.72E-05	6.59E-03	0	2.55E-05
5	3	200	0.9	0.3	0.5	0.7	3.48E-48	0	2.69E-05	1.97E-02	0	3.95
6	5	10	0.3	0.3	0.3	0.3	1.33E-46	2.43E-07	2.30E-04	6.73E-02	0	73.61
7	5	30	0.5	0.9	0.1	0.7	3.58E-47	4.53E-28	1.14E-04	1.16E-02	0	4.06
8	5	50	0.9	0.1	0.7	0.5	1.50E-47	0	8.06E-05	1.21E-01	0	60.23
9	5	100	0.1	0.7	0.5	0.9	7.88E-48	0	3.14E-05	9.86E-04	0	3.32E-05
10	5	200	0.7	0.5	0.9	0.1	3.99E-48	0	1.78E-05	3.71E-03	0	3.95
11	7	10	0.5	0.5	0.5	0.5	1.37E-46	3.12E-02	2.31E-04	8.38E-02	0	24.34
12	7	30	0.9	0.7	0.3	0.1	3.68E-47	2.26E-14	1.20E-04	1.40E-01	0	1.00
13	7	50	0.7	0.3	0.1	0.9	1.79E-47	0	6.81E-05	1.49E-02	0	15.08
14	7	100	0.3	0.1	0.9	0.7	9.35E-48	0	2.96E-05	2.22E-03	0	27.67
15	7	200	0.1	0.9	0.7	0.3	4.51E-48	0	1.73E-05	0	0	2.55E-05
16	9	10	0.7	0.7	0.7	0.7	1.59E-46	4.20E-01	2.19E-04	9.17E-02	0	20.89
17	9	30	0.1	0.3	0.9	0.5	3.27E-47	0	7.00E-05	2.96E-03	0	26.93
18	9	50	0.3	0.9	0.5	0.1	1.77E-47	0	5.92E-05	1.97E-03	0	3.58E-01
19	9	100	0.9	0.5	0.1	0.3	8.71E-48	0	3.58E-05	4.81E-02	0	3.85E-02
20	9	200	0.5	0.1	0.3	0.9	3.81E-48	0	1.77E-05	4.93E-04	0	5.60
21	10	10	0.9	0.9	0.9	0.9	1.64E-46	1.58E-03	2.89E-04	1.35E-01	0	4.90
22	10	30	0.7	0.1	0.5	0.3	3.42E-47	0	8.97E-05	1.65E-01	0	52.74
23	10	50	0.1	0.5	0.3	0.7	1.95E-47	0	8.51E-05	0	0	3.49E-01
24	10	100	0.5	0.3	0.7	0.1	7.88E-48	0	4.54E-05	6.00E-03	0	9.10
25	10	200	0.3	0.7	0.1	0.5	5.36E-48	0	2.20E-05	0	0	2.55E-05

Table 3.15: Statistical results of parameter settings obtained by the Friedman test, where * indicates the best average rank of parameter setting.

No.	Average rank	Unadjusted p	P_{Bonf}	P_{Holm}	$P_{Hochberg}$	$\alpha = 0.05$
1	18.8333	0.004742	0.113802	0.113802	0.109061	Yes
11	18.8333	0.004742	0.113802	0.113802	0.109061	Yes
6	18.6667	0.005355	0.128526	0.117816	0.112461	Yes
16	18.6667	0.005355	0.128526	0.117816	0.112461	Yes
21	18.5	0.00604	0.144949	0.120791	0.120791	Yes
22	16.5833	0.021758	0.522202	0.41341	0.41341	Yes
12	16.3333	0.02537	0.608877	0.456657	0.456657	Yes
8	15.9167	0.032544	0.781053	0.553246	0.553246	Yes
2	14.6667	0.065257	1	1	0.906329	No
7	13.5833	0.112164	1	1	0.906329	No
13	13.4167	0.121305	1	1	0.906329	No
17	12.9167	0.152245	1	1	0.906329	No
24	11.9167	0.231576	1	1	0.906329	No
14	11.5833	0.263626	1	1	0.906329	No
5	11.1667	0.307821	1	1	0.906329	No
19	11.0833	0.317217	1	1	0.906329	No
3	10.3333	0.410117	1	1	0.906329	No
18	10.25	0.421353	1	1	0.906329	No
23	10.0833	0.444359	1	1	0.906329	No
4	9.6667	0.504903	1	1	0.906329	No
10	9.6667	0.504903	1	1	0.906329	No
20	9.4167	0.543214	1	1	0.906329	No
9	8.75	0.651941	1	1	0.906329	No
25	7.3333	0.906329	1	1	0.906329	No
*15	6.8333					

Table 3.16: The experimental results obtained by BSO_{bp} on benchmark functions and CEC'05 test functions with three dimensions.

Function	$D = 2$	$D = 10$	$D = 30$
Sphere	$4.51E - 48(\pm 4.63E - 48)$	$2.61E - 44(\pm 9.41E - 45)$	$3.80E - 43(\pm 6.08E - 44)$
Rosenbrock	$0(\pm 0)$	$5.79(\pm 0.73)$	$30.33(\pm 13.01)$
Quartic	$1.73E - 05(\pm 1.22E - 05)$	$4.61E - 05(\pm 2.39E - 05)$	$6.75E - 04(\pm 3.68E - 04)$
Griewank	$0(\pm 0)$	$0.59(\pm 0.33)$	$7.06E - 03(\pm 6.87E - 03)$
Rastrigin	$0(\pm 0)$	$2.69(\pm 1.26)$	$19.31(\pm 5.67)$
Schwefel	$2.55E - 05(\pm 0)$	$1450.37(\pm 271.51)$	$5467.97(\pm 729.54)$
F1	$-450(\pm 0)$	$-450(\pm 0)$	$-450(\pm 0)$
F2	$-450(\pm 0)$	$-450(\pm 0)$	$-448.75(\pm 0.62)$
F3	$-450(\pm 0)$	$61468.04(\pm 29747.80)$	$1893647(\pm 515078.9)$
F4	$-450(\pm 0)$	$-442.49(\pm 31.82)$	$20569.12(\pm 3171.15)$
F5	$-310(\pm 0)$	$-309.41(\pm 0.54)$	$4060.34(\pm 702.73)$
F6	$390(\pm 0)$	$395.64(\pm 0.83)$	$969.88(\pm 327.11)$
F7	$-140.85(\pm 0)$	$1224.52(\pm 60.75)$	$6644.19(\pm 262.50)$
F8	$-139.20(\pm 3.16)$	$-119.91(\pm 3.66E - 02)$	$-119.51(\pm 0.11)$
F9	$-330(\pm 0)$	$-327.08(\pm 1.04)$	$-299.92(\pm 6.31)$
F10	$-330(\pm 0)$	$-326.82(\pm 1.24)$	$-300.96(\pm 10.51)$
F11	$90(\pm 0)$	$92.72(\pm 0.85)$	$113.95(\pm 2.99)$
F12	$-460(\pm 0)$	$-447.06(\pm 11.57)$	$15761.19(\pm 10756.16)$
F13	$-130(\pm 0)$	$-129.39(\pm 0.19)$	$-125.03(\pm 1.17)$
F14	$-300(\pm 0)$	$-296.88(\pm 0.31)$	$-287.61(\pm 0.40)$
F15	$120(\pm 0)$	$208.57(\pm 99.86)$	$515.42(\pm 93.43)$
F16	$120(\pm 0)$	$206.33(\pm 19.72)$	$201.61(\pm 92.58)$
F17	$120(\pm 0)$	$213.08(\pm 18.67)$	$311.96(\pm 164.71)$
F18	$10(\pm 0)$	$762.28(\pm 183.64)$	$901.35(\pm 46.48)$
F19	$106.67(\pm 49.01)$	$713.12(\pm 205.71)$	$897.12(\pm 48.90)$
F20	$60(\pm 62.97)$	$824.40(\pm 104.58)$	$901.38(\pm 46.49)$
F21	$360(\pm 0)$	$766.67(\pm 170.06)$	$860(\pm 2.75E - 13)$
F22	$366.67(\pm 36.51)$	$934.37(\pm 228.85)$	$1252.58(\pm 9.15)$
F23	$360(\pm 0)$	$1035.54(\pm 125.46)$	$907.59(\pm 73.55)$
F24	$438.43(\pm 44.51)$	$470(\pm 54.77)$	$460(\pm 0)$
F25	$360(\pm 0)$	$2006.79(\pm 5.21)$	$1931.31(\pm 6.39)$

Table 3.17: Statistical results obtained by the Wilcoxon signed ranks test between BSO_{bp} and BSO_{op} in three dimensions.

Algorithm	Dim	R^+	R^-	p-value	$\alpha=0.05$	$\alpha=0.1$
BSO_{bp}	2	428.0	68.0	1.9536E-04	Yes	Yes
vs.	10	362.5	133.5	0.02399	Yes	Yes
BSO_{op}	30	340.5	155.5	0.07107	No	Yes

apply it to BSO on the whole thirty one functions with three different dimensions. The experimental results are listed in Table 3.16. BSO with the best combinatorial parameter setting and the original parameter setting is called BSO_{bp} and BSO_{op} , respectively. The comparison between them is conducted by the Wilcoxon signed ranks and shown in Table 3.17. According to Table 3.17, it is obvious that BSO_{bp} significantly outperforms BSO_{op} on functions with 2 and 10 dimensions. In 30 dimension, BSO_{bp} can be remarkably superior to BSO_{op} at a significant level of $\alpha = 0.1$. Consequently, on the one hand, these statistical results demonstrate that the best combinatorial parameter setting can notably enhance the performance of BSO on functions with various dimensions. On the other hand, they also illustrate that the interactive effect among parameters can effectively boost the population interaction to significantly influence the performance of BSO.

3.4.5 Analysis for different related algorithms

BSO has shown that its degree of population interaction obeys a power law distribution on functions with low dimension. To further demonstrate the effect of the power law distribution, we compare BSO with two related algorithms, i.e., DE and PSO. DE has been verified that its degree meets a poisson law distribution in PIN [47]. PSO has shown a truncated power law distribution in terms of its search dynamics [122]. Thus, in this experiment, we contrast the performances of three algorithms on twenty five CEC'05 test functions with three dimensions to discuss their characteristics. BSO adopts the best combinatorial parameter setting mentioned before. DE uses $F = 0.5, CR = 0.9, p = 200, T = 2000$. PSO uses $p = 200, \gamma = 0.72984, c_1 = c_2 = 2.05, T = 2000$. Each algorithm is run 30 times for each function. Their mean and standard deviation are listed in Table 3.18. The comparison between BSO and two algorithms is obtained by the Wilcoxon signed ranks test at a significant level of $\alpha = 0.05$, exhibited in Table 3.19.

From Table 3.19, we can observe that BSO_{bp} significantly outperforms DE and PSO on functions with three dimensions, suggesting that BSO is the most effective algorithm

Table 3.18: The experimental results obtained by BSO_{bp} , DE and PSO on CEC'05 test functions with three dimensions.

Func tion	$D = 2$			$D = 10$			$D = 30$		
	BSO_{bp}	DE	PSO	BSO_{bp}	DE	PSO	BSO_{bp}	DE	PSO
F1	-450 (± 0)	-450 (± 0)	-450 (± 0)	-450 (± 0)	-450 ($\pm 9.28E - 07$)	-450 (± 0)	-450 (± 0)	-443.22 (± 2.40)	-450 (± 0)
F2	-450 (± 0)	-450 (± 0)	-450 (± 0)	-450 (± 0)	-449.98 ($\pm 9.10E - 03$)	-450 (± 0)	-448.75 (± 0.62)	4347.09 (± 914.46)	-450 (± 0)
F3	-450 (± 0)	-450 ($\pm 1.44E - 11$)	-450 (± 0)	61468.04 (± 118318.97)	321328.36 (± 1543.48)	-450 (± 0)	1893646.97 (± 515078.88)	38864770.59 (± 9344780)	-450 (± 0)
F4	-450 (± 0)	-450 (± 0)	-450 (± 0)	-442.49 (± 31.82)	-420.75 (± 6.28)	-450 (± 0)	20569.12 (± 3171.15)	9071.91 (± 2432.20)	-450 (± 0)
F5	-310 (± 0)	-310 ($\pm 7.44E - 09$)	-310 (± 0)	-309.41 (± 0.54)	-305.56 (± 1.50)	-310 (± 0)	4060.34 (± 702.73)	3401.96 (± 532.75)	-310 (± 0)
F6	390 (± 0)	390.01 ($\pm 3.43E - 02$)	390 (± 0)	395.64 (± 0.83)	989.38 (± 215.30)	390 (± 0)	969.88 (± 327.11)	20137.12 (± 11166.03)	390 (± 0)
F7	-140.85 (± 0)	-140.85 (± 0)	1365.43 ($\pm 4.21E - 05$)	1224.52 (± 60.75)	1233.03 (± 61.64)	16117.14 (± 123.31)	6644.19 (± 262.50)	4516.46 ($\pm 5.04E - 02$)	91818.51 (± 25170.02)
F8	-139.20 (± 3.16)	-133.91 (± 3.43)	637.07 ($\pm 2.31E - 13$)	-119.91 ($\pm 3.66E - 02$)	-119.62 ($\pm 9.77E - 02$)	8370.59 (± 5.77)	-119.51 (± 0.11)	-119.01 ($\pm 4.73E - 02$)	27464.96 (± 599.79)
F9	-330 (± 0)	-330 ($\pm 2E - 08$)	3752.51 ($\pm 2.80E - 13$)	-327.08 (± 1.04)	-301.11 (± 5.15)	23806.84 (± 6.62)	-299.92 (± 6.31)	-134.76 (± 14.32)	76610.87 (± 244.42)
F10	-330 (± 0)	-330 ($\pm 1.41E - 03$)	3752.51 ($\pm 8.44E - 14$)	-326.82 (± 1.24)	-293.15 (± 4.90)	23809.71 (± 11.41)	-300.96 (± 10.51)	-106.03 (± 15.18)	76610.28 (± 239.58)
F11	90 (± 0)	90.04 ($\pm 2.29E - 02$)	5006.91 ($\pm 1.69E - 13$)	92.72 (± 0.85)	99.34 (± 0.57)	28034.39 (± 0.75)	113.95 (± 2.99)	130.05 (± 1.15)	88556.31 (± 39.33)
F12	-460 (± 0)	-460 ($\pm 5.71E - 08$)	3957.28 ($\pm 7.36E - 13$)	-447.06 (± 11.57)	-315.62 (± 189.19)	25201.81 (± 7.82)	15761.19 (± 10756.16)	331923.67 (± 87780.46)	81112.90 (± 186.49)
F13	-130 (± 0)	-130 ($\pm 7.28E - 14$)	4540.95 ($\pm 1.85E - 12$)	-129.39 (± 0.19)	-127.07 (± 0.43)	26346.74 (± 1.60)	-125.03 (± 1.17)	-109.68 (± 1.56)	84291.93 (± 65.53)
F14	-300 (± 0)	-299.99 ($\pm 7.56E - 03$)	-300 (± 0)	-296.88 (± 0.31)	-296.24 (± 0.14)	-300 (± 0)	-287.61 (± 0.40)	-286.46 (± 0.11)	-300 (± 0)
F15	120 (± 0)	120 ($\pm 1.34E - 07$)	4202.51 ($\pm 1.69E - 13$)	208.57 (± 99.86)	454.54 (± 127.47)	24261.18 (± 13.69)	515.42 (± 93.43)	538.15 (± 58.32)	77007.77 (± 309.43)
F16	120 (± 0)	120 ($\pm 1.12E - 05$)	4202.51 (± 0)	206.33 (± 19.72)	294.42 (± 12.15)	24260.04 (± 11.26)	201.61 (± 92.58)	383.64 (± 39.16)	77070.08 (± 259.51)
F17	120 (± 0)	120 ($\pm 9.52E - 04$)	4202.51 (± 0)	213.08 (± 18.67)	316.62 (± 11.42)	24256.32 (± 7.68)	311.96 (± 164.71)	399.57 (± 26.96)	77128.95 (± 243.88)
F18	10 (± 0)	113.33 (± 103.34)	4092.51 (± 0)	762.28 (± 183.64)	395.35 (± 81.23)	24145.09 (± 4.66)	901.35 (± 46.48)	917.35 (± 0.16)	76904.68 (± 282.50)
F19	106.67 (± 49.01)	206.67 (± 18.26)	4092.51 ($\pm 2.53E - 13$)	713.12 (± 205.71)	376.67 (± 172.87)	24145.78 (± 5.31)	897.12 (± 48.90)	917.25 (± 0.21)	76917.20 (± 253.95)
F20	60 (± 62.97)	170 (± 81.37)	4092.51 (± 0)	824.40 (± 104.58)	310 ($\pm 4.77E - 03$)	24150.94 (± 11.30)	901.38 (± 46.49)	917.22 (± 0.26)	77056.71 (± 315.04)
F21	360 (± 0)	540 (± 61.03)	4442.51 (± 0)	766.67 (± 170.06)	860 ($\pm 1.55E - 06$)	24495.08 (± 8.47)	860.00 ($\pm 2.75E - 13$)	861.38 (± 0.53)	77306.95 (± 281.31)
F22	366.67 (± 36.51)	560 ($\pm 4.36E - 11$)	4442.51 (± 0)	934.37 (± 228.85)	1087.78 (± 144.97)	24495.06 (± 5.50)	1252.58 (± 9.15)	1275.96 (± 10.71)	77313.94 (± 378.95)
F23	360 (± 0)	597.43 (± 62.67)	4442.51 (± 0)	1035.54 (± 125.46)	1421.40 (± 204.20)	24497.67 (± 8.01)	907.59 (± 73.55)	895.20 (± 1.33)	77357.57 (± 280.56)
F24	438.43 (± 44.51)	457.97 (± 11.09)	4342.51 (± 0)	470 (± 54.77)	841.50 (± 315.68)	24403.47 (± 15.78)	460 (± 0)	462.63 (± 0.85)	77186.56 (± 265.88)
F25	360 (± 0)	367.09 (± 13.20)	4871.87 ($\pm 9.17E - 07$)	2006.78 (± 5.21)	2010.63 (± 6.00)	28030.92 (± 12.62)	1931.31 (± 6.39)	1910.50 (± 5.60)	86930.68 (± 301.92)

Table 3.19: Statistical results obtained by the Wilcoxon signed ranks test among BSO_{bp} , DE and PSO on CEC'05 test functions with three dimensions.

Algorithm	Dim	R^+	R^-	p-value	$\alpha=0.05$
BSO_{bp}	2	257.0	68.0	9.636E-03	Yes
vs.	10	263.0	62.0	5.578E-03	Yes
DE	30	246.5	78.5	0.02277	Yes
BSO_{bp}	2	289.5	10.5	5.841E-06	Yes
vs.	10	280.5	44.5	8.60E-04	Yes
PSO	30	261.0	39.0	8.462E-04	Yes

in contrast to DE and PSO . In 2 dimension, BSO possessing a power law distribution is remarkably superior to DE owning a poisson law distribution and PSO showing a truncated power law distribution, manifesting that the power law distribution effectively guides the population interaction to enhance the performance of algorithm comparing with a poisson law or a truncated power law distribution. A poisson law distribution indicates a random property of population interaction. A truncated power law distribution shows an incompletely power law attribute based on cutting off a part of data. Compared with these two distributions, a complete power law distribution has a more compact population interaction and maintains the relationship among the whole individuals. Thus, the effect of power law distribution can be more obvious and efficient than a poisson law or a truncated power law distribution. In 10 and 30 dimensions, although BSO can not completely implement a power law distribution, the trend towards a power law distribution also plays an essential role in the population interaction. This trend partially leads the evolution of population to gradually improve the qualities of individuals. Hence, BSO still performs better than DE and PSO . According to this characteristic, we can reasonably consider that the power law distribution is conducive to boosting the population interaction of BSO so as to refine its property. In the future work, modifying the structure of population to totally meet a power law distribution in high dimension is a promising research for enhancing the performance of BSO .

3.5 Conclusions

In this chapter, the population interaction of BSO is investigated by the PIN to analyze the performance of algorithm. The PIN is able to establish the connection among individuals and shows the characteristics of constructed network. Four experiments are conducted to discuss the population interaction of BSO in different dimensions, parameters, combinato-

rial parameter settings and related algorithms, respectively. The experimental results with 2, 10 and 30 dimensions demonstrate that the performance of BSO is the best on six benchmark functions and twenty five CEC'05 test functions with 2 dimension, and is worse and worse along with the increase of dimension. Meanwhile, the frequency of average degree in 2 dimension obviously shows a power law distribution comparing with that in 10 and 30 dimensions where the high dimension significantly influences the structures of functions so that the relationship among individuals can not completely satisfy a power law distribution anymore. Therefore, the occurrence of power law distribution indicates the validity and efficiency of BSO on the functions with low dimension and represents the good performance of BSO, which can effectively promote the population interaction to achieve the evolution of individuals.

The experimental results in different parameters verify that the respective parameter can influence the population interaction of BSO whereas the performance of algorithm is similar. Thus, the interactive influence among parameters is taken into account to investigate their best combinatorial result. The final combinatorial parameter setting manifests its efficiency for enhancing the performance of BSO. In the end, the comparisons among BSO, DE and PSO are discussed to illustrate that a complete power law distribution is beneficial for the population interaction so as to reinforce the performance of BSO.

Chapter 4

The research of gravitational search algorithm

4.1 Introduction

Since an effective population topology can remarkably influence the performances of EAs [48, 57], it is worth noticing and investigating to improve the GSA from the viewpoint of population structure. Based on the principle of conventional GSA, a hierarchical population structure can be implemented to further guide the evolution direction of individuals in the population. In this chapter, a three-layered hierarchical GSA with an effective gravitational constant (HGSA) is devised to address the premature convergence and low search ability of GSA. The hierarchical structure not only provides an effective guideline for individuals on each layer but also is beneficial for alleviating the stagnation of HGSA. A new gravitational constant strengthens the exploration ability of HGSA. Two weighted coefficients with time are designed to balance the exploration and exploitation process in HGSA. To evaluate the performance of HGSA, three experiments are conducted to compare it with six variants of GSA, five heuristic algorithms and seven variants of PSO on a number of benchmark functions. The results between HGSA and other six GSAs demonstrate that HGSA significantly enhances its exploration and exploitation abilities owing to its effective population structure and gravitational constant. The results between HGSA and five heuristic algorithms indicate that HGSA is a competitive and promising algorithm. The comparison between HGSA and seven kinds of PSOs verifies the notable performance of the hierarchical structure in HGSA. A component-wise experiment is carried out to analyze the effect of HGSA using a hierarchical structure and an improved gravitational constant. In addition, HGSA is used to resolve four real-world optimization problems and experimental

results manifest its effectiveness and practicability. Finally, the time complexity analysis is discussed to demonstrate that HGSA is the same computational efficient in comparison with other GSAs.

4.2 Conventional GSA

GSA inspired by the law of gravity and implemented by the gravitational force among individuals is a swarm intelligent algorithm. The gravitational force acts on everything and is different from other physical force. In particular, its effect is much significant for particles in the universe. The gravitational force among particles decides their motion trajectories where one particle with a higher mass tends to attract other particles with lower masses so as to change their motion direction and reduce their distance. Thus, the gravitational force between two particles is proportional to the product of their masses and inversely proportional to the square of their distance. The velocity and position of each particle are frequently altered due to the gravitational force among them. According to this mechanism, GSA is initially proposed to optimize the continuous functions [17].

In GSA, each particle is deemed as one individual. The influence of gravitational force on individuals is conducted by their masses expressed by the variant of fitness on functions, their distance and the gravitational constant. The gravitational force among individuals interacts with each one to guide their movement towards several individuals with higher masses. A high mass indicates a good fitness value. Hence, the movement direction of each individual stands for its evolutionary process from a low mass to a high mass. In other words, the communication among individuals is to use the gravitational force to enable the whole population to move towards a global optimal individual with the highest mass. For each individual, it possesses the attribute of position and mass, which indicates the composition and quality of a solution, respectively. The mass of each individual is improved by continually changing its position according to the gravitational force among individuals over the iterations.

The realizable process of GSA is described as follows. Firstly, the initialization of population is randomly generated by n individuals in which the i -th individual is formulated as $X_i = (x_i^1, x_i^2, \dots, x_i^d)$ where x_i^d is its position in the d -th dimension. Secondly, individuals X_i and X_j interact with each other in the d -th dimension with the iteration t via the

gravitational force $F_{ij}^d(t)$, expressed as

$$F_{ij}^d(t) = G(t) \frac{M_i(t) \times M_j(t)}{R_{ij}(t) + \epsilon} (x_j^d(t) - x_i^d(t)), \quad (4.1)$$

where $G(t)$ is a gravitational constant related with the iteration t , $M_i(t)$ and $M_j(t)$ are masses of two individuals. $R_{ij}(t)$ indicates the Euclidean distance between two individuals, defined as $R_{ij}(t) = \|X_i(t), X_j(t)\|_2$, and ϵ is a small constant. The gravitational constant $G(t)$ is described as

$$G(t) = G_0 \times e^{-\alpha \frac{t}{T}}, \quad (4.2)$$

where G_0 is an initial value and α is a constant. t and T indicate the current iteration number and the maximum iteration number, respectively. The mass $M_i(t)$ of individual X_i is formulated as follows:

$$m_i(t) = \frac{f_i(t) - w(t)}{b(t) - w(t)}, \quad (4.3)$$

$$M_i(t) = \frac{m_i(t)}{\sum_{l=1}^n m_l(t)}, \quad (4.4)$$

where $f_i(t)$ manifests the fitness value of individual X_i . $w(t)$ and $b(t)$ denote the worst and best fitness values of current population in the iteration t , respectively. For an individual X_i , the whole gravitational force $F_i^d(t)$ from other individuals in the d -th dimension is calculated as follow:

$$F_i^d(t) = \sum_{j \in K_b, j \neq i} rand_j F_{ij}^d(t), \quad (4.5)$$

where K_b indicates the K best individuals in the current population, and the K value is declined linearly from the initial n to 2. $rand_j$ is a uniform random value in the interval $[0,1]$ for the individual X_j . Thirdly, the acceleration $a_i^d(t)$ of individual X_i in the d -th dimension is formed by the gravitational force as follow:

$$a_i^d(t) = \frac{F_i^d(t)}{M_i(t)}. \quad (4.6)$$

Finally, the velocity $v_i^d(t+1)$ of individual X_i is updated to change its position in the next iteration $t+1$, given as follows:

$$v_i^d(t+1) = rand_i v_i^d(t) + a_i^d(t), \quad (4.7)$$

$$x_i^d(t+1) = x_i^d(t) + v_i^d(t+1), \quad (4.8)$$

where $rand_i$ indicates a uniform random value in the interval $[0,1]$ for the individual X_i .

4.3 Hierarchical GSA

4.3.1 Motivation

GSA has been widely used in diverse optimization and engineering application problems [123–126]. These results have also demonstrated that GSA is an effective and promising algorithm. However, its performance is limited by its potential mechanism such that a premature convergence is prone to occur and the search ability is low. This is because GSA uses the interactive information among individuals in the whole population to constantly evolve new individuals, whereas it is difficult for them to escape from the local optima once individuals are stagnated into the premature situation. Besides, the movement of individuals depend on their velocities controlled by their gravitational force and masses during the entire search process. In the late stage of searching process, the update velocities of individuals are so small that results in a low exploitation behavior for finding a better solution, implying that an inefficient update operation is used for further optimizing the search space. Thus, it is effective and valuable for balancing the search ability of GSA between exploration and exploitation in order to improve its performance from the beginning to the ending of optimization process. Taking into account these two disadvantages, a hierarchical population structure is adopted to alleviate them and enhance the search performance of GSA.

A hierarchical population structure is that individuals are ordered and placed on different layers according to some certain properties. On different layers, individuals have distinctive characteristics and function. The relationship among various layers can provide an effective guideline for individuals to efficiently evolve so that the whole population can be improved gradually [49,72]. As a result, these layers are defined as different levels from the top to bottom like a tree structure according to the actual influence of each layer on individuals. Top layer leads its next layer, and its next layer continues to lead its second layer. In this way, the interactive relationship among layers is constructed to form a hierarchical structure used to guide the evolution direction of individuals. The reason why a hierarchical population structure is effective for GSA is that the conventional GSA only uses the K best individuals to attract other individuals, and other individuals face the same circumstance and hardly escape from them once these K best individuals are trapped into

local optima. In the meantime, a slow exploitation operation further deteriorates this premature phenomenon and causes an adverse effect on the population evolution. Therefore, these K best individuals should need to be prevented from generating the premature convergence or be apt to get away from the local optima by a more effective guideline. From this point of view, a three-layered hierarchical population structure is proposed to strengthen the performance of GSA.

HGSA uses the hierarchical interaction among three layers to alleviate the above issues. Each layer has different properties of individuals. The population, K best individuals and global optimal individual are placed on different layers. For the population, the K best individuals act on them according to the gravitational force, which constructs a kind of interaction between two layers. However, this interaction can easily cause a premature convergence without any guidelines for the K best individuals. Thus, a global optimal individual is used to further attract the K best individuals, which also establishes a kind of interaction between two layers. According to the hierarchical interaction among three layers, the K best individuals are effectively guided to ameliorate the stagnation of GSA and the exploitation ability of population is enhanced. Moreover, to improve the exploration ability of population, a new log-sigmoid gravitational constant is proposed to replace the previous exponential one. It remarkably strengthens the gravitational force among individuals to expand their search ranges for finding a better solution. Two weighted coefficients with time cooperate with the hierarchical structure to finally implement an effective population interaction. In terms of the above motivation and mechanism, HGSA effectively achieves the hierarchical interaction among individuals and reinforces its performance.

4.3.2 Proposed HGSA

Conventional GSA adopts the gravitational force to associate individuals in the population and the K best individuals as better ones facilitate the population evolution. This kind of behavior actually constructs a specific population topology which can be regarded as a two-layered structure. To be specific, all the individuals in current population are on the bottom layer, and are evolved and guided by those K best individuals on the top layer. This kind of two-layered structure is able to guarantee that individuals on the bottom layer move towards those K best individuals on the top layer according to their gravitational force. Nevertheless, the K best individuals only rely on the gravitational force among them to further enhance themselves. This behavior brings an issue that they may be trapped into local optima and have no ability to escape so that the other individuals on the bottom layer

also move towards the local optima, and finally the whole population meets a premature convergence.

To address this issue, a three-layered hierarchical structure consisting of top, medium and bottom layers is established for GSA. Based on the original structure of GSA, we newly add a top layer and let the K best individuals be on the medium layer. On the top layer, a global optimal individual is adopted to be a better one than the K best individuals. The global optimal individual on the top layer attracts the K best individuals on the medium layer which guide the other ones on the bottom layer. On the basis of this structure, a hierarchical control is implemented from the top layer to medium layer and from the medium layer to bottom layer. That is to say, a global optimal individual leads the evolution of the K best individuals, and the K best individuals direct the movement of other individuals. In this way, a premature convergence can be effectively alleviated and individuals can derive valid interactive information to achieve a better evolution and development. Concrete construction and function of three layers are described as follows.

(1) Bottom layer: The whole population is placed on this layer, i.e., the distribution of all the individuals in current population is shown on this layer. Individuals move and evolve towards better ones in terms of the K best individuals on the medium layer. For a function optimization, this layer can reveal the landscape of function constructed by a large number of evolved individuals. In other words, the bottom layer provides a complete search space for the population, and individuals can implement their survival, elimination and reformation on it. Thus, this layer is defined as a bottom layer.

(2) Medium layer: In order to effectively guide the evolution of general individuals, the K best individuals are arranged on this layer. In each iteration, the medium layer always leads the bottom layer to accomplish the velocity update of individuals. It is worth noticing that each individual needs a great velocity so as to globally explore the entire search space in the beginning stage of search process, and gradually decreases the updated velocity over iterations. In the late stage of search process, an approximate optimum is found. Thus, the exploitation ability of individuals should play an essential role in further optimizing this approximate optimum. For the conventional GSA, the update velocity of each individual depends on its gravitational force and mass where the gravitational constant $G(t)$ significantly determines the value of gravitational force. That is to say, the exploration ability of GSA needs to be supported by a great gravitational constant $G(t)$ and its exploitation ability needs a small one. The conventional GSA adopts an exponential $G(t)$ to calculate the gravitational force. However, this kind of exponential change can make its exploration ability

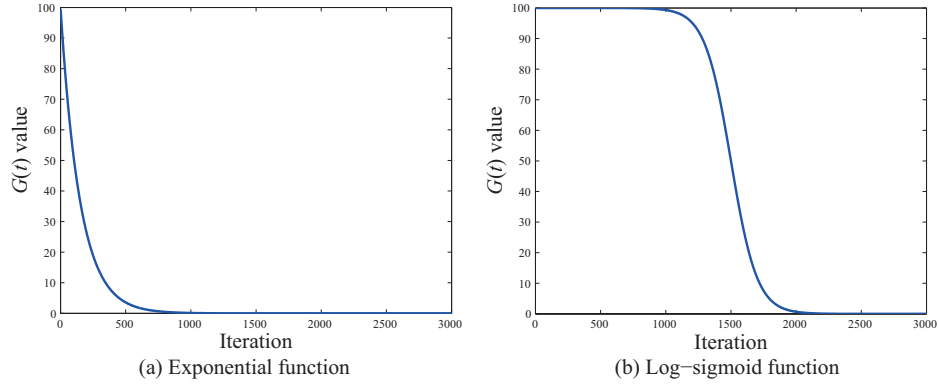


Figure 4.1: The graphs of conventional and new gravitational constant $G(t)$.

weak, meaning that GSA insufficiently explores the entire search space in the early phase so that the exploitation operation acts on an inferior optimum, and the resultant optimum is not the best. Thus, to improve its exploration ability, a new $G(t)$ is proposed to replace the exponential one.

We use a log-sigmoid transfer function to create a new gravitational constant $G(t)$, and the formula is given as follow:

$$G(t) = \frac{G_0}{1 + e^{\frac{t-T}{L}}}, \quad (4.9)$$

where t indicates the current iteration number and T is the maximum iteration number. L is a step length. According to this log-sigmoid transfer function, the value of $G(t)$ is obviously different from the original one. The graphs of both changing values with 3000 iterations and $G_0 = 100$ are shown in Fig. 4.1. From Fig. 4.1(a), it can be seen that the value of $G(t)$ declines quickly before 1500 iterations, suggesting the exploration ability of GSA weakens quickly. However, in Fig. 4.1(b), the value of $G(t)$ consistently maintains great before 1500 iterations, and subsequently it decreases quickly to approximate 0. This effect can guarantee a strong exploration ability of GSA in the early phase such that it has sufficient time to seek for an approximate optimum which can be further refined by its next exploitation ability. Therefore, both difference primarily focuses on the value of $G(t)$ in the early search process. In other words, new proposed $G(t)$ can obviously enhance the exploration ability of GSA. On the medium layer, this new revision is executed to change the gravitational force among individuals so as to influence their velocities and eventually implement the evolution of individuals on the bottom layer. In addition, since the K value decreases gradually with iterations, meaning the number of best individuals on this layer

dynamically reduces. It is beneficial for the global optimal individual on the top layer to efficiently and promisingly guide several elite individuals in current population in order to offer a better evolution direction to all the individuals on the bottom layer.

(3) Top layer: To provide an effective management for the medium layer, a global optimal individual is selected and placed on this layer. In each iteration, the K best individuals on the medium layer are chosen to be compared with the global optimal individual. If a better individual exists, this global optimal individual is replaced by it. The global optimal individual possesses the highest mass and the best position in current population. Thus, it can further attract several best individuals to move towards it. This method can bring two advantages to GSA. On the one hand, it can keep the K best individuals from trapping into the local optima. This is because the conventional GSA is liable to converge into a local optimum only by the gravitational force without the assistance of other mechanisms, while a global optimal individual can persistently attract other best individuals to enable them to escape from the stagnation so as to help the whole population continue to seek for a better position. On the other hand, this global optimal individual can accelerate the convergence speed of population. When the K best individuals without occurring a premature situation are further attracted by it, the movement speed of individuals is increased quickly to reduce the distance between them and the global optimal individual. According to this mechanism, the formula of update velocity of the K best individuals guided by the global optimal individual is described as follows:

$$v'_{i \in K_b}(t+1) = g_{opt}^d - X_{i \in K_b}^d(t), \quad (4.10)$$

where g_{opt} indicates the global optimal individual. Adding this kind of extra update velocity on the top layer can effectively alleviate the premature convergence of GSA and enhance its performance. Hence, an ultimate three-layered hierarchical population structure is completely constructed to boost the evolution of individuals in GSA, and its illustrative graph is plotted in Fig. 4.2. In Fig. 4.2, there are n (e.g., $n = 6$) individuals in the population on the bottom layer. They are attracted by the K (e.g., $K = 2$) best individuals consisting of individuals 2 and 3 on the medium layer. Finally, a global optimal individual on the top layer guides the $K = 2$ best individuals on the medium layer.

Another disadvantage of GSA which should be concerned is that its exploitation ability is low in the late stage of search process. Moreover, our new added top layer may influence the exploration ability of GSA in the early stage. Taking into account these two issues, we adopt two weighted coefficients with time $w_1(t)$ and $w_2(t)$ to balance their relationship. The

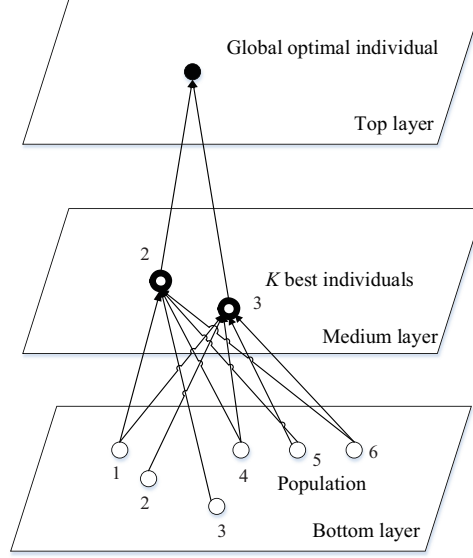


Figure 4.2: A three-layered structure of HGSA.

formulas of final update velocity of individuals on the medium layer and the bottom layer are given, respectively as follows:

$$v'_{i \in K_b}(t+1) = w_2(t) \times (g_{opt}^d - X_{i \in K_b}^d(t)), \quad (4.11)$$

$$v_i^d(t+1) = rand_i v_i^d(t) + w_1(t) \times a_i^d(t) + v'_{i \in K_b}(t+1), \quad (4.12)$$

where $w_1(t) = 1 - \frac{t^6}{T^6}$ and $w_2(t) = \frac{t^6}{T^6}$. Two weighted coefficients are set to not only intensify the relationship among three layers but also guarantee the effective transformation between exploration and exploitation abilities of GSA in different search phases. Their purpose is to use $w_1(t)$ to enhance the exploration ability of GSA in the early half stage of search process and use $w_2(t)$ to reinforce the exploitation ability of GSA in the late half stage of search process. The figure regarding two weighted coefficients in 3000 iterations is plotted in Fig. 4.3. From it, we can observe that $w_1(t)$ maintains a great value before 1500 iterations, and then declines gradually to 0. Nevertheless, $w_2(t)$ is the opposite. This kind of operation can correspond to our proposed new $G(t)$. In a early half stage of search process, a great value of $w_1(t)$ takes charge of a strong exploration of GSA whereas $w_2(t)$ approximating to 0 disables the exploitation of GSA. Whereafter, the values of $w_1(t)$ and $w_2(t)$ progressively decline and ascend, respectively, suggesting that the exploration ability of GSA begins to decay and its exploitation ability is gradually improved. Based on this manipulation, we can effectively balance the exploration and exploitation of GSA and enhance its property

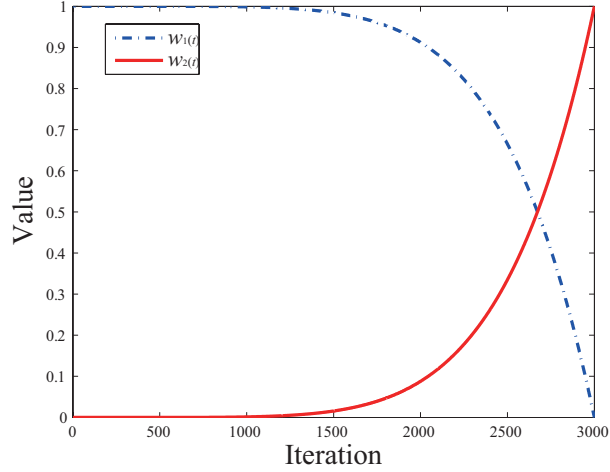


Figure 4.3: The curves of two weighted coefficients $w_1(t)$ and $w_2(t)$.

in the whole search period. Therefore, a complete HGSA is established.

The primary procedures of HGSA are described as follows: 1) Set up the parameters of GSA; 2) Initialize a random population on the bottom layer and construct two empty populations on the medium and top layers; 3) Justify the search boundary of each individual on the bottom layer; 4) Evaluate the fitness (i.e., objective function value) of each individual on the bottom layer according to the objective function; 5) Calculate the mass of each individual on the bottom layer according to Eqs. (4.3) and (4.4); 6) Calculate the current gravitational constant according to Eq. (4.9); 7) Select the K best individuals in current population to be placed on the medium layer according to their K values and masses; 8) Determine the best individual among the K best individuals as a global optimal one on the top layer; 9) The global optimal individual on the top layer updates the velocities of the K best individuals on the medium layer according to Eq. (4.11); 10) The resultant gravitational force of each individual on the bottom layer is obtained by the K best individuals on the medium layer according to Eqs. (4.1) and (4.5); 11) The corresponding acceleration of each individual is calculated by Eq. (4.6); 12) The K best individuals on the medium layer update the velocities of individuals on the bottom layer according to Eq. (4.12), and then the movement of each individual is implemented by Eq. (4.8); 13) Repeat procedures 3) - 12) until the termination criteria is satisfied. The implementation of HGSA is shown in Algorithm 2.

In order to further illustrate the explicit characteristics of HGSA, Fig. 4.4 is plotted to show its operating principle on the multi-modal landscape with local optima. Figs.

Algorithm 2: HGSA

Input: Parameters $n, d, K, G_0, L, w_1, w_2, t, T$
Output: The optimal solution

- 1 **Initialization:** Randomly generate an initial population $\{X_1, X_2, \dots, X_n\}$ on the bottom layer. The medium and top layers are empty;
- 2 **while** the termination criterion is not satisfied **do**
- 3 **for** $i = 1$ to n **do**
- 4 **if** individual X_i on the bottom layer is beyond the boundary **then**
- 5 Individual X_i is randomly initialized;
- 6 **for** $i = 1$ to n **do**
- 7 Evaluate the fitness $f_i(t)$ of individual X_i on the bottom layer according to the objective function;
- 8 **for** $i = 1$ to n **do**
- 9 Calculate the mass $M_i(t)$ of individual X_i on the bottom layer according to Eqs. (4.3) and (4.4);
- 10 Calculate the current gravitational constant $G(t)$ according to Eq. (4.9);
- 11 Select the K best individuals in current population as a set K_b to be placed on the medium layer according to their K values and masses;
- 12 **if** $t == 1$ **then**
- 13 Select the minimum $f_{K_{b_i}}(t)$ among the K_b as the fitness $f_{opt}(t)$ of global optimal individual g_{opt} , and the individual K_{b_i} as the global optimal individual g_{opt} is placed on the top layer ;
- 14 **else**
- 15 **if** $f_{opt}(t) > \text{minimum } f_{K_{b_i}}(t)$ **then**
- 16 $g_{opt} = K_{b_i}$;
- 17 $f_{opt}(t) = \text{minimum } f_{K_{b_i}}(t)$;
- 18 **for** $j = 1$ to K **do**
- 19 g_{opt} on the top layer updates the velocity of individual K_{b_j} on the medium layer according to Eq. (4.11);
- 20 **for** $i = 1$ to n **do**
- 21 **for** $j = 1$ to K **do**
- 22 Individual K_{b_j} on the medium layer attracts individual X_i on the bottom layer according to Eqs. (4.1) and (4.5);
- 23 **for** $i = 1$ to n **do**
- 24 The velocity and position of individual X_i on the bottom layer are updated according to Eqs. (4.6), (4.12) and (4.8);
- 25 $t = t + 1$;

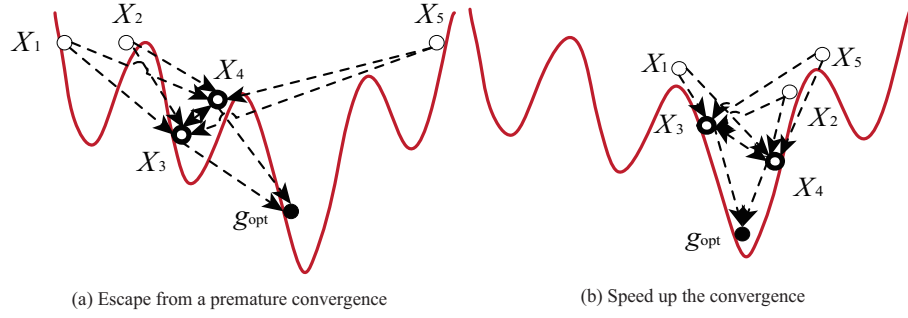


Figure 4.4: The illustrative graphs of the operating principle of HGSA.

4.4(a) and (b) explain why our proposed HGSA is effective for handling the premature convergence or accelerating the convergence. There are n (e.g., $n = 5$) individuals in the population where individuals X_3 and X_4 are the K (e.g., $K = 2$) best individuals. In Fig. 4.4(a), it can be observed that individuals X_3 and X_4 are moving towards a local optimum, whereas a global optimal individual g_{opt} provides an extra direction for them to help them escape from the local optimum. In Fig. 4.4(b), when individuals X_3 and X_4 are not trapped into a premature convergence, they can effectively attract other individuals to move towards them. Meanwhile, the global optimal individual g_{opt} further accelerates the movement of individuals X_3 and X_4 so as to enhance the convergence speed of population. Consequently, HGSA can effectively enhance its exploration and exploitation abilities in the search process.

4.4 Experiment and analysis

To evaluate the performance of HGSA, three comparative experiments are carried out. The first experiment compares HGSA with six kinds of GSAs on fifty seven benchmark functions with three kinds of dimensions from CEC2013 and CEC2017 [127, 128]. The second experiment conducts a contrast between HGSA and five heuristic algorithms on fifty seven benchmark functions. The last experiment analyzes the performances of HGSA and seven variants of PSO on twenty eight benchmark functions from CEC2013.

4.4.1 Experimental setup

In order to assess the property of HGSA, fifty seven benchmark functions (F1-F57) consisting of twenty eight CEC2013 benchmark functions (F1-F28) and twenty nine CEC2017

benchmark functions (F29-F57) are adopted. A large number of benchmark functions are used so as to avoid a potential risk such as trapping into the local optima caused by some algorithms, assure the accuracy and reliability of experimental results, and provide a fair contrast among various algorithms. In CEC2013 benchmark functions, F1-F5 are unimodal functions and F6-F20 are multimodal functions. F21-F28 indicate composition functions. In them, numerous functions are rotated to increase their complexity. In CEC2017 benchmark functions, there are two unimodal functions (F29-F30), seven multimodal functions (F31-F37), ten hybrid functions (F38-F47) and ten composition functions (F48-F57). Compared with CEC2013 functions, CEC2017 have many shifted and rotated functions which are more complex and difficult to be resolved. Both optimal solutions are obviously different. According to these two sets of test functions, HGSA can be effectively measured to show its performance.

For three experiments, the common parameters of all the algorithms are set as follows: The termination criterion is the maximum number of function evaluations (NFEs) set to be $D * 10000$ where D is the dimension of the benchmark function. The search range is in $[-100, 100]^D$. Other parameters of each algorithm are set according to its corresponding reference. For each function, each algorithm is independently run 30 times to acquire its statistical results. All the algorithm are implemented by a Matlab software on a PC with 3.30GHz Intel(R) Core(TM) i5 CPU and 8GB RAM.

4.4.2 Comparison between HGSA and other GSAs

To observe the performance of HGSA, six kinds of GSAs including GSA [17], GGSA [123], CGSA-M [86], PSO-GSA [87], MGSA [129] and DNLGSA [130] are adopted to make a comparison. Conventional GSA is compared to primarily show the degree of improvement of HGSA. GGSA uses the best individual to enhance its exploitation ability in the search process. CGSA-M memory-selectively incorporates multiple chaotic maps into GSA to further exploit a small search space. PSO-GSA combines the exploration of GSA with the exploitation of PSO to improve its overall performance. MGSA adds a memory ability into GSA from the viewpoint of global and local optimal solutions to strengthen its search accuracy. DNLGSA uses a dynamic neighborhood learning scheme to change its local and global neighborhood topologies for balancing its exploration and exploitation abilities. To explicitly show the property of each algorithm, fifty seven benchmark functions with three different dimensions, i.e., $D = 10, 30$ and 50 , are used to test their performances on low, medium and high dimensions. The population size n is set to be 100. Their pa-

rameters are listed in Table 4.1. The experimental results composed of mean and standard deviation are summarized in Tables 4.2, 4.3 and 4.4, and the best result on each function is highlighted by a bold font.

From Tables 4.2, 4.3 and 4.4, we can find that HGSA can obtain the best solutions on numerous benchmark functions with 10, 30 and 50 dimensions, suggesting that HGSA has a strong exploration and exploitation ability for finding an optimal solution. To provide more accurate conclusions, the statistical analysis is conducted by the Wilcoxon signed ranks test at a significant level of $\alpha = 0.05$ in Table 4.5. From it, we can see that HGSA significantly outperforms other six GSAs on all the benchmark functions with 10, 30 and 50 dimensions according to *p-value*. It demonstrates that a hierarchical structure can notably change the search ability of individuals and an improved gravitational constant can effectively enhance the exploration ability of GSA. In addition, although HGSA performs the best among seven algorithms on all the benchmark functions with three dimensions, *p-values* in $D = 30$ and 50 are less, indicating that it can more effectively act on medium and high dimensions. It manifests that HGSA can effectively optimize the functions with diverse dimensions due to its hierarchical structure, and especially has a better performance in medium and high dimensions. Furthermore, DNLGSA which is a kind of state-of-the-art GSA adopts a neighborhood structure to randomly divide the whole population and control the gravitational force among neighborhoods. In fact, it belongs to a kind of distributed population structure, which includes several subpopulations to enhance the diversity of GSA. The comparison between HGSA and DNLGSA demonstrates that HGSA has a better performance. In other words, a hierarchical structure is more suitable than a distributed structure for the evolution of population in GSA. To be specific, on the one hand, HGSA uses an effective gravitational constant to reinforce its exploration ability. On the other hand, a hierarchical structure is also beneficial for further guiding the evolution of individuals on different layers so as to eventually enhance the performance of GSA. Experimental results indicate this kind of mechanism is more effective than DNLGSA with neighborhoods. Hence, we can conclude that HGSA is a superior and competitive algorithm among various variants of GSA for numerous functions with different dimensions.

To intuitively show the performances of seven kinds of GSAs, Fig. 4.5 is plotted to reveal the box-and-whisker diagrams of thirty optimal solutions obtained by each algorithm on F7 and F38 with 10, 30 and 50 dimensions. In it, the vertical axis indicates the optimal solution and the horizontal axis denotes seven algorithms. From Figs. 4.5(a) and (d), we can see that each algorithm finds different optimal solutions which have a distinct

Table 4.1: Parameter settings of HGSA and other GSAs.

Algorithm	Parameters
HGSA	$G_0 = 100, L = 100, w_1(t) = 1 - t^6/T^6, w_2(t) = t^6/T^6, K \in [n, 2]$
GSA	$G_0 = 100, \alpha = 20, K \in [n, 2]$
GGSA	$G_0 = 100, \alpha = 20, w_1(t) = 2 - 2t^3/T^3, w_2(t) = 2t^3/T^3, K \in [n, 2]$
CGSA-M	$G_0 = 100, \alpha = 20, LP = 50, K \in [n, 2]$
PSOGSA	$G_0 = 100, \alpha = 20, w_1(t) = 0.5, w_2(t) = 1.5, K \in [n, 2]$
MGSA	$G_0 = 100, \alpha = 20, w_1(t) = 0.5, w_2(t) = 0.5, K \in [n, 2]$
DNLGSA	$G_0 = 100, \alpha = 20, w_1(t) = 0.5 - 0.5t^{1/6}/T^{1/6}, w_2(t) = 1.5t^{1/6}/T^{1/6}, K = 10, gm = 5$

Table 4.2: Experimental results of benchmark functions (F1-F57) with $D = 10$ dimensions using HGSA, GSA, GGSA, CGSA-M, PSO GSA, MGSA and DNLGSA.

Algorithm	F1	F2	F3	F4	F5	F6
HGSA	-1.40E+03 ± 2.00E-09	7.96E+03 ± 1.04E+04	-1.20E+03 ± 5.37E-01	1.01E+04 ± 2.62E+03	-1.00E+03 ± 1.12E-08	-8.91E+02 ± 3.05E+00
GSA	-1.40E+03 ± 0.00E+00	5.00E+06 ± 7.31E+05	7.67E+08 ± 6.56E+08	1.63E+04 ± 2.10E+03	-1.00E+03 ± 8.61E-05	-8.30E+02 ± 1.78E+00
GGSA	-1.40E+03 ± 0.00E+00	3.73E+06 ± 7.79E+05	1.61E+08 ± 1.31E+08	1.13E+04 ± 2.05E+03	-1.00E+03 ± 3.86E-07	-8.37E+02 ± 6.80E+00
CGSA-M	-1.40E+03 ± 0.00E+00	4.86E+06 ± 7.82E+05	7.48E+08 ± 4.34E+08	1.61E+04 ± 2.43E+03	-1.00E+03 ± 6.28E-05	-8.31E+02 ± 1.82E+00
PSO GSA	-1.40E+03 ± 0.00E+00	9.60E+05 ± 1.67E+06	4.60E+07 ± 2.01E+08	4.02E+03 ± 3.24E+03	-1.00E+03 ± 5.91E-13	-8.84E+02 ± 2.06E+01
MGSA	-1.40E+03 ± 0.00E+00	8.75E+05 ± 9.65E+05	9.39E+07 ± 1.33E+08	1.83E+04 ± 6.98E+03	-1.00E+03 ± 8.83E-07	-8.76E+02 ± 2.75E+01
DNLGSA	-1.40E+03 ± 0.00E+00	2.96E+06 ± 2.09E+06	7.04E+08 ± 1.59E+09	1.89E+04 ± 8.39E+03	-1.00E+03 ± 1.08E-08	-8.76E+02 ± 2.69E+01
	F7	F8	F9	F10	F11	F12
HGSA	-8.00E+02 ± 2.78E-04	-6.80E+02 ± 6.53E-02	-5.98E+02 ± 9.61E-01	-5.00E+02 ± 8.13E-03	-3.95E+02 ± 2.11E+00	-2.98E+02 ± 1.40E+00
GSA	-7.73E+02 ± 1.65E+01	-6.80E+02 ± 8.06E-02	-5.94E+02 ± 1.24E+00	-5.00E+02 ± 1.06E-01	-3.51E+02 ± 7.61E+00	-2.47E+02 ± 9.77E+00
GGSA	-7.74E+02 ± 1.82E+01	-6.80E+02 ± 9.29E-02	-5.97E+02 ± 1.16E+00	-5.00E+02 ± 5.46E-02	-3.91E+02 ± 3.28E+00	-2.93E+02 ± 2.64E+00
CGSA-M	-7.68E+02 ± 2.13E+01	-6.80E+02 ± 8.16E-02	-5.95E+02 ± 1.40E+00	-5.00E+02 ± 9.84E-02	-3.53E+02 ± 9.32E+00	-2.49E+02 ± 1.04E+01
PSO GSA	-7.44E+02 ± 3.21E+01	-6.80E+02 ± 7.97E-02	-5.95E+02 ± 1.96E+00	-5.00E+02 ± 2.19E-01	-3.86E+02 ± 7.99E+00	-2.66E+02 ± 2.05E+01
MGSA	-7.49E+02 ± 2.52E+01	-6.80E+02 ± 9.84E-02	-5.96E+02 ± 1.39E+00	-5.00E+02 ± 1.24E-01	-3.86E+02 ± 7.26E+00	-2.77E+02 ± 9.27E+00
DNLGSA	-7.43E+02 ± 2.88E+01	-6.80E+02 ± 1.16E-01	-5.94E+02 ± 1.80E+00	-4.92E+02 ± 9.23E+00	-3.77E+02 ± 1.18E+01	-2.69E+02 ± 2.05E+01
	F13	F14	F15	F16	F17	F18
HGSA	-1.97E+02 ± 2.28E+00	4.83E+02 ± 1.77E+02	3.33E+02 ± 1.02E+02	2.00E+02 ± 3.87E-03	3.12E+02 ± 1.20E+00	4.13E+02 ± 1.79E+00
GSA	-1.19E+02 ± 9.50E+00	9.28E+02 ± 2.78E+02	8.39E+02 ± 1.76E+02	2.00E+02 ± 2.40E-02	3.13E+02 ± 1.13E+00	4.13E+02 ± 1.11E+00
GGSA	-1.82E+02 ± 8.80E+00	5.63E+02 ± 2.15E+02	3.69E+02 ± 1.41E+02	2.00E+02 ± 9.17E-02	3.11E+02 ± 5.02E-01	4.12E+02 ± 1.04E+00
CGSA-M	-1.26E+02 ± 8.84E+00	8.33E+02 ± 2.88E+02	8.11E+02 ± 2.11E+02	2.00E+02 ± 2.86E-02	3.13E+02 ± 1.39E+00	4.12E+02 ± 8.72E-01
PSO GSA	-1.48E+02 ± 1.60E+01	3.44E+02 ± 1.67E+02	1.06E+03 ± 3.47E+02	2.00E+02 ± 1.70E-01	3.33E+02 ± 1.35E+01	4.42E+02 ± 1.27E+01
MGSA	-1.55E+02 ± 1.43E+01	4.87E+02 ± 2.36E+02	7.14E+02 ± 2.82E+02	2.01E+02 ± 3.53E-01	3.18E+02 ± 4.03E+00	4.21E+02 ± 5.75E+00
DNLGSA	-1.41E+02 ± 2.33E+01	6.31E+02 ± 2.54E+02	1.15E+03 ± 2.65E+02	2.00E+02 ± 1.98E-01	3.37E+02 ± 1.26E+01	4.43E+02 ± 1.38E+01
	F19	F20	F21	F22	F23	F24
HGSA	5.01E+02 ± 2.65E-01	6.03E+02 ± 4.51E-01	1.10E+03 ± 1.75E-10	1.69E+03 ± 3.69E+02	1.74E+03 ± 1.99E+02	1.22E+03 ± 4.37E+00
GSA	5.02E+02 ± 2.33E-01	6.04E+02 ± 3.07E-01	1.10E+03 ± 4.63E-13	3.08E+03 ± 2.24E+02	2.47E+03 ± 2.82E+02	1.23E+03 ± 4.71E+00
GGSA	5.01E+02 ± 2.78E-01	6.04E+02 ± 2.86E-01	1.10E+03 ± 4.63E-13	2.39E+03 ± 4.20E+02	1.82E+03 ± 2.37E+02	1.22E+03 ± 4.29E+00
CGSA-M	5.02E+02 ± 3.32E-01	6.04E+02 ± 3.07E-01	1.10E+03 ± 4.63E-13	2.90E+03 ± 2.84E+02	2.43E+03 ± 2.78E+02	1.23E+03 ± 5.05E+00
PSO GSA	5.01E+02 ± 3.89E-01	6.03E+02 ± 6.52E-01	1.07E+03 ± 6.52E+01	1.43E+03 ± 2.54E+02	2.16E+03 ± 3.97E+02	1.22E+03 ± 6.12E+00
MGSA	5.01E+02 ± 2.30E-01	6.03E+02 ± 5.16E-01	1.10E+03 ± 4.63E-13	1.84E+03 ± 4.89E+02	2.19E+03 ± 4.13E+02	1.22E+03 ± 5.82E+00
DNLGSA	5.02E+02 ± 6.09E-01	6.04E+02 ± 4.48E-01	1.06E+03 ± 8.95E+01	1.73E+03 ± 2.87E+02	2.32E+03 ± 4.09E+02	1.22E+03 ± 1.51E+01
	F25	F26	F27	F28	F29	F30
HGSA	1.31E+03 ± 9.09E+00	1.44E+03 ± 5.81E+01	1.70E+03 ± 2.89E-05	1.80E+03 ± 6.09E-04	4.72E+02 ± 6.85E+02	3.00E+02 ± 1.18E-08
GSA	1.32E+03 ± 3.52E+00	1.50E+03 ± 4.44E+01	1.70E+03 ± 1.83E-10	2.19E+03 ± 8.86E+01	2.73E+02 ± 1.17E+02	1.01E+04 ± 1.58E+03
GGSA	1.31E+03 ± 1.07E+01	1.45E+03 ± 6.41E+01	1.70E+03 ± 6.17E-11	2.05E+03 ± 2.46E+01	2.10E+02 ± 2.12E+02	5.49E+03 ± 1.47E+03
CGSA-M	1.32E+03 ± 3.34E+00	1.49E+03 ± 4.27E+01	1.70E+03 ± 2.46E-10	2.17E+03 ± 6.88E+01	3.00E+02 ± 3.27E+02	1.06E+04 ± 1.58E+03
PSO GSA	1.32E+03 ± 2.10E+01	1.38E+03 ± 5.28E+01	1.79E+03 ± 1.27E+02	1.83E+03 ± 2.06E+02	8.87E+04 ± 4.76E+05	3.00E+02 ± 1.83E-14
MGSA	1.32E+03 ± 9.13E+00	1.40E+03 ± 6.89E+01	1.69E+03 ± 9.62E+01	1.89E+03 ± 1.94E+02	1.19E+03 ± 9.72E+02	3.21E+02 ± 5.21E+01
DNLGSA	1.31E+03 ± 2.26E+01	1.41E+03 ± 6.41E+01	1.75E+03 ± 8.51E+01	1.88E+03 ± 2.29E+02	2.42E+03 ± 2.40E+03	3.92E+02 ± 1.24E+02
	F31	F32	F33	F34	F35	F36
HGSA	4.00E+02 ± 4.33E-02	5.18E+02 ± 3.84E+00	6.00E+02 ± 1.77E-01	7.12E+02 ± 1.04E+00	8.17E+02 ± 2.65E+00	9.00E+02 ± 1.45E-09
GSA	4.07E+02 ± 4.53E-01	5.58E+02 ± 7.77E+00	6.28E+02 ± 6.86E+00	7.14E+02 ± 1.54E+00	8.21E+02 ± 3.68E+00	9.00E+02 ± 0.00E+00
GGSA	4.06E+02 ± 5.00E-01	5.19E+02 ± 5.04E+00	6.00E+02 ± 3.51E-01	7.12E+02 ± 8.04E-01	8.11E+02 ± 2.84E-01	9.00E+02 ± 2.11E-14
CGSA-M	4.07E+02 ± 3.79E+00	5.61E+02 ± 8.19E+00	6.27E+02 ± 6.18E+00	7.14E+02 ± 1.94E+00	8.20E+02 ± 4.09E+00	9.03E+02 ± 1.76E+01
PSO GSA	4.03E+02 ± 5.56E+00	5.22E+02 ± 7.55E+00	6.02E+02 ± 3.48E+00	7.34E+02 ± 8.29E+00	8.21E+02 ± 7.90E+00	1.08E+03 ± 3.93E+02
MGSA	4.05E+02 ± 1.13E+01	5.26E+02 ± 1.12E+01	6.02E+02 ± 2.42E+00	7.19E+02 ± 5.15E+00	8.16E+02 ± 6.87E+00	9.08E+02 ± 3.06E+01
DNLGSA	4.09E+02 ± 1.30E+01	5.27E+02 ± 8.97E+00	6.08E+02 ± 8.38E+00	7.38E+02 ± 1.59E+01	8.18E+02 ± 6.93E+00	1.03E+03 ± 1.82E+02
	F37	F38	F39	F40	F41	F42
HGSA	2.26E+03 ± 2.02E+02	1.12E+03 ± 7.38E+00	8.70E+03 ± 3.22E+03	6.73E+03 ± 1.56E+03	4.39E+03 ± 9.68E+02	3.56E+03 ± 1.29E+03
GSA	2.74E+03 ± 2.85E+02	1.16E+03 ± 2.21E+01	8.12E+05 ± 3.79E+05	1.08E+04 ± 1.25E+03	6.12E+03 ± 1.66E+03	1.74E+04 ± 3.36E+03
GGSA	2.45E+03 ± 2.20E+02	1.13E+03 ± 9.86E+00	4.26E+05 ± 2.49E+05	1.03E+04 ± 1.76E+03	2.62E+03 ± 3.36E+02	3.81E+03 ± 1.17E+03
CGSA-M	2.79E+03 ± 2.29E+02	1.15E+03 ± 2.10E+01	7.51E+05 ± 3.92E+05	1.10E+04 ± 1.79E+03	4.89E+03 ± 1.82E+03	1.45E+04 ± 4.67E+03
PSO GSA	1.72E+03 ± 3.48E+02	1.12E+03 ± 1.41E+01	1.72E+04 ± 1.26E+04	9.06E+03 ± 6.93E+03	2.05E+03 ± 4.73E+02	4.72E+03 ± 4.83E+03
MGSA	1.94E+03 ± 2.96E+02	1.14E+03 ± 1.86E+01	3.53E+04 ± 3.18E+04	1.02E+04 ± 5.18E+03	4.85E+03 ± 3.49E+03	5.42E+03 ± 4.07E+03
DNLGSA	1.92E+03 ± 2.57E+02	1.15E+03 ± 2.77E+01	1.46E+05 ± 7.39E+05	9.50E+03 ± 7.83E+03	2.73E+03 ± 1.45E+03	5.65E+03 ± 4.72E+03
	F43	F44	F45	F46	F47	F48
HGSA	1.98E+03 ± 7.42E+01	1.76E+03 ± 1.28E+01	5.48E+03 ± 2.34E+03	5.86E+03 ± 1.87E+03	2.15E+03 ± 4.40E+00	2.31E+03 ± 4.33E+01
GSA	2.12E+03 ± 9.49E+01	1.86E+03 ± 1.11E+02	9.85E+03 ± 3.50E+03	6.22E+04 ± 2.51E+04	2.24E+03 ± 5.77E+01	2.35E+03 ± 3.10E+01
GGSA	2.02E+03 ± 1.18E+02	1.77E+03 ± 2.37E+01	3.35E+03 ± 9.11E+02	4.92E+03 ± 1.01E+03	2.17E+03 ± 4.61E+01	2.31E+03 ± 3.88E+01
CGSA-M	2.14E+03 ± 9.69E+01	1.83E+03 ± 7.69E+01	7.80E+03 ± 2.44E+03	4.96E+04 ± 3.12E+04	2.25E+03 ± 7.93E+01	2.36E+03 ± 1.97E+01
PSO GSA	1.78E+03 ± 1.23E+02	1.77E+03 ± 4.88E+01	5.54E+03 ± 3.79E+03	5.56E+03 ± 3.57E+03	2.10E+03 ± 5.90E+01	2.29E+03 ± 5.18E+01
MGSA	1.86E+03 ± 1.37E+02	1.79E+03 ± 6.21E+01	1.03E+04 ± 7.37E+03	6.73E+03 ± 3.90E+03	2.12E+03 ± 6.55E+01	2.29E+03 ± 5.87E+01
DNLGSA	1.82E+03 ± 1.53E+02	1.79E+03 ± 4.69E+01	5.68E+03 ± 3.79E+03	5.82E+03 ± 4.15E+03	2.13E+03 ± 7.78E+01	2.28E+03 ± 5.90E+01
	F49	F50	F51	F52	F53	F54
HGSA	2.30E+03 ± 5.23E-02	2.64E+03 ± 7.89E+00	2.52E+03 ± 6.20E+01	2.94E+03 ± 8.28E+00	2.82E+03 ± 4.07E+01	3.10E+03 ± 4.54E+00
GSA	2.30E+03 ± 2.26E-11	2.76E+03 ± 4.04E+01	2.52E+03 ± 7.18E+01	2.94E+03 ± 1.36E+01	3.55E+03 ± 7.22E+02	3.26E+03 ± 3.85E+01
GGSA	2.30E+03 ± 8.53E-12	2.65E+03 ± 1.26E+01	2.67E+03 ± 1.34E+02	2.94E+03 ± 8.04E+00	2.83E+03 ± 4.79E+01	3.18E+03 ± 2.03E+01
CGSA-M	2.30E+03 ± 2.02E-01	2.76E+03 ± 2.54E+01	2.59E+03 ± 1.45E+02	2.94E+03 ± 8.05E+00	3.53E+03 ± 6.22E+02	3.27E+03 ± 4.73E+01
PSO GSA	2.30E+03 ± 6.14E+00	2.63E+03 ± 1.57E+01	2.72E+03 ± 8.17E+01	2.92E+03 ± 2.41E+01	2.96E+03 ± 2.22E+02	3.12E+03 ± 2.44E+01
MGSA	2.30E+03 ± 2.16E+01	2.65E+03 ± 1.97E+01	2.72E+03 ± 1.06E+02	2.93E+03 ± 2.21E+01	3.14E+03 ± 3.92E+02	3.15E+03 ± 4.01E+01
DNLGSA	2.31E+03 ± 4.47E+00	2.63E+03 ± 1.28E+01	2.74E+03 ± 6.90E+01	2.94E+03 ± 2.61E+01	3.04E+03 ± 2.94E+02	3.13E+03 ± 3.96E+01
	F55	F56	F57			
HGSA	3.38E+03 ± 2.14E+01	3.21E+03 ± 4.66E+01	1.42E+04 ± 7.16E+03			
GSA	3.46E+03 ± 2.54E+01	3.45E+03 ± 1.21E+02	1.19E+06 ± 3.26E+05			
GGSA	3.44E+03 ± 2.49E+01	3.33E+03 ± 1.20E+02	7.12E+05 ± 1.93E+05			
CGSA-M	3.45E+03 ± 2.72E+01	3.44E+03 ± 1.10E+02	1.12E+06 ± 2.80E+05			
PSO GSA	3.30E+03 ± 1.85E+02	3.24E+03 ± 6.28E+01	1.15E+06 ± 2.08E+06			
MGSA	3.36E+03 ± 1.63E+02	3.24E+03 ± 6.52E+01	1.48E+06 ± 2.57E+06			
DNLGSA	3.23E+03 ± 9.38E+01	3.23E+03 ± 5.42E+01	5.78E+05 ± 6.74E+05			

Table 4.3: Experimental results of benchmark functions (F1-F57) with $D = 30$ dimensions using HGSA, GSA, GGSA, CGSA-M, PSO GSA, MGSA and DNLGSA.

Algorithm	F1	F2	F3	F4	F5	F6
HGSA	-1.40E+03 ± 1.98E-13	3.19E+05 ± 1.08E+05	-1.20E+03 ± 3.29E-07	5.30E+04 ± 5.52E+03	-1.00E+03 ± 4.87E-13	-8.88E+02 ± 1.42E+01
GSA	-1.40E+03 ± 0.00E+00	7.32E+06 ± 1.39E+06	5.33E+09 ± 2.35E+09	6.70E+04 ± 3.50E+03	-1.00E+03 ± 6.20E-13	-8.33E+02 ± 1.36E+01
GGSA	-1.40E+03 ± 5.97E-14	4.20E+06 ± 7.47E+05	2.78E+09 ± 1.25E+09	5.47E+04 ± 4.60E+03	-1.00E+03 ± 4.26E-12	-8.49E+02 ± 2.39E+01
CGSA-M	-1.40E+03 ± 0.00E+00	7.44E+06 ± 8.98E+05	5.46E+09 ± 1.90E+09	6.68E+04 ± 4.02E+03	-1.00E+03 ± 7.49E-13	-8.30E+02 ± 6.99E+00
PSO GSA	-1.40E+03 ± 2.15E-13	6.71E+07 ± 7.32E+07	6.72E+11 ± 3.08E+12	9.23E+03 ± 5.56E+03	-1.00E+03 ± 3.64E-13	-5.06E+02 ± 2.12E+02
MGSA	-1.40E+03 ± 0.00E+00	4.44E+06 ± 5.09E+06	6.70E+08 ± 7.07E+08	6.71E+04 ± 1.27E+04	-1.00E+03 ± 5.22E-13	-8.18E+02 ± 4.71E+01
DNLGSA	-1.40E+03 ± 6.21E-04	4.53E+07 ± 2.63E+07	2.78E+10 ± 2.10E+10	7.20E+04 ± 2.39E+04	-9.94E+02 ± 2.05E+01	-6.92E+02 ± 8.83E+01
	F7	F8	F9	F10	F11	F12
HGSA	-7.99E+02 ± 1.63E+00	-6.79E+02 ± 7.51E-02	-5.81E+02 ± 3.72E+00	-5.00E+02 ± 4.08E-03	-3.47E+02 ± 9.94E+00	-2.83E+02 ± 3.65E+00
GSA	-7.33E+02 ± 1.20E+01	-6.79E+02 ± 4.61E-02	-5.67E+02 ± 2.64E+00	-5.00E+02 ± 4.78E-02	-1.05E+02 ± 2.01E+01	3.12E+01 ± 2.58E+01
GGSA	-7.48E+02 ± 1.05E+01	-6.79E+02 ± 8.78E-02	-5.81E+02 ± 2.94E+00	-5.00E+02 ± 3.78E-02	-3.08E+02 ± 1.63E+01	-2.43E+02 ± 1.17E+01
CGSA-M	-7.34E+02 ± 7.91E+00	-6.79E+02 ± 5.99E-02	-5.67E+02 ± 2.58E+00	-5.00E+02 ± 5.55E-02	-1.10E+02 ± 2.02E+01	3.82E+01 ± 2.62E+01
PSO GSA	-6.14E+02 ± 1.41E+02	-6.79E+02 ± 8.14E-02	-5.69E+02 ± 4.89E+00	-1.75E+02 ± 5.50E+02	-3.09E+02 ± 2.46E+01	-9.62E+01 ± 6.84E+01
MGSA	-6.96E+02 ± 3.12E+01	-6.79E+02 ± 5.02E-02	-5.73E+02 ± 3.82E+00	-5.00E+02 ± 4.51E-02	-2.47E+02 ± 3.46E+01	-4.80E+01 ± 5.43E+01
DNLGSA	-3.67E+02 ± 7.14E+02	-6.79E+02 ± 9.74E-02	-5.68E+02 ± 2.95E+00	-3.48E+02 ± 7.39E+01	-1.69E+02 ± 4.92E+01	-5.12E+01 ± 5.85E+01
	F13	F14	F15	F16	F17	F18
HGSA	-1.33E+02 ± 1.92E+01	2.51E+03 ± 4.21E+02	2.45E+03 ± 3.01E+02	2.00E+02 ± 2.15E-03	3.39E+02 ± 2.31E+00	4.40E+02 ± 2.53E+00
GSA	2.65E+02 ± 3.89E+01	3.91E+03 ± 5.71E+02	3.64E+03 ± 5.08E+02	2.00E+02 ± 3.41E-03	3.66E+02 ± 8.21E+00	4.56E+02 ± 5.02E+00
GGSA	-6.43E+01 ± 2.11E+01	3.12E+03 ± 3.95E+02	3.04E+03 ± 4.66E+02	2.00E+02 ± 2.61E-03	3.36E+02 ± 1.67E+00	4.36E+02 ± 1.85E+00
CGSA-M	2.68E+02 ± 3.34E+01	4.09E+03 ± 3.89E+02	3.70E+03 ± 5.35E+02	2.00E+02 ± 2.75E-03	3.64E+02 ± 8.22E+00	4.54E+02 ± 5.45E+00
PSO GSA	1.54E+02 ± 1.07E+02	1.95E+03 ± 3.88E+02	4.14E+03 ± 7.49E+02	2.00E+02 ± 2.68E-01	5.07E+02 ± 3.75E+01	6.83E+02 ± 7.62E+01
MGSA	1.56E+02 ± 6.02E+01	2.50E+03 ± 6.53E+02	3.81E+03 ± 6.90E+02	2.01E+02 ± 8.42E-01	4.38E+02 ± 2.80E+01	5.57E+02 ± 3.76E+01
DNLGSA	1.60E+02 ± 7.30E+01	3.60E+03 ± 6.28E+02	4.51E+03 ± 5.66E+02	2.00E+02 ± 3.06E-01	6.06E+02 ± 7.05E+01	7.00E+02 ± 7.77E+01
	F19	F20	F21	F22	F23	F24
HGSA	5.05E+02 ± 5.96E-01	6.15E+02 ± 4.15E-01	1.01E+03 ± 3.38E+01	3.65E+03 ± 5.26E+02	5.61E+03 ± 4.07E+02	1.20E+03 ± 1.43E+01
GSA	5.10E+02 ± 2.63E+00	6.15E+02 ± 1.68E-01	1.01E+03 ± 4.64E+01	7.22E+03 ± 4.88E+02	6.79E+03 ± 3.93E+02	1.32E+03 ± 5.82E+01
GGSA	5.04E+02 ± 1.47E+00	6.15E+02 ± 4.27E-01	1.01E+03 ± 4.38E+01	4.97E+03 ± 5.56E+02	6.02E+03 ± 4.99E+02	1.22E+03 ± 1.13E+01
CGSA-M	5.09E+02 ± 2.23E+00	6.15E+02 ± 1.71E-01	1.02E+03 ± 4.96E+01	7.28E+03 ± 4.49E+02	6.88E+03 ± 3.29E+02	1.33E+03 ± 5.49E+01
PSO GSA	5.11E+02 ± 3.81E+00	6.15E+02 ± 7.78E-01	1.01E+03 ± 8.53E+01	3.85E+03 ± 1.03E+03	5.94E+03 ± 8.57E+02	1.30E+03 ± 1.67E+01
MGSA	5.06E+02 ± 1.88E+00	6.15E+02 ± 1.50E-01	1.04E+03 ± 9.96E+01	4.87E+03 ± 1.05E+03	6.59E+03 ± 7.64E+02	1.29E+03 ± 1.38E+01
DNLGSA	9.64E+02 ± 3.25E+02	6.15E+02 ± 2.76E-01	1.10E+03 ± 1.32E+02	5.38E+03 ± 8.67E+02	6.16E+03 ± 8.97E+02	1.31E+03 ± 1.10E+01
	F25	F26	F27	F28	F29	F30
HGSA	1.30E+03 ± 1.33E+01	1.49E+03 ± 6.58E+01	1.71E+03 ± 1.40E+02	1.63E+03 ± 9.80E+01	2.68E+03 ± 2.50E+03	4.36E+04 ± 5.49E+03
GSA	1.49E+03 ± 1.31E+01	1.56E+03 ± 1.97E+01	2.23E+03 ± 9.49E+01	5.07E+03 ± 3.41E+02	2.00E+03 ± 1.82E+03	8.30E+04 ± 4.33E+03
GGSA	1.31E+03 ± 2.51E+01	1.51E+03 ± 5.39E+01	1.85E+03 ± 8.07E+01	2.79E+03 ± 1.07E+03	2.18E+03 ± 1.12E+03	6.02E+04 ± 6.73E+03
CGSA-M	1.49E+03 ± 9.70E+00	1.55E+03 ± 2.34E+01	2.19E+03 ± 8.78E+01	4.97E+03 ± 2.72E+02	1.82E+03 ± 7.79E+02	5.11E+04 ± 6.80E+03
PSO GSA	1.44E+03 ± 1.81E+01	1.52E+03 ± 8.91E+01	2.46E+03 ± 1.51E+02	2.74E+03 ± 8.83E+02	4.12E+03 ± 3.26E+03	3.56E+03 ± 7.87E+03
MGSA	1.43E+03 ± 1.77E+01	1.54E+03 ± 5.74E+01	2.33E+03 ± 1.09E+02	4.03E+03 ± 1.16E+03	4.63E+03 ± 4.30E+03	4.23E+04 ± 1.28E+04
DNLGSA	1.44E+03 ± 1.61E+01	1.53E+03 ± 8.08E+01	2.43E+03 ± 1.04E+02	4.34E+03 ± 4.69E+02	1.22E+05 ± 1.81E+05	1.49E+04 ± 1.24E+04
	F31	F32	F33	F34	F35	F36
HGSA	5.19E+02 ± 2.63E+00	6.53E+02 ± 1.28E+01	6.08E+02 ± 4.54E+00	7.41E+02 ± 3.01E+00	9.00E+02 ± 9.03E+00	9.00E+02 ± 9.67E-14
GSA	5.42E+02 ± 1.59E+01	7.26E+02 ± 2.01E+01	6.50E+02 ± 2.75E+00	7.87E+02 ± 1.19E+01	9.51E+02 ± 1.31E+01	2.93E+03 ± 3.92E+02
GGSA	5.33E+02 ± 2.30E+01	6.11E+02 ± 1.22E+01	6.09E+02 ± 5.29E+00	7.37E+02 ± 1.49E+00	8.88E+02 ± 9.79E+00	9.00E+02 ± 0.00E+00
CGSA-M	5.36E+02 ± 1.95E+01	7.18E+02 ± 1.76E+01	6.51E+02 ± 4.18E+00	7.84E+02 ± 9.91E+00	9.52E+02 ± 7.97E+00	2.87E+03 ± 3.34E+02
PSO GSA	1.04E+03 ± 5.05E+02	6.46E+02 ± 3.40E+01	6.24E+02 ± 8.94E+00	9.72E+02 ± 6.32E+01	9.36E+02 ± 3.25E+01	4.54E+03 ± 1.67E+03
MGSA	5.33E+02 ± 5.86E+01	6.35E+02 ± 3.01E+01	6.27E+02 ± 8.09E+00	8.38E+02 ± 2.65E+01	9.08E+02 ± 2.29E+01	3.41E+03 ± 8.50E+02
DNLGSA	7.11E+02 ± 1.46E+02	6.50E+02 ± 3.67E+01	6.41E+02 ± 7.86E+00	9.86E+02 ± 6.78E+01	9.16E+02 ± 2.85E+01	3.93E+03 ± 1.10E+03
	F37	F38	F39	F40	F41	F42
HGSA	4.21E+03 ± 2.93E+02	1.20E+03 ± 2.98E+01	1.29E+05 ± 8.15E+04	1.46E+04 ± 5.32E+03	6.72E+03 ± 3.05E+03	2.20E+03 ± 7.21E+02
GSA	4.87E+03 ± 4.34E+02	1.45E+03 ± 8.92E+01	1.03E+07 ± 1.93E+07	3.10E+04 ± 6.45E+03	4.74E+05 ± 1.31E+05	1.17E+04 ± 1.93E+03
GGSA	4.38E+03 ± 3.89E+02	1.25E+03 ± 3.23E+01	4.83E+05 ± 2.11E+05	1.87E+04 ± 4.70E+03	1.96E+05 ± 7.59E+04	4.12E+03 ± 1.57E+03
CGSA-M	4.94E+03 ± 4.11E+02	1.47E+03 ± 1.06E+02	1.46E+07 ± 2.66E+07	2.83E+04 ± 5.26E+03	4.84E+05 ± 1.19E+05	1.15E+04 ± 1.93E+03
PSO GSA	4.70E+03 ± 6.23E+02	1.49E+03 ± 3.14E+02	6.00E+07 ± 1.48E+08	2.39E+07 ± 7.46E+07	9.87E+04 ± 2.69E+05	5.31E+05 ± 2.82E+06
MGSA	4.92E+03 ± 8.11E+02	1.23E+03 ± 4.53E+01	5.27E+05 ± 5.78E+05	2.81E+05 ± 1.42E+06	1.87E+04 ± 3.80E+04	6.08E+03 ± 4.72E+03
DNLGSA	4.96E+03 ± 8.84E+02	1.51E+03 ± 2.44E+02	1.58E+08 ± 2.63E+08	1.62E+06 ± 8.72E+06	6.07E+04 ± 1.02E+05	1.29E+04 ± 1.02E+04
	F43	F44	F45	F46	F47	F48
HGSA	2.83E+03 ± 2.32E+02	2.77E+03 ± 1.99E+02	6.16E+04 ± 1.47E+04	5.42E+03 ± 1.25E+03	2.86E+03 ± 2.24E+02	2.41E+03 ± 5.90E+01
GSA	3.18E+03 ± 2.84E+02	2.90E+03 ± 1.70E+02	3.20E+05 ± 1.76E+05	1.42E+04 ± 5.13E+03	3.03E+03 ± 2.36E+02	2.56E+03 ± 1.95E+01
GGSA	2.88E+03 ± 3.22E+02	2.67E+03 ± 2.06E+02	1.68E+05 ± 7.28E+04	5.93E+03 ± 1.46E+03	2.82E+03 ± 1.64E+02	2.41E+03 ± 2.11E+01
CGSA-M	3.20E+03 ± 2.90E+02	2.83E+03 ± 1.92E+02	2.78E+05 ± 1.01E+05	1.34E+04 ± 4.79E+03	3.01E+03 ± 1.88E+02	2.57E+03 ± 2.71E+01
PSO GSA	3.05E+03 ± 4.59E+02	2.27E+03 ± 2.29E+02	3.07E+05 ± 1.01E+06	1.43E+04 ± 1.33E+04	2.57E+03 ± 2.35E+02	2.43E+03 ± 3.53E+01
MGSA	2.83E+03 ± 2.89E+02	2.37E+03 ± 2.07E+02	1.44E+05 ± 1.28E+05	9.28E+03 ± 6.23E+03	2.67E+03 ± 1.86E+02	2.44E+03 ± 3.14E+01
DNLGSA	2.74E+03 ± 3.13E+02	2.30E+03 ± 2.31E+02	1.88E+05 ± 1.86E+05	1.72E+04 ± 5.34E+04	2.72E+03 ± 2.15E+02	2.43E+03 ± 3.73E+01
	F49	F50	F51	F52	F53	F54
HGSA	2.30E+03 ± 3.91E-09	2.76E+03 ± 1.33E+02	2.92E+03 ± 3.58E+01	2.89E+03 ± 7.59E+00	2.85E+03 ± 5.07E+01	3.25E+03 ± 2.08E+01
GSA	6.39E+03 ± 1.69E+03	3.56E+03 ± 1.23E+02	3.29E+03 ± 5.57E+01	2.93E+03 ± 1.22E+01	6.86E+03 ± 8.95E+02	4.67E+03 ± 3.21E+02
GGSA	2.30E+03 ± 2.05E-10	2.86E+03 ± 3.94E+01	2.91E+03 ± 3.70E+01	2.93E+03 ± 1.03E+01	2.94E+03 ± 5.28E+02	3.39E+03 ± 3.57E+01
CGSA-M	5.89E+03 ± 2.08E+03	3.62E+03 ± 1.06E+02	3.29E+03 ± 5.28E+01	2.94E+03 ± 8.49E+00	6.73E+03 ± 6.61E+02	4.55E+03 ± 2.73E+02
PSO GSA	4.68E+03 ± 1.91E+03	2.93E+03 ± 8.75E+01	3.21E+03 ± 1.43E+02	3.02E+03 ± 7.53E+01	5.70E+03 ± 1.30E+03	3.52E+03 ± 1.36E+02
MGSA	4.19E+03 ± 2.22E+03	3.00E+03 ± 8.12E+01	3.27E+03 ± 1.12E+02	2.92E+03 ± 1.66E+01	5.56E+03 ± 1.63E+03	3.52E+03 ± 1.19E+02
DNLGSA	4.50E+03 ± 2.32E+03	3.00E+03 ± 8.74E+01	3.18E+03 ± 7.29E+01	3.00E+03 ± 4.61E+01	5.98E+03 ± 1.26E+03	3.43E+03 ± 1.50E+02
	F55	F56	F57			
HGSA	3.11E+03 ± 2.82E+01	4.05E+03 ± 1.88E+02	1.10E+04 ± 2.60E+03			
GSA	3.31E+03 ± 4.94E+01	4.71E+03 ± 2.10E+02	1.70E+05 ± 1.24E+05			
GGSA	3.23E+03 ± 3.28E+01	4.25E+03 ± 2.30E+02	4.39E+04 ± 1.91E+04			
CGSA-M	3.32E+03 ± 4.92E+01	4.71E+03 ± 1.91E+02	1.67E+05 ± 9.29E+04			
PSO GSA	3.52E+03 ± 2.00E+02	4.24E+03 ± 3.80E+02	3.39E+06 ± 1.42E+07			
MGSA	3.21E+03 ± 7.43E+01	4.12E+03 ± 3.03E+02	7.95E+04 ± 1.81E+05			
DNLGSA	3.44E+03 ± 9.79E+01	4.47E+03 ± 3.17E+02	3.60E+06 ± 6.27E+06			

Table 4.4: Experimental results of benchmark functions (F1-F57) with $D = 50$ dimensions using HGSA, GSA, GGSA, CGSA-M, PSO GSA, MGSA and DNLGSA.

Algorithm	F1	F2	F3	F4	F5	F6
HGSA	-1.40E+03 ± 1.89E-13	5.27E+05 ± 1.66E+05	-1.19E+03 ± 2.59E+01	7.21E+04 ± 5.42E+03	-1.00E+03 ± 5.59E-13	-8.27E+02 ± 2.43E+01
GSA	-1.40E+03 ± 2.23E-13	3.57E+06 ± 1.68E+06	4.14E+09 ± 1.87E+09	9.00E+04 ± 4.04E+03	-1.00E+03 ± 4.02E-13	-8.06E+02 ± 1.91E+01
GGSA	-1.40E+03 ± 0.00E+00	2.13E+06 ± 1.49E+06	1.24E+09 ± 8.58E+08	7.74E+04 ± 4.22E+03	-1.00E+03 ± 8.83E-13	-8.14E+02 ± 2.60E+01
CGSA-M	-1.40E+03 ± 2.11E-13	3.34E+06 ± 7.42E+05	4.25E+09 ± 1.69E+09	8.73E+04 ± 3.48E+03	-1.00E+03 ± 4.38E-13	-8.06E+02 ± 1.02E+01
PSO GSA	-1.40E+03 ± 7.31E-14	1.89E+08 ± 1.44E+08	6.24E+10 ± 1.94E+11	1.13E+04 ± 5.64E+03	-1.00E+03 ± 3.84E-13	-5.49E+02 ± 3.63E+02
MGSA	-1.40E+03 ± 1.12E-13	6.34E+06 ± 7.13E+06	4.52E+08 ± 3.16E+08	7.97E+04 ± 1.31E+04	-1.00E+03 ± 3.48E-13	-8.12E+02 ± 4.52E+01
DNLGSA	-1.40E+03 ± 4.20E-03	1.15E+08 ± 7.72E+07	4.68E+10 ± 2.20E+10	1.10E+05 ± 2.80E+04	-9.61E+02 ± 9.46E+01	-6.45E+02 ± 5.52E+01
	F7	F8	F9	F10	F11	F12
HGSA	-8.00E+02 ± 9.32E-01	-6.79E+02 ± 5.26E-02	-5.68E+02 ± 4.64E+00	-5.00E+02 ± 6.18E-03	-2.82E+02 ± 1.08E+01	-1.96E+02 ± 1.02E+01
GSA	-7.32E+02 ± 5.23E+00	-6.79E+02 ± 3.49E-02	-5.53E+02 ± 4.66E+00	-5.00E+02 ± 1.16E-01	1.83E+01 ± 2.99E+01	4.22E+02 ± 5.04E+01
GGSA	-7.53E+02 ± 5.89E+00	-6.79E+02 ± 5.80E-02	-5.69E+02 ± 4.28E+00	-5.00E+02 ± 4.89E-02	-2.37E+02 ± 1.74E+01	-1.65E+02 ± 1.63E+01
CGSA-M	-7.34E+02 ± 6.20E+00	-6.79E+02 ± 4.08E-02	-5.54E+02 ± 3.82E+00	-5.00E+02 ± 1.01E-01	2.79E+01 ± 3.09E+01	4.18E+02 ± 5.35E+01
PSO GSA	-5.80E+02 ± 1.98E+02	-6.79E+02 ± 7.00E-02	-5.38E+02 ± 6.21E+00	1.08E+03 ± 1.57E+03	-2.00E+02 ± 4.73E+01	2.48E+02 ± 1.34E+02
MGSA	-6.90E+02 ± 2.02E+01	-6.79E+02 ± 3.61E-02	-5.51E+02 ± 5.96E+00	-5.00E+02 ± 8.56E-02	-9.65E+01 ± 4.56E+01	2.01E+02 ± 7.26E+01
DNLGSA	-6.04E+02 ± 8.07E+01	-6.79E+02 ± 6.13E-02	-5.39E+02 ± 4.01E+00	-7.37E+01 ± 1.44E+02	3.25E+01 ± 7.31E+01	1.72E+02 ± 7.70E+01
	F13	F14	F15	F16	F17	F18
HGSA	8.54E+01 ± 3.27E+01	4.07E+03 ± 5.65E+02	6.39E+03 ± 4.96E+02	2.00E+02 ± 1.78E-03	3.69E+02 ± 3.45E+00	4.70E+02 ± 4.52E+00
GSA	6.66E+02 ± 6.30E+01	6.90E+03 ± 7.54E+02	8.61E+03 ± 6.99E+02	2.00E+02 ± 1.26E-03	4.43E+02 ± 1.70E+01	5.11E+02 ± 1.09E+01
GGSA	7.21E+01 ± 3.85E+01	5.15E+03 ± 7.17E+02	6.96E+03 ± 6.63E+02	2.00E+02 ± 1.53E-03	3.64E+02 ± 2.86E+00	4.63E+02 ± 2.71E+00
CGSA-M	6.51E+02 ± 7.29E+01	6.77E+03 ± 7.00E+02	8.53E+03 ± 5.65E+02	2.00E+02 ± 1.29E-03	4.36E+02 ± 1.40E+01	5.13E+02 ± 1.07E+01
PSO GSA	5.70E+02 ± 1.35E+02	3.22E+03 ± 5.33E+02	9.00E+03 ± 2.83E+03	2.00E+02 ± 1.43E-01	7.24E+02 ± 8.51E+01	1.26E+03 ± 1.42E+02
MGSA	4.65E+02 ± 1.06E+02	4.30E+03 ± 1.02E+03	7.72E+03 ± 6.88E+02	2.01E+02 ± 1.17E+00	6.59E+02 ± 5.94E+01	8.15E+02 ± 8.12E+01
DNLGSA	4.90E+02 ± 1.19E+02	6.82E+03 ± 9.82E+02	8.38E+03 ± 1.49E+03	2.01E+02 ± 3.41E-01	1.08E+03 ± 1.66E+02	1.17E+03 ± 1.32E+02
	F19	F20	F21	F22	F23	F24
HGSA	5.08E+02 ± 9.07E-01	6.24E+02 ± 2.71E-01	1.61E+03 ± 1.29E+02	7.51E+03 ± 2.18E+03	1.03E+04 ± 3.88E+02	1.20E+03 ± 6.40E+00
GSA	5.13E+02 ± 2.27E+00	6.25E+02 ± 2.46E-01	1.64E+03 ± 1.34E+02	1.32E+04 ± 5.54E+02	1.21E+04 ± 3.87E+02	1.33E+03 ± 1.82E+01
GGSA	5.06E+02 ± 1.66E+00	6.24E+02 ± 3.90E-01	1.63E+03 ± 1.37E+02	1.10E+04 ± 1.47E+03	1.08E+04 ± 3.74E+02	1.24E+03 ± 1.63E+01
CGSA-M	5.14E+02 ± 2.92E+00	6.24E+02 ± 2.02E-01	1.61E+03 ± 1.29E+02	1.31E+04 ± 5.17E+02	1.20E+04 ± 3.92E+02	1.34E+03 ± 1.36E+01
PSO GSA	5.37E+02 ± 2.34E+01	6.24E+02 ± 7.78E-01	1.54E+03 ± 3.78E+02	6.77E+03 ± 2.12E+03	1.14E+04 ± 2.29E+03	1.42E+03 ± 2.79E+01
MGSA	5.13E+02 ± 2.62E+00	6.24E+02 ± 7.06E-01	1.66E+03 ± 2.47E+02	8.81E+03 ± 1.90E+03	1.15E+04 ± 1.06E+03	1.39E+03 ± 2.28E+01
DNLGSA	2.50E+03 ± 1.03E+03	6.25E+02 ± 3.03E-01	2.01E+03 ± 5.99E+02	1.03E+04 ± 1.67E+03	1.18E+04 ± 1.22E+03	1.44E+03 ± 2.37E+01
	F25	F26	F27	F28	F29	F30
HGSA	1.33E+03 ± 6.91E+01	1.57E+03 ± 4.57E+01	2.36E+03 ± 1.59E+02	2.10E+03 ± 9.10E+02	9.42E+02 ± 1.17E+03	1.19E+05 ± 1.15E+04
GSA	1.72E+03 ± 1.41E+01	1.61E+03 ± 5.68E+01	3.01E+03 ± 6.99E+02	8.52E+03 ± 3.42E+02	8.71E+02 ± 8.68E+02	1.69E+05 ± 1.03E+04
GGSA	1.47E+03 ± 5.40E+01	1.57E+03 ± 5.77E+01	2.52E+03 ± 1.36E+02	2.42E+03 ± 1.30E+03	9.98E+02 ± 1.57E+03	1.37E+05 ± 7.98E+03
CGSA-M	1.71E+03 ± 1.53E+01	1.61E+03 ± 5.71E+01	3.01E+03 ± 1.11E+02	8.73E+03 ± 3.54E+02	8.62E+02 ± 1.06E+03	1.70E+05 ± 8.92E+03
PSO GSA	1.61E+03 ± 3.42E+01	1.66E+03 ± 2.09E+01	3.33E+03 ± 1.77E+02	4.66E+03 ± 2.39E+03	1.69E+09 ± 4.33E+09	3.67E+04 ± 6.07E+04
MGSA	1.59E+03 ± 3.50E+01	1.63E+03 ± 4.51E+01	3.11E+03 ± 1.50E+02	6.55E+03 ± 1.98E+03	3.38E+03 ± 6.28E+03	1.12E+05 ± 2.49E+04
DNLGSA	1.61E+03 ± 2.92E+01	1.65E+03 ± 4.71E+01	3.41E+03 ± 1.46E+02	7.07E+03 ± 7.24E+02	4.19E+06 ± 7.15E+06	8.33E+04 ± 6.15E+04
	F31	F32	F33	F34	F35	F36
HGSA	6.02E+02 ± 2.91E+01	7.68E+02 ± 1.36E+01	6.25E+02 ± 3.97E+00	7.70E+02 ± 3.44E+00	1.09E+03 ± 2.04E+01	9.00E+02 ± 1.01E-13
GSA	5.99E+02 ± 6.18E+01	8.23E+02 ± 1.91E+01	6.57E+02 ± 3.03E+00	9.28E+02 ± 3.10E+01	1.16E+03 ± 2.15E+01	9.27E+03 ± 6.58E+02
GGSA	5.78E+02 ± 6.56E+01	7.33E+02 ± 2.01E+01	6.26E+02 ± 4.73E+00	7.67E+02 ± 3.05E+00	1.04E+03 ± 2.03E+01	1.51E+03 ± 4.40E+02
CGSA-M	6.23E+02 ± 6.62E+01	8.30E+02 ± 1.75E+01	6.57E+02 ± 2.47E+00	9.40E+02 ± 2.70E+01	1.16E+03 ± 1.79E+01	9.14E+03 ± 4.80E+02
PSO GSA	3.70E+03 ± 2.22E+03	7.87E+02 ± 7.88E+01	6.35E+02 ± 7.66E+00	1.46E+03 ± 1.51E+02	1.09E+03 ± 6.46E+01	1.26E+04 ± 3.13E+03
MGSA	6.42E+02 ± 7.90E+01	7.78E+02 ± 4.38E+01	6.40E+02 ± 7.05E+00	1.08E+03 ± 4.60E+01	1.07E+03 ± 3.90E+01	9.67E+03 ± 1.98E+03
DNLGSA	1.49E+03 ± 9.04E+02	7.80E+02 ± 4.79E+01	6.49E+02 ± 5.27E+00	1.49E+03 ± 1.02E+02	1.10E+03 ± 4.06E+01	1.04E+04 ± 1.76E+03
	F37	F38	F39	F40	F41	F42
HGSA	6.83E+03 ± 5.55E+02	1.23E+03 ± 1.92E+01	7.11E+05 ± 3.35E+05	1.90E+03 ± 5.38E+02	2.71E+04 ± 3.76E+04	8.61E+03 ± 1.64E+03
GSA	7.98E+03 ± 6.19E+02	2.27E+03 ± 3.04E+02	1.92E+06 ± 5.40E+05	2.81E+04 ± 3.84E+03	3.00E+05 ± 1.14E+05	1.53E+04 ± 3.66E+03
GGSA	6.87E+03 ± 5.56E+02	1.50E+03 ± 7.46E+01	1.39E+06 ± 4.25E+05	1.78E+04 ± 2.49E+03	6.78E+04 ± 2.86E+04	9.19E+03 ± 1.40E+03
CGSA-M	7.72E+03 ± 5.77E+02	2.35E+03 ± 2.81E+02	1.76E+06 ± 3.88E+05	2.73E+04 ± 2.97E+03	3.60E+05 ± 4.18E+05	1.71E+04 ± 3.12E+03
PSO GSA	7.67E+03 ± 1.80E+03	5.20E+03 ± 4.61E+03	1.19E+09 ± 2.38E+09	2.36E+08 ± 7.44E+08	3.33E+06 ± 5.41E+06	2.14E+06 ± 1.09E+07
MGSA	7.47E+03 ± 8.91E+02	1.34E+03 ± 6.66E+01	1.50E+06 ± 1.02E+06	2.01E+04 ± 1.27E+04	2.82E+05 ± 7.01E+05	1.29E+04 ± 2.61E+04
DNLGSA	8.07E+03 ± 8.63E+02	2.15E+03 ± 1.28E+03	4.26E+08 ± 6.24E+08	3.38E+04 ± 2.98E+04	1.44E+06 ± 2.16E+06	4.62E+06 ± 1.63E+07
	F43	F44	F45	F46	F47	F48
HGSA	3.55E+03 ± 3.50E+02	3.44E+03 ± 3.14E+02	1.74E+05 ± 7.74E+04	1.69E+04 ± 3.36E+03	3.38E+03 ± 2.75E+02	2.56E+03 ± 3.22E+01
GSA	3.73E+03 ± 3.60E+02	3.58E+03 ± 3.66E+02	1.39E+06 ± 8.69E+05	2.68E+04 ± 4.51E+03	3.61E+03 ± 2.84E+02	2.74E+03 ± 2.62E+01
GGSA	3.37E+03 ± 3.45E+02	3.45E+03 ± 3.62E+02	9.57E+05 ± 6.76E+05	1.68E+04 ± 2.83E+03	3.30E+03 ± 2.09E+02	2.54E+03 ± 2.83E+01
CGSA-M	3.64E+03 ± 3.67E+02	3.50E+03 ± 3.31E+02	1.35E+06 ± 8.39E+05	2.65E+04 ± 6.33E+03	3.48E+03 ± 2.79E+02	2.73E+03 ± 3.30E+01
PSO GSA	4.39E+03 ± 7.44E+02	3.13E+03 ± 2.78E+02	1.14E+07 ± 1.42E+07	1.21E+04 ± 1.06E+04	3.32E+03 ± 4.38E+02	2.62E+03 ± 1.02E+02
MGSA	3.68E+03 ± 5.08E+02	3.33E+03 ± 3.23E+02	1.95E+06 ± 2.68E+06	1.64E+04 ± 1.16E+04	3.23E+03 ± 3.52E+02	2.61E+03 ± 4.87E+01
DNLGSA	3.85E+03 ± 5.17E+02	3.28E+03 ± 3.07E+02	5.56E+06 ± 6.28E+06	9.83E+04 ± 4.24E+05	3.39E+03 ± 3.05E+02	2.62E+03 ± 5.57E+01
	F49	F50	F51	F52	F53	F54
HGSA	1.01E+04 ± 4.22E+02	3.30E+03 ± 1.80E+02	3.29E+03 ± 4.71E+01	3.08E+03 ± 1.89E+01	2.90E+03 ± 7.51E-13	4.02E+03 ± 3.01E+02
GSA	1.13E+04 ± 5.11E+02	4.34E+03 ± 1.60E+02	3.76E+03 ± 6.39E+01	3.25E+03 ± 7.27E+01	6.74E+03 ± 2.69E+03	6.38E+03 ± 3.58E+02
GGSA	9.72E+03 ± 1.49E+03	3.13E+03 ± 6.52E+01	3.21E+03 ± 5.75E+01	3.16E+03 ± 2.98E+01	2.90E+03 ± 4.17E-10	4.03E+03 ± 1.42E+02
CGSA-M	1.14E+04 ± 4.45E+02	4.33E+03 ± 1.66E+02	3.76E+03 ± 7.09E+01	3.23E+03 ± 8.13E+01	6.68E+03 ± 2.40E+03	6.47E+03 ± 4.87E+02
PSO GSA	8.86E+03 ± 1.52E+03	3.53E+03 ± 2.19E+02	3.81E+03 ± 2.44E+02	4.75E+03 ± 1.06E+03	9.89E+03 ± 1.49E+03	4.71E+03 ± 4.32E+02
MGSA	1.02E+04 ± 1.00E+03	3.54E+03 ± 1.02E+02	3.83E+03 ± 1.51E+02	3.19E+03 ± 6.82E+01	9.45E+03 ± 2.37E+03	4.54E+03 ± 2.16E+02
DNLGSA	9.97E+03 ± 1.06E+03	3.59E+03 ± 2.08E+02	3.82E+03 ± 1.79E+02	3.59E+03 ± 2.60E+02	1.06E+04 ± 8.14E+02	4.55E+03 ± 6.46E+02
	F55	F56	F57			
HGSA	3.31E+03 ± 1.56E+01	4.70E+03 ± 3.13E+02	1.33E+06 ± 1.17E+05			
GSA	3.54E+03 ± 1.15E+02	5.57E+03 ± 4.38E+02	4.11E+07 ± 5.18E+06			
GGSA	3.45E+03 ± 6.51E+01	5.11E+03 ± 3.23E+02	3.00E+07 ± 4.50E+06			
CGSA-M	3.50E+03 ± 1.02E+02	5.57E+03 ± 4.12E+02	4.11E+07 ± 6.46E+06			
PSO GSA	6.22E+03 ± 1.10E+03	6.16E+03 ± 1.22E+03	1.27E+08 ± 9.98E+07			
MGSA	3.43E+03 ± 9.29E+01	5.19E+03 ± 6.04E+02	3.63E+07 ± 1.51E+07			
DNLGSA	4.07E+03 ± 3.68E+02	6.43E+03 ± 1.00E+03	1.97E+08 ± 9.15E+07			

Table 4.5: Statistical results obtained by the Wilcoxon signed ranks test between HGSA and GSA, GGSA, CGSA-M, PSO-GSA, MGS-A and DNLGSA in $D = 10, 30$ and 50 dimensions.

HGSA vs.	$D = 10$			$D = 30$			$D = 50$		
	R^+	R^-	p -value $\alpha=0.05$	R^+	R^-	p -value $\alpha=0.05$	R^+	R^-	p -value $\alpha=0.05$
GSA	1576.0	77.0	0	1550.5	45.5	0	1568.0	28.0	0
GGSA	1327.5	325.5	3.00E-05	1354.0	242.0	4.00E-06	1255.0	398.0	5.83E-04
CGSA-M	1530.5	65.5	0	1606.0	47.0	0	1566.5	29.5	0
PSO-GSA	1061.5	534.5	2.86E-02	1431.5	221.5	1.00E-06	1363.0	290.0	1.80E-05
MGSA	1322.0	274.0	1.10E-05	1511.5	141.5	0	1456.5	139.5	0
DNLGSA	1261.5	334.5	6.90E-05	1530.0	123.0	0	1577.5	75.5	0

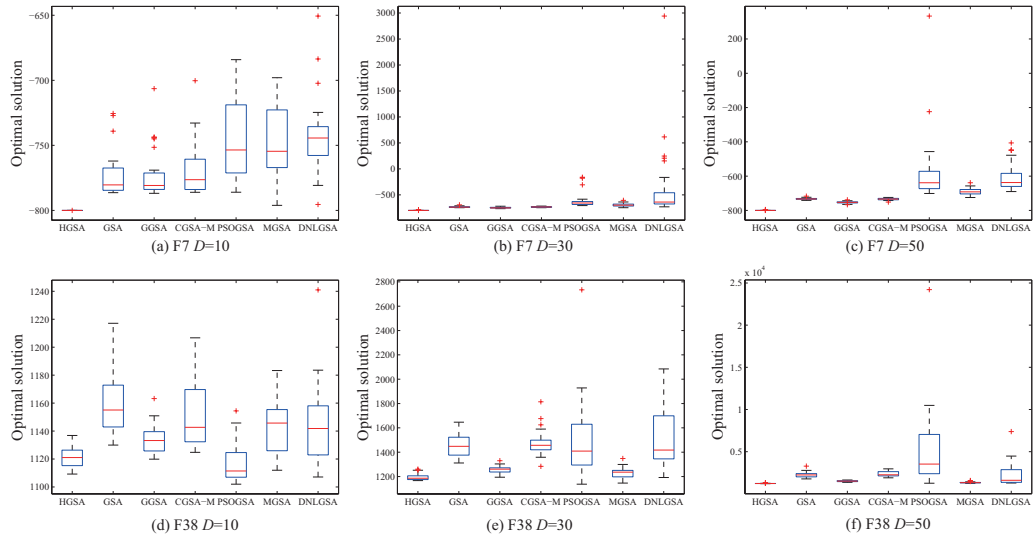


Figure 4.5: The box-and-whisker diagrams of optimal solutions obtained by seven kinds of GSAs on F7 and F38 with 10, 30 and 50 dimensions.

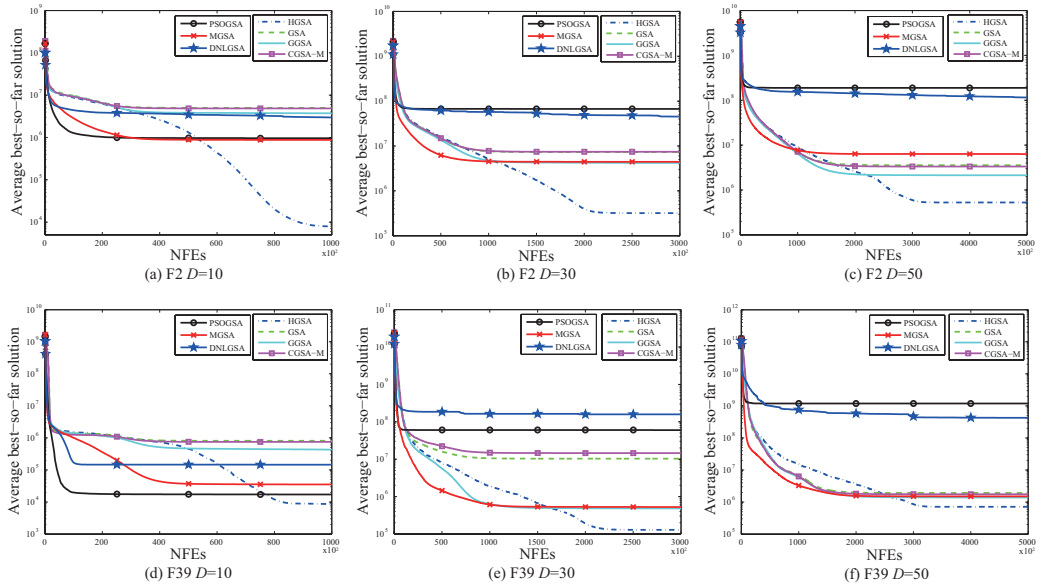


Figure 4.6: The convergence graphs of average best-so-far solutions obtained by seven kinds of GSAs on F2 and F39 with 10, 30 and 50 dimensions.

difference in comparison with the others in 10 dimensions whereas HGSA maintains the less values and the shorter distribution of optimal solutions, indicating a good and steady performance of HGSA in low dimensions. In Figs. 4.5(b), (c), (e) and (f), the complexity of two functions is enhanced owing to the increase of dimensions. Thus, we can observe that optimal solutions obtained by each algorithm are greater, suggesting that their performances gradually decrease with the increase of dimensions. Nevertheless, HGSA can still find a better optimal solution than the others, implying that it is an more effective algorithm among seven algorithms for optimizing functions with different dimensions. In order to display the convergence characteristic of each algorithm, Fig. 4.6 is depicted to show their average best-so-far solutions on F2 and F39 with 10, 30 and 50 dimensions. In it, the vertical axis indicates the log value of average best-so-far solution which aims to provide a more distinct difference of average best-so-far solutions among seven algorithms, and the horizontal axis indicates the number of function evaluations. According to Fig. 4.6, it can be found that other six GSAs converge quickly in the early stage of search process so that they are trapped into the local optima in the late stage of search process. However, HGSA shows a different convergence characteristic. It consistently converges in the early half stage of search process and finally obtains the best solution among seven algorithms in a later stage, denoting that it effectively alleviates a premature convergence and significantly enhances its performance during its execution. Therefore, this result verifies that HGSA enhances its exploration and exploitation abilities in the search process due to an effective hierarchical structure and an improved gravitational constant.

4.4.3 Comparison between HGSA and other heuristic algorithms

The first experiment implements an internal comparison among seven kinds of GSAs and demonstrates a superior performance of HGSA. To further illustrate its property, an external comparison is adopted to analyze the difference of performances between it and other heuristic algorithms including DE [101], CMA-ES [131], GABC [132], GWO [133] and SCA [134]. DE is an efficient and strong-robustness global optimization algorithm using a differential mutation and a crossover operation. CMA-ES uses a novel evolution strategy with covariance matrix adaptation to decrease the number of iterations needed to find an optimal solution. GABC incorporates the global best individual into the artificial bee colony algorithm to enhance its exploitation ability. GWO and SCA are two relatively new population-based optimization algorithms where GWO called grey wolf optimizer emulates the leadership hierarchy and hunting behavior of grey wolves to seek for an optimal

solution, and SCA called sine cosine algorithm uses a mathematical model based on sine and cosine functions to update the positions of individuals so as to guarantee its exploration and exploitation abilities. These five distinctive algorithms compare with HGSA on fifty seven benchmark functions with 30 dimensions. HGSA uses the same parameters above mentioned. DE sets parameters F and CR to be 0.9 and 0.9. The parameters of CMA-ES are set to be $\lambda = 100$, $\mu = \lfloor \lambda/2 \rfloor$, $w_i = \ln[(\lambda + 1)/2] - \ln(i)$, $c_c = 4/(D + 4)$, $c_{cov} = 2/(D + \sqrt{2})^2$, $c_\sigma = 4/(D + 4)$, $d_\sigma = c_\sigma^{-1} + 1$. GABC uses $C = 1.5$. GWO adopts the parameter a to linearly decrease from 2 to 0 with iterations. In SCA, $a = 2$.

The mean and standard deviation obtained by each algorithm are shown in Table 4.6. From Table 4.6, we can observe that HGSA still derives the best solutions on many functions whereas other heuristic algorithms also show competitive performances on several functions. To further distinguish the difference of their performances, the statistical results obtained by the Wilcoxon signed ranks test at two significant levels of $\alpha = 0.05$ and $\alpha = 0.01$ are listed in Table 4.7. According to Table 4.7, we can find that HGSA significantly outperforms other five heuristic algorithms in terms of p -value, suggesting that it is more effective. Thus, it can be concluded that HGSA can show a strong and competitive performance in contrast to other heuristic algorithms.

In order to exhibit the distribution of optimal solutions obtained by six algorithms, three box-and-whisker diagrams on F17, F27 and F53 with 30 dimensions are plotted in Fig. 4.7. From it, we can see that HGSA has the smaller values of optimal solutions in comparison with other five algorithms, indicating it has a better performance. Fig. 4.8 is given to display the convergence graphs of average best-so-far solutions among six algorithms on F14, F29 and F39 with 30 dimensions. In Fig. 4.8, it can be observed that DE, SCA and GWO have inferior solutions due to their slow convergence speed. Figs. 4.8(b) and (c) show that CMA-ES and GABC trap into the local optima although they converge quickly. Nevertheless, HGSA reveals a good convergence characteristic where it gradually converges in the early stage of search process and ultimately obtains a better solution in the late stage of search process. Consequently, this experiment also demonstrates a superior performance of HGSA in comparison with other heuristic algorithms owing to its hierarchical structure and gravitational constant.

4.4.4 Comparison between HGSA and other PSOs

HGSA uses a global optimal individual to facilitate its population evolution. Similar mechanisms have also been utilized in various PSOs [135]. Although HGSA and PSOs overall

Table 4.6: Experimental results of benchmark functions (F1-F57) with $D = 30$ dimensions using HGSA, DE, CMA-ES, GABC, GWO and SCA.

Algorithm	F1	F2	F3	F4	F5	F6
HGSA	-1.40E+03 ± 1.98E-13	3.19E+05 ± 1.08E+05	-1.20E+03 ± 3.29E-07	5.30E+04 ± 5.52E+03	-1.00E+03 ± 4.87E-13	-8.88E+02 ± 1.42E+01
DE	-7.26E+02 ± 3.32E+02	1.13E+08 ± 2.05E+07	1.32E+10 ± 2.63E+09	5.72E+04 ± 9.55E+03	-9.32E+02 ± 1.42E+01	-7.37E+02 ± 2.44E+01
CMA-ES	-1.40E+03 ± 0.00E+00	2.41E+07 ± 1.02E+07	-1.20E+03 ± 0.00E+00	1.94E+05 ± 3.89E+04	-1.00E+03 ± 1.06E-04	-8.96E+02 ± 2.90E+00
GABC	-1.40E+03 ± 1.58E-13	1.68E+07 ± 5.42E+06	2.06E+09 ± 2.27E+09	6.70E+04 ± 6.85E+03	-1.00E+03 ± 3.45E-04	-8.48E+02 ± 3.05E+01
GWO	-7.16E+02 ± 6.54E+02	1.58E+07 ± 9.24E+06	2.80E+09 ± 2.86E+09	2.69E+04 ± 7.43E+03	-4.45E+02 ± 2.31E+02	-7.74E+02 ± 4.24E+01
SCA	9.08E+03 ± 1.72E+03	1.31E+08 ± 3.26E+07	3.12E+10 ± 8.79E+09	3.17E+04 ± 6.61E+03	9.15E+02 ± 3.40E+02	-2.06E+02 ± 2.22E+02
	F7	F8	F9	F10	F11	F12
HGSA	-7.99E+02 ± 1.63E+00	-6.79E+02 ± 7.51E-02	-5.81E+02 ± 3.72E+00	-5.00E+02 ± 4.08E-03	-3.47E+02 ± 9.94E+00	-2.83E+02 ± 3.65E+00
DE	-6.88E+02 ± 1.16E+01	-6.79E+02 ± 4.22E-02	-5.61E+02 ± 1.10E+00	-4.30E+01 ± 1.05E+02	-1.59E+02 ± 2.11E+01	-9.86E+00 ± 1.22E+01
CMA-ES	-8.00E+02 ± 0.00E+00	-6.79E+02 ± 5.73E-02	-5.59E+02 ± 1.57E+00	-4.98E+02 ± 4.83E-01	-2.99E+02 ± 6.81E+01	-1.40E+02 ± 9.72E+00
GABC	-6.84E+02 ± 3.42E+01	-6.79E+02 ± 5.53E-02	-5.61E+02 ± 1.27E+00	-4.99E+02 ± 5.12E-01	-3.62E+02 ± 1.28E+01	-1.15E+02 ± 6.48E+01
GWO	-7.54E+02 ± 1.82E+01	-6.79E+02 ± 4.24E-02	-5.82E+02 ± 2.23E+00	-3.06E+02 ± 1.42E+02	-3.14E+02 ± 3.19E+01	-1.82E+02 ± 4.85E+01
SCA	-6.27E+02 ± 4.28E+01	-6.79E+02 ± 6.99E-02	-5.61E+02 ± 1.21E+00	1.01E+03 ± 3.28E+02	-4.43E+01 ± 2.90E+01	7.99E+01 ± 3.52E+01
	F13	F14	F15	F16	F17	F18
HGSA	-1.33E+02 ± 1.92E+01	2.51E+03 ± 4.21E+02	2.45E+03 ± 3.01E+02	2.00E+02 ± 2.15E-03	3.39E+02 ± 2.31E+00	4.40E+02 ± 2.53E+00
DE	9.85E+01 ± 8.77E+00	6.61E+03 ± 4.55E+02	7.47E+03 ± 2.43E+02	2.02E+02 ± 3.33E-01	6.31E+02 ± 3.76E+01	7.47E+02 ± 3.22E+01
CMA-ES	-4.25E+01 ± 1.13E+01	7.24E+03 ± 3.25E+02	7.52E+03 ± 2.71E+02	2.00E+02 ± 0.00E+00	4.85E+02 ± 8.70E+00	5.86E+02 ± 9.57E+00
GABC	1.62E+01 ± 2.85E+01	7.16E+03 ± 2.40E+02	7.44E+03 ± 2.16E+02	2.02E+02 ± 2.67E-01	4.86E+02 ± 4.25E+01	6.48E+02 ± 1.63E+01
GWO	-2.68E+01 ± 3.66E+01	2.78E+03 ± 9.75E+02	3.41E+03 ± 1.09E+03	2.02E+02 ± 3.05E-01	4.67E+02 ± 4.51E+01	6.41E+02 ± 2.87E+01
SCA	1.67E+02 ± 3.69E+01	7.00E+03 ± 3.40E+02	7.49E+03 ± 2.06E+02	2.02E+02 ± 2.55E-01	7.88E+02 ± 4.68E+01	8.88E+02 ± 3.94E+01
	F19	F20	F21	F22	F23	F24
HGSA	5.05E+02 ± 5.96E-01	6.15E+02 ± 4.15E-01	1.01E+03 ± 4.38E+01	3.65E+03 ± 5.26E+02	5.61E+03 ± 4.07E+02	1.20E+03 ± 1.43E+01
DE	5.37E+02 ± 1.24E+01	6.13E+02 ± 1.37E-01	1.57E+03 ± 1.87E+02	7.76E+03 ± 4.13E+02	8.44E+03 ± 3.02E+02	1.30E+03 ± 2.66E+00
CMA-ES	5.12E+02 ± 2.38E+00	6.15E+02 ± 2.20E-01	9.70E+02 ± 4.66E+01	8.26E+03 ± 2.93E+02	8.52E+03 ± 2.82E+02	1.30E+03 ± 2.92E+00
GABC	5.17E+02 ± 6.84E+00	6.15E+02 ± 2.16E-01	1.02E+03 ± 8.32E+01	8.67E+03 ± 2.79E+02	8.90E+03 ± 2.86E+02	1.28E+03 ± 1.17E+01
GWO	5.69E+02 ± 2.05E+02	6.12E+02 ± 1.63E+00	1.53E+03 ± 2.64E+02	3.57E+03 ± 1.01E+03	4.82E+03 ± 1.51E+03	1.25E+03 ± 9.95E+00
SCA	2.99E+03 ± 1.30E+03	6.14E+02 ± 3.54E-01	2.58E+03 ± 1.79E+02	8.35E+03 ± 4.43E+02	8.70E+03 ± 3.72E+02	1.32E+03 ± 5.05E+00
	F25	F26	F27	F28	F29	F30
HGSA	1.30E+03 ± 1.33E+01	1.49E+03 ± 6.58E+01	1.71E+03 ± 1.40E+02	1.63E+03 ± 9.80E+01	2.68E+03 ± 2.50E+03	4.36E+04 ± 5.49E+03
DE	1.42E+03 ± 3.38E+00	1.41E+03 ± 2.06E+00	2.63E+03 ± 2.62E+01	2.66E+03 ± 1.29E+02	1.32E+09 ± 4.55E+08	8.04E+04 ± 1.05E+04
CMA-ES	1.40E+03 ± 2.83E+00	1.58E+03 ± 4.82E+01	2.60E+03 ± 1.96E+01	1.70E+03 ± 0.00E+00	1.74E+04 ± 2.32E+04	3.10E+05 ± 7.67E+04
GABC	1.40E+03 ± 8.67E+00	1.40E+03 ± 5.82E+00	2.39E+03 ± 9.01E+01	1.85E+03 ± 4.05E+02	5.27E+03 ± 5.71E+03	9.20E+04 ± 1.02E+04
GWO	1.37E+03 ± 9.54E+00	1.49E+03 ± 7.02E+01	2.10E+03 ± 5.93E+01	2.43E+03 ± 2.78E+02	1.02E+09 ± 8.91E+08	2.85E+04 ± 9.70E+03
SCA	1.43E+03 ± 4.21E+00	1.41E+03 ± 5.66E+00	2.66E+03 ± 4.51E+01	3.92E+03 ± 1.98E+02	1.18E+10 ± 1.77E+09	3.50E+04 ± 6.31E+03
	F31	F32	F33	F34	F35	F36
HGSA	5.19E+02 ± 2.63E+00	6.53E+02 ± 1.28E+01	6.08E+02 ± 4.54E+00	7.41E+02 ± 3.01E+00	9.00E+02 ± 9.03E+00	9.00E+02 ± 9.67E-14
DE	6.25E+02 ± 2.90E+01	7.50E+02 ± 1.31E+01	6.24E+02 ± 4.43E+00	1.17E+03 ± 9.96E+01	1.06E+03 ± 1.14E+01	4.14E+03 ± 7.85E+02
CMA-ES	4.11E+02 ± 1.98E+00	6.48E+02 ± 2.89E+01	6.00E+02 ± 1.03E-07	8.83E+02 ± 7.56E+00	9.56E+02 ± 8.45E+00	9.00E+02 ± 0.00E+00
GABC	4.82E+02 ± 3.32E+01	5.96E+02 ± 2.01E+01	6.00E+02 ± 1.15E-01	8.38E+02 ± 3.40E+01	8.91E+02 ± 2.13E+01	2.08E+03 ± 1.08E+03
GWO	5.70E+02 ± 4.98E+01	5.92E+02 ± 2.63E+01	6.04E+02 ± 2.33E+00	8.35E+02 ± 4.95E+01	8.81E+02 ± 1.25E+01	1.18E+03 ± 1.39E+02
SCA	1.40E+03 ± 2.74E+02	7.71E+02 ± 2.17E+01	6.49E+02 ± 5.34E+00	1.12E+03 ± 2.88E+01	1.05E+03 ± 1.63E+01	5.52E+03 ± 1.10E+03
	F37	F38	F39	F40	F41	F42
HGSA	4.21E+03 ± 2.93E+02	1.20E+03 ± 2.98E+01	1.29E+05 ± 8.15E+04	1.46E+04 ± 5.32E+03	6.72E+03 ± 3.05E+03	2.20E+03 ± 7.21E+02
DE	8.17E+03 ± 2.51E+02	1.33E+03 ± 2.16E+01	5.43E+07 ± 1.60E+07	4.13E+03 ± 5.37E+02	1.49E+03 ± 7.57E+00	1.72E+03 ± 3.06E+01
CMA-ES	8.34E+03 ± 3.49E+02	3.26E+03 ± 9.70E+02	1.31E+07 ± 6.07E+06	5.09E+06 ± 2.67E+06	1.88E+05 ± 1.02E+05	2.53E+06 ± 1.71E+06
GABC	8.20E+03 ± 2.16E+02	1.71E+03 ± 7.64E+02	1.30E+06 ± 1.06E+06	8.32E+03 ± 7.15E+03	1.88E+05 ± 9.66E+04	7.32E+03 ± 7.67E+03
GWO	3.73E+03 ± 5.49E+02	1.51E+03 ± 4.42E+02	3.31E+07 ± 3.81E+07	6.63E+06 ± 2.33E+07	8.10E+04 ± 1.76E+05	2.44E+05 ± 5.82E+05
SCA	8.12E+03 ± 3.34E+02	2.19E+03 ± 3.99E+02	1.21E+09 ± 2.30E+08	4.07E+08 ± 1.98E+08	1.19E+05 ± 7.05E+04	1.56E+07 ± 1.29E+07
	F43	F44	F45	F46	F47	F48
HGSA	2.83E+03 ± 2.32E+02	2.77E+03 ± 1.99E+02	6.16E+04 ± 1.47E+04	5.42E+03 ± 1.25E+03	2.86E+03 ± 2.24E+02	2.41E+03 ± 5.90E+01
DE	3.19E+03 ± 3.08E+02	2.41E+03 ± 2.16E+02	6.90E+03 ± 1.84E+03	1.96E+03 ± 4.88E+00	2.31E+03 ± 2.03E+02	2.54E+03 ± 1.26E+01
CMA-ES	2.95E+03 ± 1.71E+02	2.28E+03 ± 1.59E+02	3.29E+06 ± 2.15E+06	2.21E+06 ± 1.45E+06	2.55E+03 ± 1.55E+02	2.44E+03 ± 2.65E+01
GABC	2.48E+03 ± 2.19E+02	2.05E+03 ± 1.34E+02	5.10E+06 ± 2.12E+06	6.00E+03 ± 5.19E+03	2.72E+03 ± 8.80E+01	2.40E+03 ± 2.35E+01
GWO	2.32E+03 ± 2.39E+02	1.93E+03 ± 1.16E+02	7.75E+05 ± 1.40E+06	2.06E+05 ± 3.88E+05	2.33E+03 ± 1.66E+02	2.37E+03 ± 1.85E+01
SCA	3.64E+03 ± 2.13E+02	2.42E+03 ± 1.64E+02	2.80E+06 ± 1.21E+06	2.48E+07 ± 1.13E+07	2.61E+03 ± 1.29E+02	2.56E+03 ± 1.92E+01
	F49	F50	F51	F52	F53	F54
HGSA	2.30E+03 ± 3.91E-09	2.76E+03 ± 1.33E+02	2.92E+03 ± 3.58E+01	2.89E+03 ± 7.59E+00	2.85E+03 ± 5.07E+01	3.25E+03 ± 2.08E+01
DE	2.52E+03 ± 4.78E+01	2.88E+03 ± 1.38E+01	3.04E+03 ± 1.07E+01	3.01E+03 ± 3.38E+01	6.15E+03 ± 1.47E+02	3.26E+03 ± 1.20E+01
CMA-ES	9.41E+03 ± 3.94E+02	2.79E+03 ± 4.13E+01	2.91E+03 ± 7.22E+01	2.88E+03 ± 1.14E-01	4.82E+03 ± 1.26E+02	3.20E+03 ± 4.94E-05
GABC	2.30E+03 ± 1.56E+00	2.78E+03 ± 3.12E+01	2.95E+03 ± 3.66E+01	2.90E+03 ± 1.45E+01	5.08E+03 ± 7.13E+02	3.25E+03 ± 1.52E+01
GWO	4.47E+03 ± 1.45E+03	2.73E+03 ± 3.04E+01	2.90E+03 ± 4.70E+01	2.96E+03 ± 2.69E+01	4.43E+03 ± 2.45E+02	3.23E+03 ± 1.78E+01
SCA	8.25E+03 ± 2.37E+03	2.99E+03 ± 2.34E+01	3.16E+03 ± 2.96E+01	3.20E+03 ± 4.91E+01	6.87E+03 ± 2.56E+02	3.39E+03 ± 4.83E+01
	F55	F56	F57			
HGSA	3.11E+03 ± 2.82E+01	4.05E+03 ± 1.88E+02	1.10E+04 ± 2.60E+03			
DE	3.39E+03 ± 3.61E+01	4.34E+03 ± 1.18E+02	1.94E+05 ± 7.07E+04			
CMA-ES	3.30E+03 ± 6.39E-05	4.34E+03 ± 1.88E+02	2.20E+06 ± 1.16E+06			
GABC	3.22E+03 ± 2.59E+01	3.73E+03 ± 1.69E+02	1.08E+04 ± 2.81E+03			
GWO	3.33E+03 ± 4.83E+01	3.71E+03 ± 1.26E+02	3.90E+06 ± 3.10E+06			
SCA	3.78E+03 ± 1.36E+02	4.62E+03 ± 2.62E+02	7.44E+07 ± 2.59E+07			

Table 4.7: Statistical results obtained by the Wilcoxon signed ranks test between HGSA and DE, CMA-ES, GABC, GWO and SCA in $D = 30$ dimensions.

HGSA vs.	R^+	R^-	p -value	$\alpha=0.05$	$\alpha=0.01$
DE	1300.0	296.0	3.30E-05	YES	YES
CMA-ES	1383.5	212.5	2.00E-06	YES	YES
GABC	1312.5	340.5	1.02E-04	YES	YES
GWO	1242.5	410.5	9.14E-04	YES	YES
SCA	1466.0	130.0	0	YES	YES

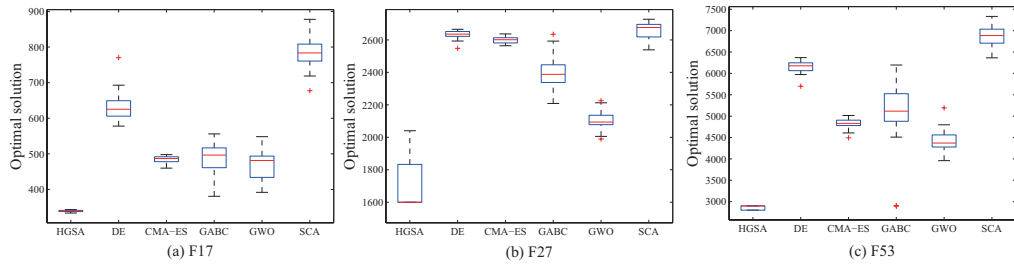


Figure 4.7: The box-and-whisker diagrams of optimal solutions obtained by HGSA and five heuristic algorithms on F17, F27 and F53 with 30 dimensions.

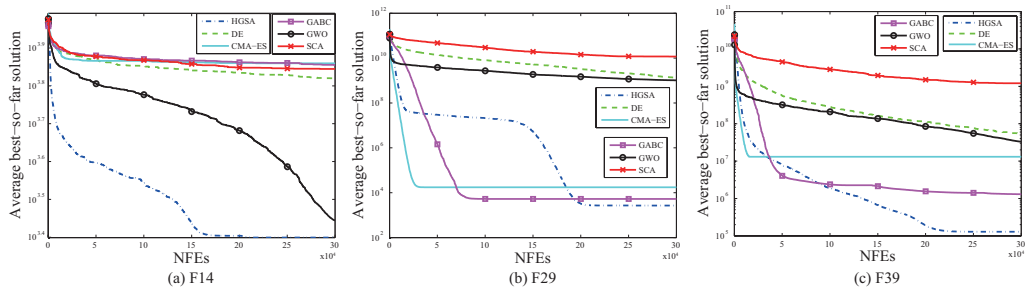


Figure 4.8: The convergence graphs of average best-so-far solutions obtained by HGSA and five heuristic algorithms on F14, F29 and F39 with 30 dimensions.

employ a global optimal individual to help to guide the movement of individuals, their performances are obviously different. In order to compare and analyze their difference, the comparative experiment among HGSA, FIPS [136], GPSO [137], CLPSO [138], OLPSO [139], GAPSO [140], DEPSO [141] and GL-PSO [142] is constructed to assess their performances on twenty eight CEC2013 test functions (F1-F28) with 30 dimensions. FIPS implements a fully informed topology of particle swarm according to its neighbors. GPSO adds an inertia weight into PSO to improve its effect. CLPSO adopts a learning strategy where other particles' historical best knowledge is recorded to update individuals. OLPSO uses an orthogonal learning strategy which selects the best information between each particle and its neighbors via an orthogonal experiment to effectively guide the movement direction of individuals. GAPSO combines GA with PSO to jointly enhance its exploration and exploitation abilities. DEPSO hybridizes DE and PSO with a random moving strategy to update individuals. GL-PSO uses genetic operators to evolve exemplars for PSO, which improves its global search ability and search efficiency. These seven variants of PSO not only use a global optimal individual but also add some other strategies so that their performances are significantly enhanced in contrast to the original PSO. Thus, they are used to compare with HGSA to further illustrate the effectiveness of the hierarchical structure. The parameters of seven PSOs are listed in Table 4.8. The population size is set to be 50. The mean and standard deviation of error values obtained by eight algorithms are shown in Table 4.9. The corresponding statistical results achieved by the Wilcoxon signed ranks test at a significant level of $\alpha = 0.05$ are revealed in Table 4.10.

Table 4.9 shows that HGSA obtains the least error values on a number of functions whereas seven variants of PSO perform better on certain functions. It illustrates that HGSA performs the best on a majority of functions and seven PSOs are more suitable for solving some specific functions due to their inherent mechanisms and characteristics. According to Table 4.10, we can conclude that HGSA significantly outperforms six variants of PSO, i.e., FIPS, GPSO, CLPSO, OLPSO, GAPSO and DEPSO, in terms of *p-value*, verifying that HGSA which adopts a hierarchical structure with an improved gravitational constant can effectively enhance its performance. However, the statistical result between HGSA and GL-PSO is not significant. This is because GL-PSO which is a kind of state-of-the-art PSO has a considerably superior search ability for functions. Genetic operators are used to generate exemplars for evolving particles. This genetic learning scheme achieves a cascade hybrid paradigm of PSO and GA so that GL-PSO is capable of providing a remarkable search performance. Although HGSA does not significantly outperform GL-PSO, the num-

Table 4.8: Parameter settings of seven variants of PSO.

Algorithm	Parameters
FIPS	$\omega = 0.7298, \sum c_i = 4.1$
GPSO	$\omega = 0.9 \sim 0.4, c_1 = 2.0, c_2 = 2.0$
CLPSO	$\omega = 0.7298, c = 1.49618, m = 7, p_c = 0.05 \sim 0.5$
OLPSO	$\omega = 0.9 \sim 0.4, c = 2.0, G = 5$
GAPSO	$\omega = 0.9 \sim 0.4, c_1 = 2.0, c_2 = 2.0, p_c = 0.5, p_m = 0.05, d_s = 7$
DEPSO	$\omega = 0.7298, c_1 = c_2 = 1.49618, C_R = 0.5, F_i \in [-1, -0.4] \cup [0.4, 1], \delta = 0.2, I = 4$
GL-PSO	$\omega = 0.7298, c = 1.49618, p_m = 0.01, s_g = 7$

Table 4.9: Experimental results of error values of CEC2013 test functions (F1-F28) with $D = 30$ dimensions using HGSA, FIPS, GPSO, CLPSO, OLPSO, GAPSO, DEPSO and GL-PSO.

Algorithm	F1	F2	F3	F4	F5	F6
HGSA	2.27E-14 ± 6.94E-14	3.44E+05 ± 1.95E+05	4.41E-04 ± 2.41E-03	4.62E+04 ± 8.27E+03	5.19E-12 ± 4.60E-12	1.92E+01 ± 2.01E+01
FIPS	1.00E+00 ± 3.46E+00	1.09E+07 ± 2.89E+06	1.88E+06 ± 2.08E+06	9.34E+03 ± 2.28E+03	4.10E-02 ± 1.16E-01	3.43E+01 ± 2.34E+01
GPSO	2.27E-13 ± 5.97E-14	2.89E+06 ± 1.17E+06	3.67E+07 ± 4.23E+07	1.24E+03 ± 3.21E+02	2.27E-13 ± 5.97E-14	4.43E+01 ± 2.98E+01
CLPSO	2.27E-13 ± 0.00E+00	2.00E+07 ± 3.91E+06	4.15E+08 ± 2.26E+08	2.90E+04 ± 5.72E+03	5.64E-11 ± 1.95E-11	3.32E+01 ± 8.86E+00
OLPSO	2.58E-13 ± 7.86E-14	1.60E+07 ± 1.96E+07	2.37E+07 ± 5.35E+07	5.83E+04 ± 1.52E+04	3.33E-13 ± 9.87E-14	2.70E+01 ± 2.15E+01
GAPSO	6.46E-11 ± 1.20E-10	1.16E+07 ± 6.64E+06	2.72E+09 ± 2.51E+09	5.08E+03 ± 2.06E+03	3.17E-06 ± 2.87E-06	5.48E+01 ± 2.73E+01
DEPSO	2.27E-13 ± 0.00E+00	1.54E+07 ± 7.83E+06	5.60E+08 ± 9.01E+08	4.14E+03 ± 1.04E+03	1.52E-13 ± 5.45E-14	4.12E+01 ± 2.75E+01
GL-PSO	1.97E-13 ± 7.86E-14	1.97E+05 ± 1.10E+05	1.95E+07 ± 2.61E+07	1.56E+04 ± 5.21E+03	1.48E-13 ± 5.30E-14	1.61E+01 ± 1.19E+01
	F7	F8	F9	F10	F11	F12
HGSA	4.86E-03 ± 1.19E-02	2.09E+01 ± 7.02E-02	1.49E+01 ± 2.80E+00	1.97E-03 ± 5.10E-03	1.88E+01 ± 4.65E+00	1.58E+01 ± 3.99E+00
FIPS	2.15E+01 ± 9.71E+00	2.10E+01 ± 5.04E-02	2.30E+01 ± 2.68E+00	4.34E+00 ± 4.62E+00	6.34E+01 ± 1.35E+01	1.83E+02 ± 8.38E+00
GPSO	2.36E+01 ± 8.41E+00	2.09E+01 ± 6.91E-02	1.94E+01 ± 3.69E+00	1.61E-01 ± 1.02E-01	2.05E+01 ± 6.11E+00	7.37E+01 ± 3.20E+01
CLPSO	7.95E+01 ± 1.02E+01	2.09E+01 ± 4.34E-02	2.84E+01 ± 1.80E+00	3.42E+00 ± 1.03E+00	1.24E+00 ± 1.42E+00	1.61E+02 ± 2.02E+01
OLPSO	2.26E+01 ± 9.35E+00	2.10E+01 ± 7.79E-02	2.26E+01 ± 7.70E+00	1.44E-01 ± 7.91E-02	6.30E-01 ± 8.05E-01	1.01E+02 ± 5.76E+01
GAPSO	7.10E+01 ± 3.23E+01	2.10E+01 ± 5.38E-02	1.66E+01 ± 3.09E+00	1.72E+01 ± 7.75E+00	1.17E+00 ± 5.36E-01	1.06E+02 ± 3.17E+01
DEPSO	4.56E+01 ± 2.78E+01	2.09E+01 ± 5.26E-02	1.53E+01 ± 4.49E+00	4.43E-02 ± 2.54E-02	1.70E+02 ± 1.90E+01	1.98E+02 ± 1.24E+01
GL-PSO	4.05E+01 ± 1.48E+01	2.09E+01 ± 7.28E-02	1.87E+01 ± 4.14E+00	1.39E-01 ± 7.75E-02	1.19E-12 ± 5.80E-12	5.07E+01 ± 1.41E+01
	F13	F14	F15	F16	F17	F18
HGSA	2.52E+01 ± 1.27E+01	1.49E+03 ± 2.64E+02	1.80E+03 ± 2.72E+02	8.79E-03 ± 5.33E-03	4.63E+01 ± 5.19E+00	4.79E+01 ± 6.30E+00
FIPS	1.59E+02 ± 1.40E+01	3.81E+03 ± 6.14E+02	6.57E+03 ± 3.80E+02	2.51E+00 ± 2.32E-01	1.71E+02 ± 1.08E+01	2.08E+02 ± 6.87E+00
GPSO	1.38E+02 ± 3.80E+01	1.11E+03 ± 2.77E+02	4.81E+03 ± 1.44E+03	1.98E+00 ± 3.98E-01	6.09E+01 ± 9.30E+00	2.27E+02 ± 2.43E+01
CLPSO	1.66E+02 ± 1.62E+01	5.35E+02 ± 1.23E+02	6.09E+03 ± 3.11E+02	2.44E+00 ± 2.43E-01	7.23E+01 ± 4.92E+00	2.22E+02 ± 1.21E+01
OLPSO	1.35E+02 ± 4.27E+01	1.79E+02 ± 1.23E+02	6.12E+03 ± 1.20E+03	1.90E+00 ± 3.78E-01	3.16E+01 ± 6.74E-01	1.81E+02 ± 3.19E+01
GAPSO	1.77E+02 ± 2.69E+01	7.81E+00 ± 2.48E+00	3.99E+03 ± 8.32E+02	1.88E+00 ± 4.03E-01	3.61E+01 ± 1.11E+00	2.23E+02 ± 2.01E+01
DEPSO	2.02E+02 ± 1.79E+01	6.04E+03 ± 5.03E+02	6.99E+03 ± 3.52E+02	2.57E+00 ± 3.12E-01	2.36E+02 ± 1.32E+01	2.42E+02 ± 1.00E+01
GL-PSO	1.16E+02 ± 3.54E+01	9.25E-01 ± 7.49E-01	3.55E+03 ± 6.99E+02	5.16E-01 ± 2.65E-01	3.14E+01 ± 5.67E-01	7.54E+01 ± 1.30E+01
	F19	F20	F21	F22	F23	F24
HGSA	3.69E+00 ± 7.35E-01	1.44E+01 ± 8.72E-01	3.22E+02 ± 7.17E+01	9.56E+02 ± 2.55E+02	4.02E+03 ± 6.97E+02	1.92E+02 ± 2.49E+01
FIPS	1.25E+01 ± 8.02E-01	1.21E+01 ± 6.28E-01	2.77E+02 ± 3.90E+01	3.07E+03 ± 5.95E+02	7.22E+03 ± 2.69E+02	2.11E+02 ± 6.17E+00
GPSO	2.96E+00 ± 6.31E-01	1.20E+01 ± 1.01E+00	3.35E+02 ± 8.91E+01	1.09E+03 ± 3.03E+02	4.31E+03 ± 9.56E+02	2.46E+02 ± 1.51E+01
CLPSO	3.23E+00 ± 8.03E-01	1.38E+01 ± 5.71E-01	3.00E+02 ± 3.17E+01	9.95E+02 ± 2.11E+02	6.62E+03 ± 4.00E+02	2.73E+02 ± 6.00E+00
OLPSO	1.74E+00 ± 4.14E-01	1.34E+01 ± 1.55E+00	3.12E+02 ± 7.64E+01	1.95E+02 ± 8.00E+01	6.19E+03 ± 1.12E+03	2.28E+02 ± 1.44E+01
GAPSO	2.20E+00 ± 4.56E-01	1.21E+01 ± 4.67E-01	3.14E+02 ± 7.63E+01	1.12E+02 ± 4.88E+01	4.20E+03 ± 9.85E+02	2.65E+02 ± 9.03E+00
DEPSO	1.79E+01 ± 1.77E+00	1.24E+01 ± 5.05E-01	3.05E+02 ± 1.17E+02	5.88E+03 ± 5.37E+02	7.22E+03 ± 4.40E+02	2.36E+02 ± 2.12E+01
GL-PSO	1.60E+00 ± 2.76E-01	1.19E+01 ± 8.60E-01	2.99E+02 ± 7.01E+01	1.04E+02 ± 3.18E+01	4.33E+03 ± 1.01E+03	2.39E+02 ± 1.07E+01
	F25	F26	F27	F28		
HGSA	2.00E+02 ± 7.60E-03	2.52E+02 ± 9.33E+01	4.29E+02 ± 1.60E+02	2.07E+02 ± 1.01E+02		
FIPS	2.49E+02 ± 2.98E+01	2.09E+02 ± 3.27E+01	5.83E+02 ± 1.26E+02	2.71E+02 ± 6.32E+01		
GPSO	2.87E+02 ± 1.61E+01	3.22E+02 ± 5.56E+01	8.05E+02 ± 1.17E+02	4.09E+02 ± 3.58E+02		
CLPSO	2.91E+02 ± 5.69E+00	2.02E+02 ± 5.76E-01	8.10E+02 ± 2.81E+02	3.00E+02 ± 1.11E-03		
OLPSO	2.65E+02 ± 8.18E+00	2.67E+02 ± 7.35E+01	6.57E+02 ± 9.66E+01	3.00E+02 ± 3.54E-13		
GAPSO	2.88E+02 ± 8.44E+00	2.75E+02 ± 7.52E+01	8.62E+02 ± 7.63E+01	3.85E+02 ± 2.67E+02		
DEPSO	2.85E+02 ± 3.53E+01	2.72E+02 ± 7.27E+01	7.90E+02 ± 1.69E+02	4.75E+02 ± 4.18E+02		
GL-PSO	2.67E+02 ± 8.12E+00	2.50E+02 ± 6.69E+01	6.65E+02 ± 1.18E+02	3.00E+02 ± 2.38E-13		

Table 4.10: Statistical results obtained by the Wilcoxon signed ranks test between HGSA and FIPS, GPSO, CLPSO, OLPSO, GAPSO, DEPSO and GL-PSO in $D = 30$ dimensions.

HGSA vs.	R^+	R^-	p -value	$\alpha=0.05$
FIPS	350.0	56.0	4.25E-04	YES
GPSO	317.0	61.0	1.39E-03	YES
CLPSO	292.0	86.0	1.21E-02	YES
OLPSO	313.0	93.0	1.10E-02	YES
GAPSO	294.0	112.0	3.79E-02	YES
DEPSO	338.0	40.0	1.25E-04	YES
GL-PSO	221.0	157.0	4.35E-01	No

ber of functions where the experimental results obtained by HGSA are better than those by GL-PSO is 16 out of 28. That is to say, both HGSA and GL-PSO are highly competitive on twenty eight functions. Thus, we can consider that HGSA still shows an effective and competitive performance in comparison with the state-of-the-art PSO. This experiment indicates that a global optimal individual is able to benefit the population evolution so that diverse PSOs can be proposed to reinforce the movement of individuals. Moreover, it is also effective for HGSA to achieve a better performance.

4.5 Discussion

4.5.1 Parameter sensitivity analysis

HGSA has two important parameters, i.e., L and K , which indicate the steepness of log-sigmoid function and the number of individuals on the medium layer, respectively. A large L value means a low steepness of log-sigmoid function whereas a small one denotes a high steepness of log-sigmoid function. Different steepness cause diverse gravitational constant values which may result in different performances of HGSA. The K value influences the hierarchical interaction among three layers. To be specific, a large K value indicates that the medium layer has many best individuals to guide the population on the bottom layer and be led by the global optimal individuals on the top layer, suggesting that HGSA is executing an exploration process. A small K value means that few best individuals act on the population and HGSA mainly exerts an exploitation ability to accelerate the convergence of population. Although the K value in HGSA linearly decreases as the same as that in the conventional GSA, its initial value may influence the performance of HGSA. Therefore, two experiments are conducted to investigate the influence of these two parameters on the performance of HGSA.

The parameter L is firstly investigated. To explore the effectiveness of L value, it is set to be 50, 100, 150, 200 and 250, implying five different steepness of log-sigmoid function. Their curves are shown in Fig. 4.9(a) where the steepness of log-sigmoid function gradually decreases according to the L value from 50 to 250. The K value linearly decreases and is set to be in the interval $[n, 2]$ where $n = 100$. Other parameter settings maintain invariant as the above experiments. Fifty seven benchmark functions with 30 dimensions are used to test the performance of HGSA with five different L values. Experimental results are summarized in Table 4.11 and statistical results calculated by the Friedman test are shown

Table 4.11: Experimental results of benchmark functions (F1-F57) with $D = 30$ dimensions using HGSA with five different L values.

Parameter	F1	F2	F3	F4	F5	F6
$L = 50$	-1.40E+03 ± 0.00E+00	8.36E+05 ± 2.78E+05	-1.20E+03 ± 1.85E+01	5.66E+04 ± 5.84E+03	-1.00E+03 ± 4.42E-09	-8.72E+02 ± 2.30E+01
$L = 100$	-1.40E+03 ± 1.98E-13	3.19E+05 ± 1.08E+05	-1.20E+03 ± 3.29E-07	5.30E+04 ± 5.52E+03	-1.00E+03 ± 4.87E-13	-8.88E+02 ± 1.42E+01
$L = 150$	-1.40E+03 ± 6.07E-13	1.70E+05 ± 6.86E+04	9.67E+04 ± 4.80E+05	5.05E+04 ± 5.26E+03	-1.00E+03 ± 2.25E-13	-8.92E+02 ± 7.28E+00
$L = 200$	-1.40E+03 ± 3.18E-11	9.95E+04 ± 5.31E+04	-1.20E+03 ± 2.00E-03	4.64E+04 ± 5.13E+03	-1.00E+03 ± 3.85E-12	-8.91E+02 ± 7.57E+00
$L = 250$	-1.40E+03 ± 7.67E-10	6.76E+04 ± 2.65E+04	7.01E+05 ± 3.81E+06	4.26E+04 ± 2.94E+03	-1.00E+03 ± 6.36E-11	-8.92E+02 ± 7.43E+00
	F7	F8	F9	F10	F11	F12
$L = 50$	-8.00E+02 ± 4.23E-01	-6.79E+02 ± 5.50E-02	-5.81E+02 ± 3.14E+00	-5.00E+02 ± 6.97E-03	-3.47E+02 ± 6.53E+00	-2.84E+02 ± 4.11E+00
$L = 100$	-7.99E+02 ± 1.63E+00	-6.79E+02 ± 7.51E-02	-5.81E+02 ± 3.72E+00	-5.00E+02 ± 4.08E-03	-3.47E+02 ± 9.94E+00	-2.83E+02 ± 3.65E+00
$L = 150$	-8.00E+02 ± 1.04E-01	-6.79E+02 ± 5.39E-02	-5.80E+02 ± 4.93E+00	-5.00E+02 ± 2.56E-03	-3.42E+02 ± 7.83E+00	-2.83E+02 ± 4.07E+00
$L = 200$	-7.99E+02 ± 1.78E+00	-6.79E+02 ± 5.05E-02	-5.82E+02 ± 4.08E+00	-5.00E+02 ± 3.59E-03	-3.41E+02 ± 9.53E+00	-2.81E+02 ± 4.66E+00
$L = 250$	-8.00E+02 ± 2.66E-01	-6.79E+02 ± 7.24E-02	-5.80E+02 ± 3.38E+00	-5.00E+02 ± 3.76E-03	-3.39E+02 ± 8.19E+00	-2.81E+02 ± 4.05E+00
	F13	F14	F15	F16	F17	F18
$L = 50$	-1.31E+02 ± 2.46E+01	2.27E+03 ± 3.36E+02	2.54E+03 ± 3.27E+02	2.00E+02 ± 6.25E-03	3.40E+02 ± 3.61E+00	4.40E+02 ± 3.57E+00
$L = 100$	-1.33E+02 ± 1.92E+01	2.51E+03 ± 4.21E+02	2.45E+03 ± 3.01E+02	2.00E+02 ± 2.15E-03	3.39E+02 ± 2.31E+00	4.40E+02 ± 2.53E+00
$L = 150$	-1.23E+02 ± 2.08E+01	2.52E+03 ± 4.47E+02	2.43E+03 ± 4.29E+02	2.00E+02 ± 1.69E-03	3.40E+02 ± 2.29E+00	4.41E+02 ± 2.44E+00
$L = 200$	-1.27E+02 ± 2.35E+01	2.48E+03 ± 3.98E+02	2.45E+03 ± 3.78E+02	2.00E+02 ± 1.12E-03	3.39E+02 ± 2.18E+00	4.41E+02 ± 3.81E+00
$L = 250$	-1.17E+02 ± 1.93E+01	2.52E+03 ± 3.91E+02	2.54E+03 ± 3.44E+02	2.00E+02 ± 1.15E-03	3.39E+02 ± 2.16E+00	4.41E+02 ± 3.31E+00
	F19	F20	F21	F22	F23	F24
$L = 50$	5.05E+02 ± 6.16E-01	6.15E+02 ± 5.57E-01	1.03E+03 ± 5.84E+01	3.63E+03 ± 7.63E+02	5.66E+03 ± 3.34E+02	1.20E+03 ± 2.02E+01
$L = 100$	5.05E+02 ± 5.96E-01	6.15E+02 ± 4.15E-01	1.01E+03 ± 4.38E+01	3.65E+03 ± 5.26E+02	5.61E+03 ± 4.07E+02	1.20E+03 ± 1.43E+01
$L = 150$	5.05E+02 ± 7.85E-01	6.15E+02 ± 3.15E-01	1.02E+03 ± 4.96E+01	3.66E+03 ± 3.79E+02	5.63E+03 ± 3.57E+02	1.20E+03 ± 1.40E+01
$L = 200$	5.04E+02 ± 6.82E-01	6.15E+02 ± 5.32E-01	1.01E+03 ± 6.37E+01	3.68E+03 ± 5.53E+02	5.67E+03 ± 3.39E+02	1.19E+03 ± 2.25E+01
$L = 250$	5.05E+02 ± 7.24E-01	6.15E+02 ± 2.64E-01	1.03E+03 ± 6.17E+01	3.91E+03 ± 5.77E+02	5.75E+03 ± 3.10E+02	1.19E+03 ± 1.99E+01
	F25	F26	F27	F28	F29	F30
$L = 50$	1.30E+03 ± 4.67E-03	1.51E+03 ± 5.18E+01	1.68E+03 ± 1.27E+02	1.65E+03 ± 9.00E+01	2.19E+03 ± 1.53E+03	5.90E+04 ± 6.85E+03
$L = 100$	1.30E+03 ± 1.33E+01	1.49E+03 ± 6.58E+01	1.71E+03 ± 1.40E+02	1.63E+03 ± 9.80E+01	2.68E+03 ± 2.50E+03	4.36E+04 ± 5.49E+03
$L = 150$	1.30E+03 ± 1.52E+01	1.51E+03 ± 5.34E+01	1.73E+03 ± 1.49E+02	1.64E+03 ± 9.32E+01	2.69E+03 ± 1.81E+03	3.18E+04 ± 4.11E+03
$L = 200$	1.30E+03 ± 4.04E-03	1.49E+03 ± 7.82E+01	1.74E+03 ± 1.68E+02	1.65E+03 ± 9.00E+01	2.32E+03 ± 1.70E+03	2.37E+04 ± 2.95E+03
$L = 250$	1.30E+03 ± 6.63E-03	1.51E+03 ± 6.01E+01	1.69E+03 ± 1.02E+02	1.64E+03 ± 9.32E+01	2.38E+03 ± 1.84E+03	1.66E+04 ± 2.53E+03
	F31	F32	F33	F34	F35	F36
$L = 50$	5.20E+02 ± 2.32E+00	6.51E+02 ± 1.21E+01	6.08E+02 ± 5.20E+00	7.41E+02 ± 2.96E+00	9.02E+02 ± 8.61E+00	9.00E+02 ± 0.00E+00
$L = 100$	5.19E+02 ± 2.63E+00	6.53E+02 ± 1.28E+01	6.08E+02 ± 4.54E+00	7.41E+02 ± 3.01E+00	9.00E+02 ± 9.03E+00	9.00E+02 ± 9.67E-14
$L = 150$	5.18E+02 ± 2.42E+00	6.54E+02 ± 1.11E+01	6.09E+02 ± 4.39E+00	7.41E+02 ± 2.64E+00	9.05E+02 ± 1.00E+01	9.00E+02 ± 4.06E-13
$L = 200$	5.18E+02 ± 2.19E+00	6.58E+02 ± 1.45E+01	6.09E+02 ± 4.29E+00	7.41E+02 ± 3.10E+00	9.09E+02 ± 9.88E+00	9.00E+02 ± 2.95E-11
$L = 250$	5.18E+02 ± 1.88E+00	6.52E+02 ± 1.22E+01	6.10E+02 ± 4.18E+00	7.41E+02 ± 3.06E+00	9.09E+02 ± 1.11E+01	9.00E+02 ± 3.02E-10
	F37	F38	F39	F40	F41	F42
$L = 50$	4.15E+03 ± 3.36E+02	1.20E+03 ± 2.84E+01	3.49E+05 ± 1.84E+05	1.44E+04 ± 4.04E+03	7.96E+03 ± 4.29E+03	2.10E+03 ± 4.62E+02
$L = 100$	4.21E+03 ± 2.93E+02	1.20E+03 ± 2.98E+01	1.29E+05 ± 8.15E+04	1.46E+04 ± 5.32E+03	6.72E+03 ± 3.05E+03	2.20E+03 ± 7.21E+02
$L = 150$	4.27E+03 ± 4.04E+02	1.19E+03 ± 2.75E+01	3.42E+04 ± 1.66E+04	1.35E+04 ± 5.53E+03	5.51E+03 ± 2.59E+03	2.26E+03 ± 5.37E+02
$L = 200$	4.32E+03 ± 3.90E+02	1.19E+03 ± 3.11E+01	1.62E+04 ± 7.44E+03	1.35E+04 ± 4.44E+03	4.78E+03 ± 1.35E+03	2.43E+03 ± 8.68E+02
$L = 250$	4.17E+03 ± 4.26E+02	1.19E+03 ± 2.81E+01	1.50E+04 ± 3.42E+03	1.28E+04 ± 5.02E+03	4.67E+03 ± 1.53E+03	2.41E+03 ± 7.37E+02
	F43	F44	F45	F46	F47	F48
$L = 50$	2.83E+03 ± 2.41E+02	2.77E+03 ± 2.03E+02	1.22E+05 ± 4.78E+04	5.36E+03 ± 1.23E+03	2.85E+03 ± 1.96E+02	2.41E+03 ± 5.89E+01
$L = 100$	2.83E+03 ± 2.32E+02	2.77E+03 ± 1.99E+02	6.16E+04 ± 1.47E+04	5.42E+03 ± 1.25E+03	2.86E+03 ± 2.24E+02	2.41E+03 ± 5.90E+01
$L = 150$	2.89E+03 ± 2.42E+02	2.70E+03 ± 2.12E+02	5.15E+04 ± 1.03E+04	4.86E+03 ± 1.39E+03	2.81E+03 ± 1.84E+02	2.43E+03 ± 1.56E+01
$L = 200$	2.86E+03 ± 2.35E+02	2.71E+03 ± 2.08E+02	4.80E+04 ± 1.30E+04	5.03E+03 ± 1.47E+03	2.86E+03 ± 1.49E+02	2.42E+03 ± 4.49E+01
$L = 250$	2.92E+03 ± 2.93E+02	2.75E+03 ± 1.92E+02	4.57E+04 ± 1.07E+04	5.03E+03 ± 9.94E+02	2.87E+03 ± 1.85E+02	2.43E+03 ± 1.51E+01
	F49	F50	F51	F52	F53	F54
$L = 50$	2.30E+03 ± 3.87E-13	2.80E+03 ± 1.08E+02	2.92E+03 ± 2.70E+01	2.89E+03 ± 8.08E+00	2.86E+03 ± 4.98E+01	3.26E+03 ± 1.87E+01
$L = 100$	2.30E+03 ± 3.91E-09	2.76E+03 ± 1.33E+02	2.92E+03 ± 3.58E+01	2.89E+03 ± 7.59E+00	2.85E+03 ± 5.07E+01	3.25E+03 ± 2.08E+01
$L = 150$	2.30E+03 ± 4.63E-07	2.83E+03 ± 1.38E+02	2.93E+03 ± 4.31E+01	2.89E+03 ± 7.68E+00	2.86E+03 ± 4.98E+01	3.26E+03 ± 1.93E+01
$L = 200$	2.30E+03 ± 6.54E-06	2.81E+03 ± 1.27E+02	2.93E+03 ± 3.92E+01	2.89E+03 ± 8.18E+00	2.85E+03 ± 5.09E+01	3.25E+03 ± 1.82E+01
$L = 250$	2.44E+03 ± 7.73E+02	2.80E+03 ± 9.88E+01	2.92E+03 ± 5.05E+01	2.89E+03 ± 6.98E+00	2.86E+03 ± 5.04E+01	3.26E+03 ± 1.90E+01
	F55	F56	F57			
$L = 50$	3.12E+03 ± 3.34E+01	4.07E+03 ± 1.80E+02	1.33E+04 ± 2.82E+03			
$L = 100$	3.11E+03 ± 2.82E+01	4.05E+03 ± 1.88E+02	1.10E+04 ± 2.60E+03			
$L = 150$	3.10E+03 ± 1.75E+01	4.09E+03 ± 1.87E+02	1.00E+04 ± 1.38E+03			
$L = 200$	3.10E+03 ± 1.30E-06	4.13E+03 ± 1.70E+02	9.12E+03 ± 1.24E+03			
$L = 250$	3.10E+03 ± 7.04E-06	4.14E+03 ± 2.00E+02	8.71E+03 ± 7.57E+02			

Table 4.12: Statistical results of parameter L obtained by the Friedman test, where * indicates the best average rank of parameter.

Parameter	Average rank	p -value	$\alpha = 0.05$
$L = 50$	3.0614	3.90E-01	No
* $L = 100$	2.807		
$L = 150$	3.1228	2.86E-01	No
$L = 200$	2.8947	7.67E-01	No
$L = 250$	3.114	3.00E-01	No

Table 4.13: Experimental results of benchmark functions (F1-F57) with $D = 30$ dimensions using HGSA with five different K value intervals, where $n = 100$.

Parameter	F1	F2	F3	F4	F5	F6
$K \in [n, 2]$	-1.40E+03 ± 1.98E-13	3.19E+05 ± 1.08E+05	-1.20E+03 ± 3.29E-07	5.30E+04 ± 5.52E+03	-1.00E+03 ± 4.87E-13	-8.88E+02 ± 1.42E+01
$K \in [75\%n, 2]$	-1.40E+03 ± 1.03E-13	1.56E+05 ± 7.27E+04	1.50E+05 ± 5.92E+05	5.52E+04 ± 5.54E+03	-1.00E+03 ± 3.07E-13	-8.91E+02 ± 7.01E+00
$K \in [50\%n, 2]$	-1.40E+03 ± 5.97E-14	9.94E+04 ± 6.88E+04	1.89E+06 ± 4.93E+06	5.23E+04 ± 5.96E+03	-1.00E+03 ± 1.23E-13	-8.87E+02 ± 1.25E+01
$K \in [25\%n, 2]$	-1.40E+03 ± 4.22E-14	5.40E+04 ± 2.03E+04	1.23E+06 ± 1.47E+06	3.86E+04 ± 5.88E+03	-1.00E+03 ± 5.97E-14	-8.82E+02 ± 2.44E+01
$K \in [15\%n, 2]$	-1.40E+03 ± 9.44E-14	5.10E+04 ± 2.56E+04	1.57E+06 ± 5.40E+06	1.79E+04 ± 3.51E+03	-1.00E+03 ± 8.44E-14	-8.55E+02 ± 4.68E+01
	F7	F8	F9	F10	F11	F12
$K \in [n, 2]$	-7.99E+02 ± 1.63E+00	-6.79E+02 ± 7.51E-02	-5.81E+02 ± 3.72E+00	-5.00E+02 ± 4.08E-03	-3.47E+02 ± 9.94E+00	-2.83E+02 ± 3.65E+00
$K \in [75\%n, 2]$	-8.00E+02 ± 3.86E-01	-6.79E+02 ± 7.59E-02	-5.76E+02 ± 4.86E+00	-5.00E+02 ± 4.39E-03	-3.29E+02 ± 9.50E+00	-2.62E+02 ± 1.09E+01
$K \in [50\%n, 2]$	-7.95E+02 ± 6.46E+00	-6.79E+02 ± 8.43E-02	-5.72E+02 ± 2.84E+00	-5.00E+02 ± 4.60E-03	-2.78E+02 ± 1.38E+01	5.68E+00 ± 3.20E+01
$K \in [25\%n, 2]$	-7.69E+02 ± 1.86E+01	-6.79E+02 ± 5.30E-02	-5.68E+02 ± 3.06E+00	-5.00E+02 ± 5.10E-03	-9.69E+01 ± 3.27E+01	1.27E+02 ± 4.29E+01
$K \in [15\%n, 2]$	-7.39E+02 ± 1.95E+01	-6.79E+02 ± 4.55E-02	-5.65E+02 ± 2.85E+00	-5.00E+02 ± 7.98E-03	-4.46E+00 ± 5.47E+01	1.20E+02 ± 5.50E+01
	F13	F14	F15	F16	F17	F18
$K \in [n, 2]$	-1.33E+02 ± 1.92E+01	2.51E+03 ± 4.21E+02	2.45E+03 ± 3.01E+02	2.00E+02 ± 2.15E-03	3.39E+02 ± 2.31E+00	4.40E+02 ± 2.53E+00
$K \in [75\%n, 2]$	-7.13E+01 ± 2.03E+01	2.35E+03 ± 3.80E+02	2.69E+03 ± 4.15E+02	2.00E+02 ± 2.65E-03	3.42E+02 ± 2.88E+00	4.42E+02 ± 3.20E+00
$K \in [50\%n, 2]$	3.20E+02 ± 4.92E+01	2.60E+03 ± 4.12E+02	3.07E+03 ± 4.15E+02	2.00E+02 ± 2.63E-03	3.48E+02 ± 4.74E+00	4.43E+02 ± 3.60E+00
$K \in [25\%n, 2]$	3.39E+02 ± 5.59E+01	3.30E+03 ± 4.31E+02	4.06E+03 ± 5.57E+02	2.00E+02 ± 5.52E-03	3.60E+02 ± 5.40E+00	4.58E+02 ± 5.84E+00
$K \in [15\%n, 2]$	3.35E+02 ± 5.16E+01	4.20E+03 ± 5.43E+02	4.28E+03 ± 5.46E+02	2.00E+02 ± 1.19E-02	3.77E+02 ± 1.06E+01	4.76E+02 ± 1.15E+01
	F19	F20	F21	F22	F23	F24
$K \in [n, 2]$	5.05E+02 ± 5.96E-01	6.15E+02 ± 4.15E-01	1.01E+03 ± 4.38E+01	3.65E+03 ± 5.26E+02	5.61E+03 ± 4.07E+02	1.20E+03 ± 1.43E+01
$K \in [75\%n, 2]$	5.04E+02 ± 4.89E-01	6.15E+02 ± 6.78E-01	1.02E+03 ± 6.80E+01	3.69E+03 ± 4.69E+02	5.74E+03 ± 3.27E+02	1.20E+03 ± 2.09E+01
$K \in [50\%n, 2]$	5.04E+02 ± 6.36E-01	6.14E+02 ± 1.87E+00	1.02E+03 ± 5.44E+01	5.03E+03 ± 9.84E+02	6.24E+03 ± 2.77E+02	1.24E+03 ± 2.05E+01
$K \in [25\%n, 2]$	5.03E+02 ± 6.56E-01	6.13E+02 ± 2.13E+00	1.04E+03 ± 6.46E+01	6.67E+03 ± 6.69E+02	6.69E+03 ± 3.87E+02	1.29E+03 ± 6.90E+01
$K \in [15\%n, 2]$	5.03E+02 ± 5.79E-01	6.13E+02 ± 1.58E+00	1.04E+03 ± 8.20E+01	7.12E+03 ± 6.64E+02	6.98E+03 ± 3.61E+02	1.30E+03 ± 3.27E+01
	F25	F26	F27	F28	F29	F30
$K \in [n, 2]$	1.30E+03 ± 1.33E+01	1.49E+03 ± 6.58E+01	1.71E+03 ± 1.40E+02	1.63E+03 ± 9.80E+01	2.68E+03 ± 2.50E+03	4.36E+04 ± 5.49E+03
$K \in [75\%n, 2]$	1.30E+03 ± 1.41E+01	1.52E+03 ± 4.40E+01	1.83E+03 ± 1.64E+02	2.09E+03 ± 8.99E+02	2.60E+03 ± 2.06E+03	3.59E+04 ± 5.50E+03
$K \in [50\%n, 2]$	1.41E+03 ± 5.99E+01	1.53E+03 ± 3.08E+01	2.02E+03 ± 1.17E+02	4.93E+03 ± 2.56E+02	3.45E+03 ± 4.08E+03	2.12E+04 ± 3.77E+03
$K \in [25\%n, 2]$	1.50E+03 ± 1.33E+01	1.55E+03 ± 2.34E+01	2.23E+03 ± 8.26E+01	5.23E+03 ± 2.73E+02	2.81E+03 ± 3.12E+03	3.00E+02 ± 1.63E-13
$K \in [15\%n, 2]$	1.49E+03 ± 1.46E+01	1.56E+03 ± 1.79E+01	2.34E+03 ± 1.18E+02	5.20E+03 ± 2.80E+02	2.56E+03 ± 3.95E+03	3.00E+02 ± 4.02E-13
	F31	F32	F33	F34	F35	F36
$K \in [n, 2]$	5.19E+02 ± 2.63E+00	6.53E+02 ± 1.28E+01	6.08E+02 ± 4.54E+00	7.41E+02 ± 3.01E+00	9.00E+02 ± 9.03E+00	9.00E+02 ± 9.67E-14
$K \in [75\%n, 2]$	5.18E+02 ± 2.31E+00	6.70E+02 ± 1.38E+01	6.14E+02 ± 6.94E+00	7.43E+02 ± 3.74E+00	9.12E+02 ± 1.03E+01	9.00E+02 ± 1.01E-13
$K \in [50\%n, 2]$	4.85E+02 ± 4.24E+01	6.83E+02 ± 1.70E+01	6.30E+02 ± 4.93E+00	7.48E+02 ± 4.40E+00	9.27E+02 ± 1.18E+01	9.05E+02 ± 2.48E+01
$K \in [25\%n, 2]$	4.98E+02 ± 4.34E+01	6.79E+02 ± 1.83E+01	6.40E+02 ± 3.56E+00	8.01E+02 ± 2.31E+01	9.17E+02 ± 1.16E+01	2.15E+03 ± 3.18E+02
$K \in [15\%n, 2]$	5.14E+02 ± 2.92E+01	6.68E+02 ± 1.56E+01	6.46E+02 ± 4.27E+00	8.98E+02 ± 3.85E+01	9.10E+02 ± 1.60E+01	3.08E+03 ± 3.41E+02
	F37	F38	F39	F40	F41	F42
$K \in [n, 2]$	4.21E+03 ± 2.93E+02	1.20E+03 ± 2.98E+01	1.29E+05 ± 8.15E+04	1.46E+04 ± 5.32E+03	6.72E+03 ± 3.05E+03	2.20E+03 ± 7.21E+02
$K \in [75\%n, 2]$	4.24E+03 ± 4.26E+02	1.19E+03 ± 2.91E+01	5.00E+04 ± 1.93E+04	1.42E+04 ± 4.18E+03	6.05E+03 ± 2.28E+03	2.23E+03 ± 5.74E+02
$K \in [50\%n, 2]$	4.74E+03 ± 4.70E+02	1.19E+03 ± 2.49E+01	2.02E+04 ± 6.27E+03	1.53E+04 ± 4.21E+03	4.44E+03 ± 8.41E+02	2.42E+03 ± 8.59E+02
$K \in [25\%n, 2]$	4.98E+03 ± 6.96E+02	1.19E+03 ± 2.00E+01	1.58E+04 ± 4.76E+03	1.41E+04 ± 5.33E+03	3.32E+03 ± 1.10E+03	1.99E+03 ± 3.77E+02
$K \in [15\%n, 2]$	5.06E+03 ± 5.74E+02	1.18E+03 ± 1.42E+01	4.83E+06 ± 2.28E+07	1.53E+04 ± 6.46E+03	2.58E+03 ± 5.67E+02	2.60E+03 ± 9.23E+02
	F43	F44	F45	F46	F47	F48
$K \in [n, 2]$	2.83E+03 ± 2.32E+02	2.77E+03 ± 1.99E+02	6.16E+04 ± 1.47E+04	5.42E+03 ± 1.25E+03	2.86E+03 ± 2.24E+02	2.41E+03 ± 5.90E+01
$K \in [75\%n, 2]$	2.98E+03 ± 3.09E+02	2.94E+03 ± 1.77E+02	4.76E+04 ± 9.61E+03	4.94E+03 ± 9.07E+02	2.89E+03 ± 2.13E+02	2.45E+03 ± 5.09E+01
$K \in [50\%n, 2]$	3.11E+03 ± 4.15E+02	2.94E+03 ± 1.84E+02	4.44E+04 ± 6.73E+03	4.53E+03 ± 1.11E+03	2.99E+03 ± 1.90E+02	2.54E+03 ± 2.46E+01
$K \in [25\%n, 2]$	3.22E+03 ± 3.38E+02	2.82E+03 ± 2.58E+02	3.95E+04 ± 7.70E+03	5.32E+03 ± 1.72E+03	2.91E+03 ± 1.61E+02	2.51E+03 ± 3.11E+01
$K \in [15\%n, 2]$	3.22E+03 ± 3.08E+02	2.77E+03 ± 2.87E+02	3.57E+04 ± 8.21E+03	5.03E+03 ± 1.94E+03	2.88E+03 ± 1.82E+02	2.49E+03 ± 2.25E+01
	F49	F50	F51	F52	F53	F54
$K \in [n, 2]$	2.30E+03 ± 3.91E-09	2.76E+03 ± 1.33E+02	2.92E+03 ± 3.58E+01	2.89E+03 ± 7.59E+00	2.85E+03 ± 5.07E+01	3.25E+03 ± 2.08E+01
$K \in [75\%n, 2]$	2.75E+03 ± 1.37E+03	3.02E+03 ± 1.58E+02	3.05E+03 ± 5.69E+01	2.89E+03 ± 2.66E+00	3.08E+03 ± 9.31E+02	3.34E+03 ± 6.78E+01
$K \in [50\%n, 2]$	5.38E+03 ± 2.08E+03	3.34E+03 ± 1.36E+02	3.25E+03 ± 4.89E+01	2.89E+03 ± 2.14E+00	6.02E+03 ± 2.00E+03	4.27E+03 ± 2.71E+02
$K \in [25\%n, 2]$	6.75E+03 ± 9.94E+02	3.47E+03 ± 1.17E+02	3.31E+03 ± 6.47E+01	2.90E+03 ± 1.30E+01	7.17E+03 ± 1.57E+03	4.41E+03 ± 2.40E+02
$K \in [15\%n, 2]$	6.28E+03 ± 1.27E+03	3.44E+03 ± 9.89E+01	3.35E+03 ± 5.80E+01	2.91E+03 ± 1.55E+01	7.79E+03 ± 1.16E+03	4.38E+03 ± 2.74E+02
	F55	F56	F57			
$K \in [n, 2]$	3.11E+03 ± 2.82E+01	4.05E+03 ± 1.88E+02	1.10E+04 ± 2.60E+03			
$K \in [75\%n, 2]$	3.10E+03 ± 1.67E-09	4.20E+03 ± 1.97E+02	7.51E+03 ± 8.20E+02			
$K \in [50\%n, 2]$	3.10E+03 ± 1.91E-09	4.30E+03 ± 1.81E+02	6.83E+03 ± 5.10E+02			
$K \in [25\%n, 2]$	3.10E+03 ± 1.89E+01	4.51E+03 ± 2.81E+02	7.19E+03 ± 5.92E+02			
$K \in [15\%n, 2]$	3.15E+03 ± 9.72E+01	4.49E+03 ± 2.66E+02	8.14E+03 ± 1.20E+03			

Table 4.14: Statistical results of parameter K obtained by the Friedman test, where * indicates the best average rank of parameter.

Parameter	Average rank	p -value	$\alpha = 0.05$
* $K \in [n, 2]$	2.2193		
$K \in [75\%n, 2]$	2.4825	3.74E-01	No
$K \in [50\%n, 2]$	3.1228	2.28E-03	Yes
$K \in [25\%n, 2]$	3.4825	2.00E-05	Yes
$K \in [15\%n, 2]$	3.693	1.00E-06	Yes

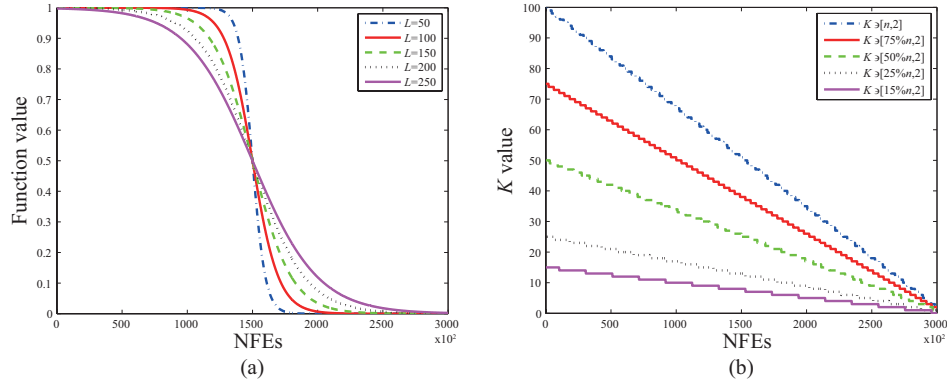


Figure 4.9: The curves of (a) log-sigmoid function with five different L values and (b) five different K value intervals.

in Table 4.12.

From Table 4.11, it can be seen that HGSA with different L values obtains the best results on different functions, indicating that each L value is effective for certain functions, respectively. Table 4.12 shows that $L = 100$ has the best average rank among five values whereas it is not significantly better than the others. That is to say, HGSA with five different L values can obtain a similar performance and their experimental results have no significant difference. Thus, we can consider that these five L values are all effective. Five different steepness of log-sigmoid function hardly influence the overall performance of HGSA. In order to determine the best L value, $L = 100$ is adopted according to the best average rank among five values.

After selecting the best value $L = 100$, the parameter K is investigated. Since the K best individuals on the medium layer come from the population on the bottom layer, its initial value is set to be n , $75\%n$, $50\%n$, $25\%n$ and $15\%n$ where $n = 100$, indicating that different number of initial individuals on the medium layer. Their curves are displayed in Fig. 4.9(b) where they linearly decrease from their initial values to 2 with iterations. Experimental and statistical results obtained by HGSA with five different K initial values on fifty seven benchmark functions with 30 dimensions are listed in Tables 4.13 and 4.14.

In Table 4.13, it can be observed that HGSA with $K \in [n, 2]$ has the best results on 34 functions, showing its good performance on numerous functions. From Table 4.14, it can be found that HGSA with $K \in [n, 2]$ has the best average rank and significantly outperforms that with $K \in [50\%n, 2]$, $K \in [25\%n, 2]$ and $K \in [15\%n, 2]$ according to p -value, suggesting that a large initial K value is better than a small one. This is because a large

number of individuals on the medium layer can enhance the hierarchical interaction among three layers to improve the exploration ability of HGSA. However, a small initial K value means that the number of individuals on the medium layer is too few to guarantee a sufficient exploration process of HGSA. Thus, the performance of HGSA with a small initial K value declines. In addition, the statistical result between $K \in [n, 2]$ and $K \in [75\%n, 2]$ shows a non-significant difference because both have approximately initial values, which also indicates the effectiveness of a large initial K value. Therefore, $K \in [n, 2]$ is adopted to be the best K value interval according to the best average rank. It demonstrates that the number of initial individuals on the medium layer which is equal to the population size n is the best selection in HGSA. Based on these two experiments, it can be concluded that $L = 100$ and $K \in [n, 2]$ are the best parameter settings for HGSA.

4.5.2 Component-wise analysis

The above experiments have demonstrated that HGSA has a superior performance due to its population structure and improved gravitational constant. In order to further verify the effect of these combination, a component-wise experiment is carried out. Two comparative algorithms consist of a hierarchical GSA with an original gravitational constant (HGSA-OG) and a conventional GSA with an improved gravitational constant (GSA-IG). Three algorithms are used to test fifty seven benchmark functions with 30 dimensions. Parameter settings are the same as the above experiments. Experimental and statistical results are shown in Tables 4.15 and 4.16.

According to Table 4.15, it can be found that HGSA, HGSA-OG and GSA-IG obtain the best results on 31, 3 and 23 functions, respectively. It illustrates that HGSA performs better than HGSA-OG and GSA-IG from the number of functions. Statistical results in Table 4.16 demonstrate that HGSA significantly outperforms HGSA-OG and GSA-IG according to *p-value*. The comparison between HGSA and HGSA-OG manifests that an improved gravitational constant effectively enhances the exploration ability of algorithm. In other words, a log-sigmoid gravitational constant is better than an exponential one because it reinforces the exploration period of algorithm such that HGSA can find a better optimal solution. The comparison between HGSA and GSA-IG demonstrates that a hierarchical population structure can better direct the evolution of individuals and enhance the overall performance of algorithm. That is to say, a hierarchical control can effectively balance the exploration and exploitation abilities of algorithm, and provide a promising guideline for evolving the population. Consequently, this component-wise experiment proves the

Table 4.15: Experimental results of benchmark functions (F1-F57) with $D = 30$ dimensions using HGSA, HGSA-OG and GSA-IG.

Algorithm	F1	F2	F3	F4	F5	F6
HGSA	-1.40E+03 ± 1.98E-13	3.19E+05 ± 1.08E+05	-1.20E+03 ± 3.29E-07	5.30E+04 ± 5.52E+03	-1.00E+03 ± 4.87E-13	-8.88E+02 ± 1.42E+01
HGSA-OG	-1.40E+03 ± 0.00E+00	7.37E+06 ± 1.41E+06	5.19E+09 ± 2.29E+09	6.69E+04 ± 3.50E+03	-1.00E+03 ± 9.53E-13	-8.33E+02 ± 1.38E+01
GSA-IG	-1.40E+03 ± 7.31E-14	3.78E+05 ± 1.51E+05	-1.20E+03 ± 1.16E-03	6.39E+04 ± 3.98E+03	-1.00E+03 ± 3.07E-13	-8.90E+02 ± 6.47E+00
	F7	F8	F9	F10	F11	F12
HGSA	-7.99E+02 ± 1.63E+00	-6.79E+02 ± 7.51E-02	-5.81E+02 ± 3.72E+00	-5.00E+02 ± 4.08E-03	-3.47E+02 ± 9.94E+00	-2.83E+02 ± 3.65E+00
HGSA-OG	-7.36E+02 ± 9.42E+00	-6.79E+02 ± 5.97E-02	-5.67E+02 ± 3.08E+00	-5.00E+02 ± 6.26E-02	-1.05E+02 ± 1.94E+01	3.12E+01 ± 2.58E+01
GSA-IG	-7.99E+02 ± 1.99E+00	-6.79E+02 ± 5.09E-02	-5.82E+02 ± 3.50E+00	-5.00E+02 ± 3.97E-03	-3.44E+02 ± 9.58E+00	-2.83E+02 ± 4.06E+00
	F13	F14	F15	F16	F17	F18
HGSA	-1.33E+02 ± 1.92E+01	2.51E+03 ± 4.21E+02	2.45E+03 ± 3.01E+02	2.00E+02 ± 2.15E-03	3.39E+02 ± 2.31E+00	4.40E+02 ± 2.53E+00
HGSA-OG	2.65E+02 ± 3.84E+01	3.90E+03 ± 5.66E+02	3.64E+03 ± 5.06E+02	2.00E+02 ± 3.88E-03	3.63E+02 ± 7.38E+00	4.55E+02 ± 6.09E+00
GSA-IG	-1.38E+02 ± 1.73E+01	2.46E+03 ± 3.84E+02	2.49E+03 ± 3.04E+02	2.00E+02 ± 1.88E-03	3.42E+02 ± 2.44E+00	4.43E+02 ± 3.01E+00
	F19	F20	F21	F22	F23	F24
HGSA	5.05E+02 ± 5.96E-01	6.15E+02 ± 4.15E-01	1.01E+03 ± 4.38E+01	3.65E+03 ± 5.26E+02	5.61E+03 ± 4.07E+02	1.20E+03 ± 1.43E+01
HGSA-OG	5.09E+02 ± 1.66E+00	6.15E+02 ± 2.05E-01	1.01E+03 ± 3.64E+01	7.20E+03 ± 5.28E+02	6.79E+03 ± 4.02E+02	1.31E+03 ± 5.64E+01
GSA-IG	5.04E+02 ± 6.71E-01	6.15E+02 ± 1.54E-01	1.04E+03 ± 6.69E+01	3.67E+03 ± 5.62E+02	5.64E+03 ± 4.05E+02	1.20E+03 ± 2.19E+01
	F25	F26	F27	F28	F29	F30
HGSA	1.30E+03 ± 1.33E+01	1.49E+03 ± 6.58E+01	1.71E+03 ± 1.40E+02	1.63E+03 ± 9.80E+01	2.68E+03 ± 2.50E+03	4.36E+04 ± 5.49E+03
HGSA-OG	1.49E+03 ± 1.32E+01	1.56E+03 ± 1.99E+01	2.22E+03 ± 8.93E+01	5.06E+03 ± 2.70E+02	1.93E+03 ± 8.32E+02	8.27E+04 ± 6.69E+03
GSA-IG	1.30E+03 ± 9.79E-04	1.52E+03 ± 9.72E+00	1.68E+03 ± 1.23E+02	1.65E+03 ± 9.00E+01	2.34E+03 ± 1.86E+03	6.34E+04 ± 9.15E+03
	F31	F32	F33	F34	F35	F36
HGSA	5.19E+02 ± 2.63E+00	6.53E+02 ± 1.28E+01	6.08E+02 ± 4.54E+00	7.41E+02 ± 3.01E+00	9.00E+02 ± 9.03E+00	9.00E+02 ± 9.67E-14
HGSA-OG	5.40E+02 ± 2.54E+01	7.24E+02 ± 1.99E+01	6.51E+02 ± 3.27E+00	7.88E+02 ± 1.40E+01	9.56E+02 ± 1.32E+01	2.99E+03 ± 3.47E+02
GSA-IG	5.18E+02 ± 2.93E+00	6.54E+02 ± 1.57E+01	6.08E+02 ± 3.92E+00	7.43E+02 ± 3.93E+00	9.07E+02 ± 8.81E+00	9.00E+02 ± 2.99E-14
	F37	F38	F39	F40	F41	F42
HGSA	4.21E+03 ± 2.93E+02	1.20E+03 ± 2.98E+01	1.29E+05 ± 8.15E+04	1.46E+04 ± 5.32E+03	6.72E+03 ± 3.05E+03	2.20E+03 ± 7.21E+02
HGSA-OG	4.89E+03 ± 3.95E+02	1.44E+03 ± 7.39E+01	9.28E+06 ± 1.74E+07	3.09E+04 ± 5.77E+03	4.77E+05 ± 1.08E+05	1.17E+04 ± 1.99E+03
GSA-IG	4.08E+03 ± 3.10E+02	1.20E+03 ± 3.08E+01	1.36E+05 ± 7.86E+04	1.46E+04 ± 4.78E+03	9.39E+03 ± 7.64E+03	2.17E+03 ± 5.54E+02
	F43	F44	F45	F46	F47	F48
HGSA	2.83E+03 ± 2.32E+02	2.77E+03 ± 1.99E+02	6.16E+04 ± 1.47E+04	5.42E+03 ± 1.25E+03	2.86E+03 ± 2.24E+02	2.41E+03 ± 5.90E+01
HGSA-OG	3.19E+03 ± 3.13E+02	2.85E+03 ± 2.02E+02	2.79E+05 ± 1.33E+05	1.25E+04 ± 5.65E+03	3.00E+03 ± 1.92E+02	2.55E+03 ± 2.73E+01
GSA-IG	2.88E+03 ± 2.90E+02	2.72E+03 ± 2.24E+02	6.64E+04 ± 2.19E+04	5.01E+03 ± 1.13E+03	2.85E+03 ± 1.83E+02	2.42E+03 ± 1.26E+01
	F49	F50	F51	F52	F53	F54
HGSA	2.30E+03 ± 3.91E-09	2.76E+03 ± 1.33E+02	2.92E+03 ± 3.58E+01	2.89E+03 ± 7.59E+00	2.85E+03 ± 5.07E+01	3.25E+03 ± 2.08E+01
HGSA-OG	6.16E+03 ± 1.86E+03	3.59E+03 ± 1.35E+02	3.28E+03 ± 5.03E+01	2.93E+03 ± 9.91E+00	6.39E+03 ± 1.25E+03	4.60E+03 ± 3.65E+02
GSA-IG	2.30E+03 ± 8.65E-08	2.78E+03 ± 8.30E+01	2.92E+03 ± 2.87E+01	2.89E+03 ± 8.73E+00	2.85E+03 ± 5.07E+01	3.26E+03 ± 2.37E+01
	F55	F56	F57			
HGSA	3.11E+03 ± 2.82E+01	4.05E+03 ± 1.88E+02	1.10E+04 ± 2.60E+03			
HGSA-OG	3.31E+03 ± 5.72E+01	4.69E+03 ± 2.46E+02	1.82E+05 ± 9.87E+04			
GSA-IG	3.11E+03 ± 2.68E+01	4.07E+03 ± 1.97E+02	1.11E+04 ± 1.93E+03			

Table 4.16: Statistical results obtained by the Wilcoxon signed ranks test between HGSA and HGSA-OG and GSA-IG in $D = 30$ dimensions.

HGSA vs.	R^+	R^-	p -value	$\alpha=0.05$
HGSA-OG	1550.5	45.5	0	YES
GSA-IG	1068.0	585.0	4.24E-02	YES

validity and superiority of combination between a hierarchical structure and an improved gravitational constant in HGSA.

4.5.3 Real-world optimization problems

To further investigate the practicability and performance of HGSA in other problems, four real-world optimization problems from CEC2011 [143] are adopted to evaluate the properties between it and GSA, GGSA, CGSA-M, MGSA, PSOGSA and DNLGSA. These four real-world problems are optimal control of a nonlinear stirred tank reactor (NLSTR), spread spectrum radar polyphase code design (SSRPCD), transmission network expansion planning (TNEP) and static economic load dispatch (ELD). NLSTR is a chemical process occurred in a nonlinear stirred tank reactor. It is a benchmark optimization problem. SSRPCD aims to design a radar system by the polyphase codes, which is a mix-max nonlinear global optimization problem with continuous variables. TNEP is to resolve the minimum cost of expansion plan and implement no overloads during the planning horizon by the set of transmission lines. It contains a DC power flow model. ELD is to minimize the fuel cost of units in order to achieve an optimal generation dispatch among them, and meet four constraints, i.e., load demand, generator operation, ramp rate limits and prohibited operating zones. The explicit implementation regarding these four problems can be referred in [143]. The parameters of seven kinds of GSAs are the same as those in Table 4.1. For each problem, each algorithm is independently run 30 times and the termination criterion is $D * 10000$ where D is set to be 1, 20, 7 and 13 according to the configuration of four problems.

The mean, standard deviation, the best and worst solutions obtained by each algorithm are shown in Table 4.17. From it, we can see that HGSA derives the least mean in four problems, indicating its effective and steady performance in comparison with other six GSAs. In addition, the worst solutions obtained by the HGSA in four problems are also the least, suggesting that when seven algorithms trap into the local optima, the influence of the premature convergence on HGSA is the lowest due to its effective structure and mechanism. Therefore, this experiment denotes that HGSA is an effective and practicable algorithm for resolving some real-world optimization problems.

Table 4.17: Experimental results of four real-world optimization problems using HGSA, GSA, GGSA, CGSA-M, MGSA, GSGA, PSOGSA and DNLGSA.

Problem		HGSA	GSA	GGSA	CGSA-M	MGSA	PSOGSA	DNLGSA
NLSTR	Mean	2.12E+01	2.15E+01	2.14E+01	2.14E+01	2.13E+01	2.15E+01	2.14E+01
	Std	1.32E+00	7.32E-01	1.16E+00	1.29E+00	1.36E+00	1.54E+00	7.61E-01
	Best	1.53E+01	2.06E+01	1.60E+01	1.53E+01	1.54E+01	1.43E+01	1.91E+01
	Worst	2.26E+01	2.43E+01	2.29E+01	2.29E+01	2.31E+01	2.39E+01	2.30E+01
SSRPCD	Mean	7.05E-01	9.16E-01	1.01E+00	1.00E+00	1.69E+00	1.14E+00	1.11E+00
	Std	1.12E-01	1.85E-01	1.72E-01	1.98E-01	2.06E-01	2.42E-01	1.78E-01
	Best	5.00E-01	5.00E-01	7.39E-01	6.37E-01	1.02E+00	6.05E-01	8.18E-01
	Worst	8.93E-01	1.28E+00	1.38E+00	1.45E+00	2.01E+00	1.60E+00	1.71E+00
TNEP	Mean	2.20E+02	2.97E+02	2.43E+02	2.69E+02	2.22E+02	2.34E+02	3.52E+02
	Std	0.00E+00	8.17E+01	2.65E+01	5.53E+01	5.49E+00	3.81E+01	2.18E+02
	Best	2.20E+02	2.20E+02	2.20E+02	2.20E+02	2.20E+02	2.20E+02	2.20E+02
	Worst	2.20E+02	5.40E+02	3.51E+02	4.45E+02	2.38E+02	3.51E+02	1.30E+03
ELD	Mean	1.91E+04	1.92E+04	1.92E+04	1.92E+04	1.93E+04	1.94E+04	1.94E+04
	Std	1.14E+02	9.20E+01	1.53E+02	1.24E+02	2.41E+02	1.83E+02	1.60E+02
	Best	1.89E+04	1.91E+04	1.88E+04	1.89E+04	1.86E+04	1.91E+04	1.90E+04
	Worst	1.94E+04	1.94E+04	1.95E+04	1.95E+04	1.97E+04	1.98E+04	1.96E+04

4.5.4 Time complexity analysis

The above experiments have demonstrated a remarkable performance of HGSA on functions and real-world optimization problems. To investigate the efficiency of HGSA, the time complexity analysis between it and other six GSAs is carried out. The population size n is analyzed in the time complexity. The corresponding time complexity of each procedure in HGSA is calculated as follows:

- (1) Initializing the parameters of HGSA needs the time complexity $O(1)$.
- (2) Establishing a three-layered hierarchical population structure requires $2O(n) + O(1)$.
- (3) Justifying the boundary of population costs $O(n)$.
- (4) Calculating the fitness of all the individuals on the bottom layer needs $O(n)$.
- (5) The masses of all the individuals on the bottom layer are calculated, which costs $4O(n)$.
- (6) The time complexity of obtaining a gravitational constant is $O(1)$.
- (7) The K best individuals on the medium layer are determined. Since the K value linearly decreases, the time complexity of this procedure in the worst condition is $O(n^2) + O(n)$.
- (8) The global optimal individual is selected to place on the top layer. The time complexity of this operation at most is $O(n)$.
- (9) The velocities of the K best individuals on the medium layer are updated by the global optimal individual on the top layer. This process at most requires $O(n)$.
- (10) The accelerations of all the individuals on the bottom layer are calculated by the K best individuals on the medium layer. This operation at most costs $2O(n^2)$.
- (11) The velocities and positions of all the individuals on the bottom layer are updated, which need $O(n)$ and $O(n)$.

Consequently, the overall time complexity of HGSA under the termination criterion is calculated as follow:

$$\begin{aligned}
 & O(1) + 2O(n) + O(1) + T * [O(n) + O(n) + 4O(n) + O(1) + O(n^2) + O(n) + \\
 & O(n) + O(n) + 2O(n^2) + O(n) + O(n)] \tag{4.13} \\
 & = 3T * O(n^2) + (11T + 2) * O(n) + (T + 2) * O(1),
 \end{aligned}$$

where T is the maximum iteration number. To be simplified, we can regard its overall time complexity as $O(n^2)$.

After calculating the time complexity of GSA, GGSA, CGSA-M, MGSA, PSO-GSA

and DNLGSA, we find that these six GSAs possess the same time complexity $O(n^2)$ which mainly occurs in generating accelerations of individuals. The results show that the time complexity of HGSA is identical with that of other six GSAs, implying that HGSA maintains the same computational efficiency in comparison with other GSAs. In other words, a hierarchical structure not only enhances the performance of HGSA but also does not decrease its efficiency, indicating that it is an effective and prospective population topology for refining the property of GSA.

4.6 Conclusions

In this chapter, a three-layered hierarchical GSA with an improved gravitational constant (HGSA) is proposed to enhance the performance of GSA from the viewpoint of population topology. Since the conventional GSA is prone to trap into the local optima and its search ability is limited, HGSA is devised to address these two issues. A hierarchical population structure is used to effectively guide the evolution of individuals and an improved gravitational constant intensifies the exploration ability of HGSA. Two weighted coefficients with time effectively control the relationship among three layers so as to balance the exploration and exploitation abilities of HGSA. Three comparative experiments are implemented to analyze the performances between HGSA and other six GSAs, five heuristic algorithms and seven PSOs on numerous benchmark functions. Three experiments demonstrate a superior performance of HGSA in comparison with other eighteen algorithms due to its effective hierarchical structure and gravitational constant, suggesting that it significantly enhances its exploration and exploitation abilities in the search process. In addition, a component-wise experiment is conducted to show the effect of combination between a hierarchical structure and an improved gravitational constant in HGSA. Afterwards, HGSA is applied to four real-world optimization problems to further investigate its property. The experiment verifies that HGSA is an effective and practicable approach for optimizing real-world problems. Finally, the time complexity analysis of HGSA shows that it is the same computational efficient in contrast to other six GSAs.

Chapter 5

Conclusions

5.1 Some general remarks

In this thesis, three kinds of evolutionary algorithms including DE, BSO and GSA are investigated from the viewpoint of population structure. Different algorithms have distinctive population structures and characteristics. For them, three chapters are written to analyze their inherent relationship and performance, respectively. Thus, some general remarks can be summarized as follows:

(1) The population structure of DE shows a cumulative Poisson distribution. The goodness of fit verifies this phenomenon on several benchmark functions according to frequency of degree among individuals. Besides, parameters of DE influence its population interaction, which reflects different number of nodes and values of λ .

(2) The population structure of BSO meets a power law distribution on functions with low dimension. Its frequency of degree can exhibit a straight slash in double logarithmic coordinates. Different dimensions and parameters also influence the population structure and performance of algorithm. To be specific, the occurrence of power law distribution can indicate good performance of BSO. In addition, combinatorial parameter setting effectively improves the property of BSO.

(3) The population structure of GSA in fact is a two-layered hierarchy. Based on this characteristic, a three-layered hierarchical GSA with a log-sigmoid gravitational constant, namely HGSA, is proposed to enhance its search ability. Hierarchical structure effectively guides interaction among individuals and improved gravitational constant reinforces search performance. Numerous contrastive experiments demonstrate the significant improvement of HGSA.

5.2 Future work

PIN provides an analytical platform for search performance metrics (such as population entropy, search step length, population dispersion, convergence speed, etc.) and topological structure metrics (such as degree distribution of network, characteristic path length, assortative mixing, etc.). It is expected that some generic relationships between search performance of EAs and topological structures of population can be drawn, thus to give some potential guidelines for designing and improving the performance of EAs. Especially, EAs constructed based on heterogeneous population structures are expected to be more effective. At present, my work only plays significant influence within DE, BSO and GSAs' community, and it opens the door to the following future researches:

(1) PIN should be used to construct population structures of other EAs such as PSO and ACO to investigate the relationship between their properties and population interaction from a theoretical viewpoint of complex network.

(2) EAs with diverse population topologies could be designed to attempt to resolve some engineering and practical problems. Their performances could also be analyzed via PIN.

(3) More topological structure metrics should be used to study the properties of population structures derived from EAs.

(4) New strategies or framework of population interaction should be added into EAs to adjust their current structures and thereafter to enhance the performance and robustness of algorithms. For instance, GSA can be further improved according to a three-layered hierarchical structure where the distribution of individuals on three layers should be changed by several new proposed strategies.

Bibliography

- [1] J. Cheng, G. Yuan, M. Zhou, S. Gao, C. Liu, and H. Duan, “A fluid mechanics-based data flow model to estimate VANET capacity,” *IEEE Transactions on Intelligent Transportation Systems*, 2019, doi: 10.1109/TITS.2019.2921074.
- [2] Y. Wang, Y. Yu, S. Cao, X. Zhang, and S. Gao, “A review of applications of artificial intelligent algorithms in wind farms,” *Artificial Intelligence Review*, 2019, doi: 10.1007/s10462-019-09768-7.
- [3] S. Gao, Q. Cao, Z. Zhang, and Z. Tang, “A chaotic clonal selection algorithm and its application to synthesize multiple-valued logic functions,” *IEEJ Transactions on Electrical and Electronic Engineering*, vol. 5, no. 1, pp. 105–114, 2010.
- [4] S. Gao, S. Song, J. Cheng, Y. Todo, and M. Zhou, “Incorporation of solvent effect into multi-objective evolutionary algorithm for improved protein structure prediction,” *IEEE/ACM Transactions on Computational Biology and Bioinformatics*, vol. 15, no. 4, pp. 1365–1378, 2018.
- [5] J. Wang, B. Cen, S. Gao, Z. Zhang, and Y. Zhou, “Cooperative evolutionary framework with focused search for many-objective optimization,” *IEEE Transactions on Emerging Topics in Computational Intelligence*, 2018, doi: 10.1109/TETCI.2018.2849380.
- [6] J. Wang, L. Yuan, Z. Zhang, S. Gao, Y. Sun, and Y. Zhou, “Multiobjective multiple neighborhood search algorithms for multiobjective fleet size and mix location-routing problem with time windows,” *IEEE Transactions on Systems, Man, and Cybernetics: Systems*, 2019, doi: 10.1109/TSMC.2019.2912194.
- [7] P. J. Van Laarhoven and E. H. Aarts, “Simulated annealing,” in *Simulated Annealing: Theory and Applications*. Springer, 1987, pp. 7–15.

- [8] F. Glover and M. Laguna, "Tabu search," in *Handbook of Combinatorial Optimization*. Springer, 1998, pp. 2093–2229.
- [9] D. S. Weile and E. Michielssen, "Genetic algorithm optimization applied to electromagnetics: A review," *IEEE Transactions on Antennas and Propagation*, vol. 45, no. 3, pp. 343–353, 1997.
- [10] X. Yao, Y. Liu, and G. Lin, "Evolutionary programming made faster," *IEEE Transactions on Evolutionary Computation*, vol. 3, no. 2, pp. 82–102, 1999.
- [11] K. V. Price, "Differential evolution," in *Handbook of Optimization*. Springer, 2013, pp. 187–214.
- [12] Y. Yu, S. Gao, Y. Wang, and Y. Todo, "Global optimum-based search differential evolution," *IEEE/CAA Journal of Automatica Sinica*, vol. 6, no. 2, pp. 379–394, 2018.
- [13] S. Gao, Y. Yu, Y. Wang, J. Wang, J. Cheng, and M. Zhou, "Chaotic local search-based differential evolution algorithms for optimization," *IEEE Transactions on Systems, Man and Cybernetics: Systems*, 2019, doi: 10.1109/TSMC.2019.2956121.
- [14] M. Dorigo and C. Blum, "Ant colony optimization theory: A survey," *Theoretical Computer Science*, vol. 344, no. 2-3, pp. 243–278, 2005.
- [15] R. Eberhart and J. Kennedy, "Particle swarm optimization," in *Proceedings of the IEEE International Conference on Neural Networks*, vol. 4. Citeseer, 1995, pp. 1942–1948.
- [16] Y. Shi, "Brain storm optimization algorithm," in *International Conference in Swarm Intelligence*. Springer, 2011, pp. 303–309.
- [17] E. Rashedi, H. Nezamabadi-Pour, and S. Saryazdi, "GSA: a gravitational search algorithm," *Information Sciences*, vol. 179, no. 13, pp. 2232–2248, 2009.
- [18] E. Atashpaz-Gargari and C. Lucas, "Imperialist competitive algorithm: an algorithm for optimization inspired by imperialistic competition," in *2007 IEEE congress on Evolutionary Computation*. IEEE, 2007, pp. 4661–4667.
- [19] H.-G. Beyer and H.-P. Schwefel, "Evolution strategies-a comprehensive introduction," *Natural Computing*, vol. 1, no. 1, pp. 3–52, 2002.

- [20] Z. W. Geem, *Music-inspired harmony search algorithm: theory and applications*. Springer, 2009, vol. 191.
- [21] S. A. Hofmeyr and S. Forrest, “Architecture for an artificial immune system,” *Evolutionary Computation*, vol. 8, no. 4, pp. 443–473, 2000.
- [22] K. M. Passino, “Bacterial foraging optimization,” *International Journal of Swarm Intelligence Research*, vol. 1, no. 1, pp. 1–16, 2010.
- [23] A. H. Gandomi, X.-S. Yang, and A. H. Alavi, “Cuckoo search algorithm: a meta-heuristic approach to solve structural optimization problems,” *Engineering with Computers*, vol. 29, no. 1, pp. 17–35, 2013.
- [24] D. Karaboga and B. Akay, “A comparative study of artificial bee colony algorithm,” *Applied Mathematics and Computation*, vol. 214, no. 1, pp. 108–132, 2009.
- [25] S. Salcedo-Sanz, J. Del Ser, I. Landa-Torres, S. Gil-López, and J. Portilla-Figueras, “The coral reefs optimization algorithm: a novel metaheuristic for efficiently solving optimization problems,” *The Scientific World Journal*, vol. 2014, Article ID 739768, 15 pages, 2014.
- [26] X.-S. Yang, “Firefly algorithm, levy flights and global optimization,” in *Research and Development in Intelligent Systems XXVI*. Springer, 2010, pp. 209–218.
- [27] R. V. Rao, V. Savsani, and J. Balic, “Teaching–learning-based optimization algorithm for unconstrained and constrained real-parameter optimization problems,” *Engineering Optimization*, vol. 44, no. 12, pp. 1447–1462, 2012.
- [28] M. Eusuff, K. Lansey, and F. Pasha, “Shuffled frog-leaping algorithm: a memetic meta-heuristic for discrete optimization,” *Engineering Optimization*, vol. 38, no. 2, pp. 129–154, 2006.
- [29] H. Duan and P. Qiao, “Pigeon-inspired optimization: a new swarm intelligence optimizer for air robot path planning,” *International Journal of Intelligent Computing and Cybernetics*, vol. 7, no. 1, pp. 24–37, 2014.
- [30] L. Shan, H. Qiang, J. Li, and Z.-q. Wang, “Chaotic optimization algorithm based on tent map,” *Control and Decision*, vol. 20, no. 2, pp. 179–182, 2005.

- [31] H. Shah-Hosseini, “The intelligent water drops algorithm: a nature-inspired swarm-based optimization algorithm,” *International Journal of Bio-inspired Computation*, vol. 1, no. 1-2, pp. 71–79, 2009.
- [32] M.-H. Tayarani-N and M. Akbarzadeh-T, “Magnetic optimization algorithms a new synthesis,” in *2008 IEEE Congress on Evolutionary Computation*. IEEE, 2008, pp. 2659–2664.
- [33] J. Cheng, J. Cheng, M. Zhou, F. Liu, S. Gao, and C. Liu, “Routing in internet of vehicles: A review,” *IEEE Transactions on Intelligent Transportation Systems*, vol. 16, no. 5, pp. 2339–2352, 2015.
- [34] Y. Liu, D. Cheng, Y. Wang, J. Cheng, and S. Gao, “A novel method for predicting vehicle state in internet of vehicles,” *Mobile Information Systems*, vol. 2018, Article ID 9728328, 2018.
- [35] S. Gao, Q. Cao, M. Ishii, and Z. Tang, “Local search with probabilistic modeling for learning multiple-valued logic networks,” *IEICE Transactions on Fundamentals of Electronics, Communications and Computer Sciences*, vol. 94, no. 2, pp. 795–805, 2011.
- [36] J. Sun, S. Gao, H. Dai, J. Cheng, M. Zhou, and J. Wang, “Bi-objective elite differential evolution for multivalued logic networks,” *IEEE Transactions on Cybernetics*, vol. 50, no. 1, pp. 233–246, 2020.
- [37] S. Gao, J. Zhang, X. Wang, and Z. Tang, “Multi-layer neural network learning algorithm based on random pattern search method,” *International Journal of Innovative Computing, Information and Control*, vol. 5, no. 2, pp. 489–502, 2009.
- [38] S. Gao, M. Zhou, Y. Wang, J. Cheng, H. Yachi, and J. Wang, “Dendritic neural model with effective learning algorithms for classification, approximation, and prediction,” *IEEE Transactions on Neural Networks and Learning Systems*, vol. 30, no. 2, pp. 601–614, 2019.
- [39] A.-L. Barabási, “Scale-free networks: a decade and beyond,” *Science*, vol. 325, no. 5939, pp. 412–413, 2009.
- [40] D. J. Watts and S. H. Strogatz, “Collective dynamics of ‘small-world’ networks,” *Nature*, vol. 393, no. 6684, pp. 440–442, 1998.

- [41] H. Dai, S. Gao, Y. Yang, and Z. Tang, “Effects of rich-gets-richer rule on small-world networks,” *Neurocomputing*, vol. 73, no. 10-12, pp. 2286–2289, 2010.
- [42] R. Bell and P. Dean, “Properties of vitreous silica: Analysis of random network models,” *Nature*, vol. 212, no. 5068, pp. 1354–1356, 1966.
- [43] M. E. Newman, “Analysis of weighted networks,” *Physical Review E*, vol. 70, no. 5, 056131, 2004.
- [44] S. Boccaletti, V. Latora, Y. Moreno, M. Chavez, and D.-U. Hwang, “Complex networks: Structure and dynamics,” *Physics Reports*, vol. 424, no. 4, pp. 175–308, 2006.
- [45] J. Cheng, X. Wu, M. Zhou, S. Gao, Z. Huang, and C. Liu, “A novel method for detecting new overlapping community in complex evolving networks,” *IEEE Transactions on Systems, Man, and Cybernetics: Systems*, 2018, doi: 10.1109/TSM-C.2017.2779138.
- [46] J. Cheng, M. Chen, M. Zhou, S. Gao, C. Liu, and C. Liu, “Overlapping community change point detection in an evolving network,” *IEEE Transactions on Big Data*, 2018, doi: 10.1109/TBDATA.2018.2880780.
- [47] S. Gao, Y. Wang, J. Wang, and J.-J. Cheng, “Understanding differential evolution: A Poisson law derived from population interaction network,” *Journal of Computational Science*, vol. 21, pp. 140–149, 2017.
- [48] B. Dorronsoro and P. Bouvry, “Improving classical and decentralized differential evolution with new mutation operator and population topologies,” *IEEE Transactions on Evolutionary Computation*, vol. 15, no. 1, pp. 67–98, 2011.
- [49] S. Janson and M. Middendorf, “A hierarchical particle swarm optimizer and its adaptive variant,” *IEEE Transactions on Systems, Man, and Cybernetics, Part B (Cybernetics)*, vol. 35, no. 6, pp. 1272–1282, 2005.
- [50] Y. Wang, S. Gao, Y. Yu, and Z. Xu, “The discovery of population interaction with a power law distribution in brain storm optimization,” *Memetic Computing*, vol. 11, no. 1, pp. 65–87, 2019.

- [51] Y. Yu, S. Gao, S. Cheng, Y. Wang, S. Song, and F. Yuan, “CBSO: a memetic brain storm optimization with chaotic local search,” *Memetic Computing*, vol. 10, no. 4, pp. 353–367, 2018.
- [52] J. Wang, W. Zhang, and J. Zhang, “Cooperative differential evolution with multiple populations for multiobjective optimization,” *IEEE Transactions on Cybernetics*, vol. 46, no. 12, pp. 2848–2861, 2016.
- [53] J. Wang, Y. Zhou, Y. Wang, J. Zhang, C. P. Chen, and Z. Zheng, “Multiobjective vehicle routing problems with simultaneous delivery and pickup and time windows: formulation, instances, and algorithms,” *IEEE Transactions on Cybernetics*, vol. 46, no. 3, pp. 582–594, 2016.
- [54] S. Gao, Y. Wang, J. Cheng, Y. Inazumi, and Z. Tang, “Ant colony optimization with clustering for solving the dynamic location routing problem,” *Applied Mathematics and Computation*, vol. 285, pp. 149–173, 2016.
- [55] J. L. Payne, M. Giacobini, and J. H. Moore, “Complex and dynamic population structures: synthesis, open questions, and future directions,” *Soft Computing*, vol. 17, no. 7, pp. 1109–1120, 2013.
- [56] E. Alba and M. Tomassini, “Parallelism and evolutionary algorithms,” *IEEE Transactions on Evolutionary Computation*, vol. 6, no. 5, pp. 443–462, 2002.
- [57] N. Lynn, M. Z. Ali, and P. N. Suganthan, “Population topologies for particle swarm optimization and differential evolution,” *Swarm and Evolutionary Computation*, vol. 39, pp. 24–35, 2018.
- [58] M. Tomassini, *Spatially structured evolutionary algorithms: artificial evolution in space and time*. Springer, 2006.
- [59] E. Alba and B. Dorronsoro, *Cellular genetic algorithms*. Springer Science & Business Media, 2009, vol. 42.
- [60] E. Cantu-Paz, *Efficient and accurate parallel genetic algorithms*. Springer Science & Business Media, 2000, vol. 1.
- [61] D. Whitley, “A genetic algorithm tutorial,” *Statistics and Computing*, vol. 4, no. 2, pp. 65–85, 1994.

- [62] W. Fang, J. Sun, H. Chen, and X. Wu, “A decentralized quantum-inspired particle swarm optimization algorithm with cellular structured population,” *Information Sciences*, vol. 330, pp. 19–48, 2016.
- [63] J. Liao, Y. Cai, T. Wang, H. Tian, and Y. Chen, “Cellular direction information based differential evolution for numerical optimization: an empirical study,” *Soft Computing*, vol. 20, no. 7, pp. 2801–2827, 2016.
- [64] I. Arnaldo, I. Contreras, D. Millán-Ruiz, J. I. Hidalgo, and N. Krasnogor, “Matching island topologies to problem structure in parallel evolutionary algorithms,” *Soft Computing*, vol. 17, no. 7, pp. 1209–1225, 2013.
- [65] J. Apolloni, J. García-Nieto, E. Alba, and G. Leguizamón, “Empirical evaluation of distributed differential evolution on standard benchmarks,” *Applied Mathematics and Computation*, vol. 236, pp. 351–366, 2014.
- [66] L. Vanneschi, D. Codecasa, and G. Mauri, “An empirical study of parallel and distributed particle swarm optimization,” in *Parallel Architectures and Bioinspired Algorithms*. Springer, 2012, pp. 125–150.
- [67] F. Zou, D. Chen, and R. Lu, “Hybrid hierarchical backtracking search optimization algorithm and its application,” *Arabian Journal for Science and Engineering*, vol. 43, no. 2, pp. 993–1014, 2018.
- [68] M. Owais and M. K. Osman, “Complete hierarchical multi-objective genetic algorithm for transit network design problem,” *Expert Systems with Applications*, vol. 114, pp. 143–154, 2018.
- [69] D. Sánchez, P. Melin, and O. Castillo, “Optimization of modular granular neural networks using a hierarchical genetic algorithm based on the database complexity applied to human recognition,” *Information Sciences*, vol. 309, pp. 73–101, 2015.
- [70] S. Rastegar, R. Araujo, and J. Mendes, “Online identification of Takagi–Sugeno fuzzy models based on self-adaptive hierarchical particle swarm optimization algorithm,” *Applied Mathematical Modelling*, vol. 45, pp. 606–620, 2017.
- [71] L. Rodríguez, O. Castillo, J. Soria, P. Melin, F. Valdez, C. I. Gonzalez, G. E. Martinez, and J. Soto, “A fuzzy hierarchical operator in the grey wolf optimizer algorithm,” *Applied Soft Computing*, vol. 57, pp. 315–328, 2017.

- [72] F. Herrera, M. Lozano, and C. Moraga, “Hierarchical distributed genetic algorithms,” *International Journal of Intelligent Systems*, vol. 14, no. 11, pp. 1099–1121, 1999.
- [73] Z. Cao, Y. Shi, X. Rong, B. Liu, Z. Du, and B. Yang, “Random grouping brain storm optimization algorithm with a new dynamically changing step size,” in *International Conference in Swarm Intelligence*. Springer, 2015, pp. 357–364.
- [74] H. Zhu and Y. Shi, “Brain storm optimization algorithms with k-medians clustering algorithms,” in *2015 Seventh International Conference on Advanced Computational Intelligence*. IEEE, 2015, pp. 107–110.
- [75] Y. Yu, S. Gao, Y. Wang, J. Cheng, and Y. Todo, “ASBSO: An improved brain storm optimization with flexible search length and memory-based selection,” *IEEE Access*, vol. 6, pp. 36 977–36 994, 2018.
- [76] Y. Yu, S. Gao, Y. Wang, Z. Lei, J. Cheng, and Y. Todo, “A multiple diversity-driven brain storm optimization algorithm with adaptive parameters,” *IEEE Access*, vol. 7, pp. 126 871–126 888, 2019.
- [77] D. Zhou, Y. Shi, and S. Cheng, “Brain storm optimization algorithm with modified step-size and individual generation,” *International Conference in Swarm Intelligence*, pp. 243–252, 2012.
- [78] Z. Yang and Y. Shi, “Brain storm optimization with chaotic operation,” in *2015 Seventh International Conference on Advanced Computational Intelligence*. IEEE, 2015, pp. 111–115.
- [79] Y. Yang, Y. Shi, and S. Xia, “Advanced discussion mechanism-based brain storm optimization algorithm,” *Soft Computing*, vol. 19, no. 10, pp. 2997–3007, 2015.
- [80] Z. Jia, H. Duan, and Y. Shi, “Hybrid brain storm optimisation and simulated annealing algorithm for continuous optimisation problems,” *International Journal of Bio-Inspired Computation*, vol. 8, no. 2, pp. 109–121, 2016.
- [81] Z. Cao, X. Hei, L. Wang, Y. Shi, and X. Rong, “An improved brain storm optimization with differential evolution strategy for applications of ANNs,” *Mathematical Problems in Engineering*, vol. 2015, Article ID 923698, 18 pages, 2015.

- [82] S. Cheng, Q. Qin, J. Chen, and Y. Shi, “Brain storm optimization algorithm: a review,” *Artificial Intelligence Review*, vol. 46, no. 4, pp. 445–458, 2016.
- [83] Y. Wang, Y. Yu, S. Gao, H. Pan, and G. Yang, “A hierarchical gravitational search algorithm with an effective gravitational constant,” *Swarm and Evolutionary Computation*, vol. 46, pp. 118–139, 2019.
- [84] M. R. Narimani, A. A. Vahed, R. Azizipanah-Abarghooee, and M. Javidsharifi, “Enhanced gravitational search algorithm for multi-objective distribution feeder reconfiguration considering reliability, loss and operational cost,” *IET Generation, Transmission & Distribution*, vol. 8, no. 1, pp. 55–69, 2014.
- [85] S. Gao, C. Vairappan, Y. Wang, Q. Cao, and Z. Tang, “Gravitational search algorithm combined with chaos for unconstrained numerical optimization,” *Applied Mathematics and Computation*, vol. 231, pp. 48–62, 2014.
- [86] Z. Song, S. Gao, Y. Yu, J. Sun, and Y. Todo, “Multiple chaos embedded gravitational search algorithm,” *IEICE Transactions on Information and Systems*, vol. 100, no. 4, pp. 888–900, 2017.
- [87] S. Mirjalili and S. Z. M. Hashim, “A new hybrid PSO-GSA algorithm for function optimization,” in *2010 International Conference on Computer and Information Application*. IEEE, 2010, pp. 374–377.
- [88] M. Khatibinia and S. Khosravi, “A hybrid approach based on an improved gravitational search algorithm and orthogonal crossover for optimal shape design of concrete gravity dams,” *Applied Soft Computing*, vol. 16, pp. 223–233, 2014.
- [89] B. Shaw, V. Mukherjee, and S. Ghoshal, “Solution of reactive power dispatch of power systems by an opposition-based gravitational search algorithm,” *International Journal of Electrical Power & Energy Systems*, vol. 55, pp. 29–40, 2014.
- [90] M. Soleimanpour-Moghadam, H. Nezamabadi-Pour, and M. M. Farsangi, “A quantum inspired gravitational search algorithm for numerical function optimization,” *Information Sciences*, vol. 267, pp. 83–100, 2014.
- [91] G. Sun, P. Ma, J. Ren, A. Zhang, and X. Jia, “A stability constrained adaptive alpha for gravitational search algorithm,” *Knowledge-Based Systems*, vol. 139, pp. 200–213, 2018.

- [92] V. K. Bohat and K. Arya, “An effective gbest-guided gravitational search algorithm for real-parameter optimization and its application in training of feedforward neural networks,” *Knowledge-Based Systems*, vol. 143, pp. 192–207, 2018.
- [93] B. González, F. Valdez, P. Melin, and G. Prado-Arechiga, “Fuzzy logic in the gravitational search algorithm for the optimization of modular neural networks in pattern recognition,” *Expert Systems with Applications*, vol. 42, no. 14, pp. 5839–5847, 2015.
- [94] ———, “Fuzzy logic in the gravitational search algorithm enhanced using fuzzy logic with dynamic alpha parameter value adaptation for the optimization of modular neural networks in echocardiogram recognition,” *Applied Soft Computing*, vol. 37, pp. 245–254, 2015.
- [95] P. Haghbayan, H. Nezamabadi-Pour, and S. Kamyab, “A niche GSA method with nearest neighbor scheme for multimodal optimization,” *Swarm and Evolutionary Computation*, vol. 35, pp. 78–92, 2017.
- [96] K. Pal, C. Saha, S. Das, and C. A. C. Coello, “Dynamic constrained optimization with offspring repair based gravitational search algorithm,” in *2013 IEEE Congress on Evolutionary Computation*. IEEE, 2013, pp. 2414–2421.
- [97] H. Sajedi and S. F. Razavi, “DGSA: discrete gravitational search algorithm for solving knapsack problem,” *Operational Research*, vol. 17, no. 2, pp. 563–591, 2017.
- [98] S. Gao, Y. Todo, T. Gong, G. Yang, and Z. Tang, “Graph planarization problem optimization based on triple-valued gravitational search algorithm,” *IEEJ Transactions on Electrical and Electronic Engineering*, vol. 9, no. 1, pp. 39–48, 2014.
- [99] P. Das, H. S. Behera, and B. K. Panigrahi, “A hybridization of an improved particle swarm optimization and gravitational search algorithm for multi-robot path planning,” *Swarm and Evolutionary Computation*, vol. 28, pp. 14–28, 2016.
- [100] S. Mallick, R. Kar, D. Mandal, and S. Ghoshal, “Optimal sizing of CMOS analog circuits using gravitational search algorithm with particle swarm optimization,” *International Journal of Machine Learning and Cybernetics*, vol. 8, no. 1, pp. 309–331, 2017.

- [101] R. Storn and K. Price, “Differential evolution—a simple and efficient heuristic for global optimization over continuous spaces,” *Journal of Global Optimization*, vol. 11, no. 4, pp. 341–359, 1997.
- [102] S. Das and P. N. Suganthan, “Differential evolution: a survey of the state-of-the-art,” *IEEE Transactions on Evolutionary Computation*, vol. 15, no. 1, pp. 4–31, 2011.
- [103] H. John, *Holland, Adaptation in natural and artificial systems*. MIT Press, Cambridge, MA, 1992.
- [104] Y. Yu and Z.-H. Zhou, “A new approach to estimating the expected first hitting time of evolutionary algorithms,” *Artificial Intelligence*, vol. 172, no. 15, pp. 1809–1832, 2008.
- [105] D. E. Goldberg and K. Deb, “A comparative analysis of selection schemes used in genetic algorithms,” *Foundations of Genetic Algorithms*, vol. 1, pp. 69–93, 1991.
- [106] A. Prügel-Bennett and J. L. Shapiro, “Analysis of genetic algorithms using statistical mechanics,” *Physical Review Letters*, vol. 72, no. 9, pp. 1305, 1994.
- [107] B. Dorronsoro and P. Bouvry, “Study of different small-world topology generation mechanisms for genetic algorithms,” in *2012 IEEE Congress on Evolutionary Computation*. IEEE, 2012, pp. 1–8.
- [108] J. M. Whitacre, R. A. Sarker, and Q. T. Pham, “Effects of adaptive social networks on the robustness of evolutionary algorithms,” *International Journal on Artificial Intelligence Tools*, vol. 20, no. 05, pp. 783–817, 2011.
- [109] C. Echegoyen, A. Mendiburu, R. Santana, and J. A. Lozano, “Estimation of bayesian networks algorithms in a class of complex networks,” in *2010 IEEE Congress on Evolutionary Computation*. IEEE, 2010, pp. 1–8.
- [110] R. Salomon, “Re-evaluating genetic algorithm performance under coordinate rotation of benchmark functions. a survey of some theoretical and practical aspects of genetic algorithms,” *BioSystems*, vol. 39, no. 3, pp. 263–278, 1996.
- [111] J. Brest, S. Greiner, B. Boskovic, M. Mernik, and V. Zumer, “Self-adapting control parameters in differential evolution: a comparative study on numerical benchmark problems,” *IEEE Transactions on Evolutionary Computation*, vol. 10, no. 6, pp. 646–657, 2006.

- [112] J. Vesterstrom and R. Thomsen, “A comparative study of differential evolution, particle swarm optimization, and evolutionary algorithms on numerical benchmark problems,” in *Proceedings of 2004 Congress on Evolutionary Computation*, vol. 2. IEEE, 2004, pp. 1980–1987.
- [113] P. N. Suganthan, N. Hansen, J. J. Liang, K. Deb, Y.-P. Chen, A. Auger, and S. Tiwari, “Problem definitions and evaluation criteria for the CEC 2005 special session on real-parameter optimization,” *KanGAL Report*, vol. 2005005, 2005.
- [114] M. Jamil and X.-S. Yang, “A literature survey of benchmark functions for global optimisation problems,” *International Journal of Mathematical Modelling and Numerical Optimisation*, vol. 4, no. 2, pp. 150–194, 2013.
- [115] Y. Wang, Z. Cai, and Q. Zhang, “Differential evolution with composite trial vector generation strategies and control parameters,” *IEEE Transactions on Evolutionary Computation*, vol. 15, no. 1, pp. 55–66, 2011.
- [116] Z.-h. Zhan, W.-n. Chen, Y. Lin, Y.-j. Gong, Y.-l. Li, and J. Zhang, “Parameter investigation in brain storm optimization,” in *2013 IEEE Symposium on Swarm Intelligence*. IEEE, 2013, pp. 103–110.
- [117] S. Cheng, Y. Shi, Q. Qin, and S. Gao, “Solution clustering analysis in brain storm optimization algorithm,” in *2013 IEEE Symposium on Swarm Intelligence*. IEEE, 2013, pp. 111–118.
- [118] J. M. Whitacre, R. A. Sarker, and Q. T. Pham, “The self-organization of interaction networks for nature-inspired optimization,” *IEEE Transactions on Evolutionary Computation*, vol. 12, no. 2, pp. 220–230, 2008.
- [119] A. Clauset, C. R. Shalizi, and M. E. Newman, “Power-law distributions in empirical data,” *SIAM Review*, vol. 51, no. 4, pp. 661–703, 2009.
- [120] J. Derrac, S. García, D. Molina, and F. Herrera, “A practical tutorial on the use of nonparametric statistical tests as a methodology for comparing evolutionary and swarm intelligence algorithms,” *Swarm and Evolutionary Computation*, vol. 1, no. 1, pp. 3–18, 2011.
- [121] R. Jugulum, S. Taguchi *et al.*, *Computer-based robust engineering: essentials for DFSS*. ASQ Quality Press, 2004.

- [122] J. Qi and Z. Rong, “The emergence of scaling laws search dynamics in a particle swarm optimization,” *Physica A: Statistical Mechanics and Its Applications*, vol. 392, no. 6, pp. 1522–1531, 2013.
- [123] S. Mirjalili and A. Lewis, “Adaptive gbest-guided gravitational search algorithm,” *Neural Computing and Applications*, vol. 25, no. 7-8, pp. 1569–1584, 2014.
- [124] E. Rashedi, H. Nezamabadi-Pour, and S. Saryazdi, “BGSA: binary gravitational search algorithm,” *Natural Computing*, vol. 9, no. 3, pp. 727–745, 2010.
- [125] ———, “Filter modeling using gravitational search algorithm,” *Engineering Applications of Artificial Intelligence*, vol. 24, no. 1, pp. 117–122, 2011.
- [126] S. Duman, U. Güvenç, Y. Sönmez, and N. Yörükeren, “Optimal power flow using gravitational search algorithm,” *Energy Conversion and Management*, vol. 59, pp. 86–95, 2012.
- [127] J. Liang, B. Qu, P. Suganthan, and A. G. Hernández-Díaz, “Problem definitions and evaluation criteria for the CEC 2013 special session on real-parameter optimization,” *Computational Intelligence Laboratory, Zhengzhou University, Zhengzhou, China and Nanyang Technological University, Singapore, Technical Report*, vol. 201212, no. 34, pp. 281–295, 2013.
- [128] N. Awad, M. Ali, J. Liang, B. Qu, and P. Suganthan, “Problem definitions and evaluation criteria for the CEC 2017 special session and competition on single objective bound constrained real-parameter numerical optimization,” *Technical Report*, 2016.
- [129] B. Gu and F. Pan, “Modified gravitational search algorithm with particle memory ability and its application,” *International Journal of Innovative Computing, Information and Control*, vol. 9, no. 11, pp. 4531–4544, 2013.
- [130] A. Zhang, G. Sun, J. Ren, X. Li, Z. Wang, and X. Jia, “A dynamic neighborhood learning-based gravitational search algorithm,” *IEEE Transactions on Cybernetics*, vol. 48, no. 1, pp. 436–447, 2018.
- [131] N. Hansen, S. D. Müller, and P. Koumoutsakos, “Reducing the time complexity of the derandomized evolution strategy with covariance matrix adaptation (CMA-ES),” *Evolutionary Computation*, vol. 11, no. 1, pp. 1–18, 2003.

- [132] G. Zhu and S. Kwong, “Gbest-guided artificial bee colony algorithm for numerical function optimization,” *Applied Mathematics and Computation*, vol. 217, no. 7, pp. 3166–3173, 2010.
- [133] S. Mirjalili, S. M. Mirjalili, and A. Lewis, “Grey wolf optimizer,” *Advances in Engineering Software*, vol. 69, pp. 46–61, 2014.
- [134] S. Mirjalili, “SCA: a sine cosine algorithm for solving optimization problems,” *Knowledge-Based Systems*, vol. 96, pp. 120–133, 2016.
- [135] R. Poli, J. Kennedy, and T. Blackwell, “Particle swarm optimization,” *Swarm Intelligence*, vol. 1, no. 1, pp. 33–57, 2007.
- [136] R. Mendes, J. Kennedy, and J. Neves, “The fully informed particle swarm: simpler, maybe better,” *IEEE Transactions on Evolutionary Computation*, vol. 8, no. 3, pp. 204–210, 2004.
- [137] Y. Shi and R. Eberhart, “A modified particle swarm optimizer,” in *1998 IEEE International Conference on Evolutionary Computation Proceedings. IEEE World Congress on Computational Intelligence*. IEEE, 1998, pp. 69–73.
- [138] J. J. Liang, A. K. Qin, P. N. Suganthan, and S. Baskar, “Comprehensive learning particle swarm optimizer for global optimization of multimodal functions,” *IEEE Transactions on Evolutionary Computation*, vol. 10, no. 3, pp. 281–295, 2006.
- [139] Z. H. Zhan, J. Zhang, Y. Li, and Y. H. Shi, “Orthogonal learning particle swarm optimization,” *IEEE Transactions on Evolutionary Computation*, vol. 15, no. 6, pp. 832–847, 2011.
- [140] K. Premalatha and A. Natarajan, “Hybrid PSO and GA for global maximization,” *Int. J. Open Problems Compt. Math*, vol. 2, no. 4, pp. 597–608, 2009.
- [141] C. Zhang, J. Ning, S. Lu, D. Ouyang, and T. Ding, “A novel hybrid differential evolution and particle swarm optimization algorithm for unconstrained optimization,” *Operations Research Letters*, vol. 37, no. 2, pp. 117–122, 2009.
- [142] Y.-J. Gong, J.-J. Li, Y. Zhou, Y. Li, H. S.-H. Chung, Y.-H. Shi, and J. Zhang, “Genetic learning particle swarm optimization,” *IEEE Transactions on Cybernetics*, vol. 46, no. 10, pp. 2277–2290, 2016.

- [143] S. Das and P. N. Suganthan, "Problem definitions and evaluation criteria for CEC 2011 competition on testing evolutionary algorithms on real world optimization problems," *Jadavpur University, Nanyang Technological University, Kolkata*, pp. 341–359, 2010.